Sorbonne University

Doctoral School of Informatics, Telecommunications and Electronics of Paris

EURECOM

Towards Dependable 5G-NR Sidelink Communication

Author : **Jin Yan**

Dissertation for Doctor of Philosophy in Information and Communication Engineering

Directed by **Prof. Jérôme Härri**

Publicly defended on **13th of December 2024**

In Front of a committee composed of:

Prof. Alexey Vinel	Karlsruhe Institute of Technology, Germany	*Reviewer*
Prof. Claudia Campolo	Mediterranea University of Reggio Calabria, Italy	*Reviewer*
Prof. Yaser Fallah	University of Central Florida, USA	*Examiners*
Prof. Meng Wang	Technische Universität Dresden, Germany	*Examiners*
Prof. Adlen Ksentini	EURECOM, France	*Examiners*
Prof. Jérôme Härri	EURECOM, France	*Advisor*

Sorbonne University

Ecole Doctorale Informatique, Télécommunications et Électronique de Paris

EURECOM

Vers une Communication Fiable en Sidelink 5G-NR

Presentée par: **Jin Yan**

Thèse de Doctorat en Informatique, Télécommunications et Électronique de l'Université Sorbonne Université

Dirigée par **Prof. Jérôme Härri**

Soutenue publiquement le **13 décembre 2024**

Devant un jury composé de :

Prof. Alexey Vinel	Karlsruhe Institute of Technology, Germany	*Reviewer*
Prof. Claudia Campolo	Mediterranea University of Reggio Calabria, Italy	*Reviewer*
Prof. Yaser Fallah	University of Central Florida, USA	*Examiners*
Prof. Meng Wang	Technische Universität Dresden, Germany	*Examiners*
Prof. Adlen Ksentini	EURECOM, France	*Examiners*
Prof. Jérôme Härri	EURECOM, France	*Advisor*

Abstract

5G New Radio (NR) is anticipated to revolutionize communication infrastructure significantly, it is designed to provide robust and reliable network services tailored to a wide range of operational demands. A crucial aspect of this advancement is the development of direct Device-to-Device (D2D) communication, termed Sidelink(SL) in the 5G-NR standards by 3GPP. 5G-NR Sidelink communication is essential due to its direct and efficient nature, significantly enhancing support for complex services such as autonomous driving systems and Internet of Things (IoT). It facilitates real-time, reliable information exchange among distributed intelligent devices in an ad-hoc manner, propelling network development into its next phase and offering streamlined and responsive connectivity. Despite these potential, research into dependable Ultra-Reliable and Low-Latency Communication (URLLC) services over Sidelink, especially for delay-sensitive and high-reliability applications, remains scarce.

This thesis addresses the significant gap in direct D2D communication by reconfiguring the 5G-NR Sidelink, particularly for Vehicle-to-Everything (V2X) communications. We initially alter standard parameter settings to accommodate diverse operational demands within V2X communications. Through adjustments to key parameters—numerology, Modulation and Coding Scheme (MCS), and MAC layer scheduling—our configuration meets stringent URLLC requirements, demonstrating the potential in a V2X Sidelink communication at the 5.9 GHz band.

Despite this newly designed system supporting URLLC services in the V2X domain, standards and industrial requirements dictate that numerous services continue to operate over standard parameter settings, with additional services potentially necessitating different types of settings. To accommodate these multiple services within the limited resources available at the V2X 5.9 GHz band, we propose a novel architecture based on network slicing. This architecture is designed to support multiple services simultaneously, employing a variety of dynamic parameter settings directly over the Sidelink PC5 link. By segmenting network resources into protected slices, each tailored to specific service needs, our system maintains service integrity and prevents interference. The Proximity Services (ProSe) standard plays a pivotal role in this configuration, enabling systematic group management for different service scenarios. This approach facilitates the management of both standard and altered parameter settings across different service slices, promoting flexibility and efficiency.

Furthermore, we apply these concepts to real-world applications such as vehicular platooning to assess the tangible benefits of URLLC services. Simulation results indicate significant improvements in mobility metrics such as stability and response times when a URLLC service slice is allocated to platoon vehicles.

This study not only proposes a novel architecture for Sidelink-based network slicing but also advances our understanding of integrating URLLC services into direct 5G-NR Sidelink communication. It lays the groundwork for future research aimed at optimizing and practically implementing advanced network slicing and URLLC strategies in diverse communication environments.

Résumé

La 5G New Radio (NR) est prévue pour révolutionner de manière significative l'infrastructure de communication, elle est conçue pour fournir des services de réseau robustes et fiables adaptés à une large gamme d'exigences opérationnelles. Un aspect crucial de cette avancée est le développement de la communication directe de dispositif à dispositif (D2D), appelée Sidelink dans les normes 5G-NR par 3GPP. La communication Sidelink 5G-NR est essentielle en raison de sa nature directe et efficace, améliorant considérablement le soutien pour des services complexes tels que les systèmes de conduite autonome et IoT. Elle facilite l'échange d'informations fiable et en temps réel entre des dispositifs intelligents distribués de manière ad hoc, propulsant le développement du réseau dans sa prochaine phase et offrant une connectivité rationalisée et réactive. Malgré ce potentiel, la recherche sur des services URLL fiables via Sidelink, en particulier pour des applications sensibles aux délais et à haute fiabilité, reste rare.

Cette thèse aborde une lacune significative dans la communication D2D directe en reconfigurant le Sidelink 5G-NR, en particulier pour les communications Vehicle-to-Everything (V2X). Nous modifions initialement les paramètres standards pour répondre aux demandes opérationnelles diverses au sein des communications V2X. Grâce aux ajustements de paramètres clés—numérologie, schéma de modulation et de codage (MCS), et planification de la couche MAC— notre configuration satisfait aux exigences strictes URLLC, démontrant le potentiel dans une communication Sidelink V2X à la bande de 5,9 GHz.

Malgré ce système nouvellement conçu soutenant les services URLLC dans le domaine V2X, les normes et les exigences industrielles dictent que de nombreux services continuent de fonctionner sur des paramètres standard, avec des services supplémentaires nécessitant potentiellement différents types de réglages. Pour accommoder ces multiples services dans les ressources limitées disponibles à la bande V2X de 5,9 GHz, nous proposons une nouvelle architecture basée sur le découpage en tranches réseau. Cette architecture est conçue pour supporter simultanément plusieurs services, utilisant une variété de réglages de paramètres dynamiques directement sur le lien Sidelink PC5. En segmentant les ressources réseau en tranches protégées, chacune adaptée aux besoins de service spécifiques, notre système maintient l'intégrité du service et évite les interférences. Le standard des Services de Proximité (ProSe) joue un rôle pivot dans cette configuration, permettant une gestion systématique de groupe pour différents scénarios de service. Cette approche facilite la gestion des réglages de paramètres standard et modifiés à travers différentes tranches de service, favorisant la flexibilité et l'efficacité.

De plus, nous appliquons ces concepts à des applications réelles telles que le platooning véhiculaire pour évaluer les avantages tangibles des services URLLC. Les résultats des simulations indiquent des améliorations significatives dans les métriques de mobilité telles que la stabilité et les temps de réponse lorsque une tranche de service URLLC est allouée à des véhicules en platoon.

Cette étude propose non seulement une nouvelle architecture pour le découpage en tranches basé sur le Sidelink, mais avance également notre compréhension de l'intégration des services URLLC dans la communication Sidelink 5G-NR directe. Elle pose les bases pour des recherches futures visant à optimiser et mettre en œuvre pratiquement des stratégies

avancées de découpage en tranches réseau et de services URLLC dans des environnements de communication diversifiés.

Acknowledgements

The years of my PhD have been an incredible and unforgettable journey, this has been about more than just research, but also about living and thinking about life.
First and foremost, I would like to express my heartfelt gratitude to my advisor, Jérôme, for his unwavering support and patience. Working with him has been an enriching experience; no matter how naive my thoughts or misunderstandings were, he always found a way to guide me with his remarkable insight. His positive attitude and support have been invaluable in helping me navigate challenges, and for that, I am truly grateful.
I would also like to thanks to my team, CATS, for our insightful discussions and shared experiences. A special thanks to Carlos for his invaluable expertise on the simulator and for his countless hours of support, which helped me navigate the challenges of my final year.
To my colleagues and friends at EURECOM, Ali, Alireza, Antonio, Arman, Cédric, Chieh-Chun, Eunjeong, Imad, Jichao, Judy, Kensuke, Matteo, Mohammad, Mohsen, Omid, Pepe, Robert, Romain, Sofia, Symeon, Roya, Zixuan, and many others, thank you all for your encouragement, the coffee breaks, the trips, and all the joyful moments under the Mediterranean sun. These are priceless memories that I will always cherish. A special thanks to Chieh-Chun—thank you for simply being there. Your endless silly jokes have always brightened my days.
I am deeply grateful to my parents back in China. Though you could not be here physically, your unwavering support has meant the world to me.
Finally, to my love, Jack, this work would not have been possible without your unconditional support. And to our new son, Edmond, I dedicate this thesis to both of you, with all my love.

Contents

List of Figures

List of Tables

Acronyms

3GPP 3rd Generation Partnership Project.

ADAS Advanced driver-assistance systems.

AI Artificial Intelligence.

C-ITS Cooperative Intelligent Transport Systems.

C-V2X Cellular-Vehicle-to-Everything.

CAM Cooperative Awareness Messages.

CBR Channel Busy Ratio.

CCAM Connected and Automated Mobility.

CCDF Complementary Cumulative Distribution Function.

CPM Collective Perception Messag.

CSMA/CA Carrier Sensing Multiple Access with Collision Avoidance.

D2D Device-to-Device.

DCC Decentralised Congestion Control.

DENM Decentralized Environmental Notification Messages.

eMBB enhanced Mobile BroadBand.

eNB evolved Node B.

gNB next Generation Node B.

GUI Graphical User Interface.

IoT Internet of Things.

ITS Intelligent Transportation Systems.

KPI Key Performances Indicator.

LTE Long Term Evolution.

MAC Medium Access Channel.

MCM Maneuver Coordination Message.

MCS Modulation and Coding Scheme.

mMTC massive Machine-Type Communication.

NFV Network Function Virtualization.

NR New Radio.

NS3 Network Simulator 3.

NSSAI Network Slice Selection Assistance Information.

O-RAN Open RAN.

OFDM Orthogonal Frequency-Division Multiplexing.

OFDMA Orthogonal Frequency-Division Multiple Access.

OSI The Open Systems Interconnection.

PCM Platooning Control Message.

PDCP Packet Data Convergence Protocol.

PHY PHysical Layer.

PMM Platooning Management Message.

PRB Physical Resource Blocks.

PRR Packet Reception Rate.

QoS Quality of Service.

RAN Radio Access Network.

RLC Radio Link Control.

RRC Radio Resource Control.

RSU Road-Side Unit.

SB-SPS Sensing Based Semi-persistent Scheduling.

SC-FDMA Single-Carrier Frequency-Division Multiple Access.

SCS Sub-Carrier Spacing.

SDAP Service Data Adaptation Protocol.

SDN Software-Defined Networking.

SL Sidelink.

SLA Service Level Agreement.

TDMA Time Division Multiple Access.

TSN Time-Sensitive Networking.

UE User Equipment.

URLLC Ultra-Reliable and Low-Latency Communication.

V2I Vehicle-to-Infrastructure.

V2N Vehicle-to-Network.

V2P Vehicle-to-Pedestrian.

V2V Vehicle-to-Vehicle.

V2X Vehicle-to-Everything.

VUE Vehicular UE.

Chapter 1
General Introduction

1.1 Introduction

Wireless communication has become indispensable in our increasingly connected world, with 5G technology at the forefront of this digital revolution. Offering significant enhancements over its predecessors, 5G introduces ultra-fast speeds, substantially reduced latency, and greater capacity to handle simultaneous connections. These capabilities are crucial as they support a broad spectrum of applications, ranging from complex Internet of Things (IoT) networks to a more wider range of advanced applications.
Particularly, 5G-NR extends beyond providing ultra-reliable low-latency communications (URLLC) [1, 2]; it supports a wide array of applications that require high reliability and minimal delay, crucial for the safe operation of autonomous vehicles. This advanced connectivity framework is key to enabling real-time decision-making and vehicle control, therefore enhancing both the safety and efficiency of autonomous driving technologies.
The 5G Americas White-paper [3] highlights the increasing range of applications across various industries that require support from URLLC services, including the smart factory, healthcare, and entertainment sectors. Specifically, industrial automation emerges as a critical application for URLLC features. Many industrial processes are governed by extremely tight Key Performance Indicators (KPIs) for 5G communication links among sensors, actuators, and controllers.
In Qualcomm white-paper [4] has pointed out, the current low latency by industrial demands, which requires 2ms cycle time, are mainly met by Ethernet systems; these systems show drawbacks as they require physical cabling between machines, which increase the hazard risks during operation and are less adaptive to dynamic environment. An immediate opportunity exists to replace these wired local-area networks with 5G in factories. While LTE and WiFi can serve some of these functions, they generally fail to meet the necessary Layer 1-2 performance (scheduling, latency, redundancy) for the most demanding applications. 5G in the meantime can fulfill these stringent, time-critical requirements.
The Qualcomm white paper [4] has also pointed out an important aspect of applying 5G to industrial automation is knowing which standards should be part of the design brief. Of which, an IEEE Ethernet standard as the Time-Sensitive Networking (TSN) for industrial networking, likely to become the baseline networking technology for real-time industrial networking.
With many of the legacy industrial Ethernet protocols able to run over TSN, one

key development for adapting 5G systems into industrial requirements is mapping TSN to the 5G radio interface. According to Qualcomm [4], the TSN physical layer resources are similar to time-slot distribute in 5G, however concept of Quality of Service (QoS) identifier, MAC layer design, and other criteria require further analysis and development within the 5G framework to ensure seamless integration and optimal performance.

Current industrial applications and advanced use cases increasingly demand that numerous devices connect in a distributed, ad-hoc manner. Thus, supporting direct Device-to-Device (D2D) communication, which defines as Sidelink via PC5 link, over 5G-NR communication is crucial. D2D communication, which evolved from ad-hoc networking principles where devices interact directly without centralized coordination, has significantly advanced. Over the years, it has seen improvements in protocol design and spectrum efficiency, becoming integral to modern communication frameworks.
While D2D technology can be broadly applied across various sectors, this paper focuses specifically on its implementation in Intelligent Transportation Systems (ITS). Our examination centers on leveraging 5G D2D to enhance the capabilities of autonomous driving systems, underscoring its critical role in advancing vehicle-to-everything (V2X) communications and the broader ITS landscape.

In the V2X domain, the increasing number of vehicles on the road, coupled with more complex applications such as vehicular platooning and advanced autonomous driving, necessitates robust wireless communication. This communication must support ubiquitous connectivity, particularly for Vehicle-to-Vehicle (V2V) interactions, to ensure seamless and efficient data exchange across diverse environments.
This growth is driven by the need to support enhanced safety features, real-time traffic management, and seamless connectivity between vehicles. From the early 2010s, the IEEE 802.11p/ITS-G5 technology was established to facilitate direct V2V communication. This standard enables devices to connect without a central access point, supporting applications such as file transfers and direct media streaming. Following this, the evolution from 4G LTE, starting with 3GPP Release 12, to 5G-NR Release 17, has formalized D2D communication under the term Sidelink (SL). This development has provided a structured framework within the cellular network for direct device communication, enhancing support for proximity-based services and public safety applications.

In the automotive sector, 5G connectivity plays a crucial role, particularly for autonomous driving systems. It enables dynamic manipulation of resources for efficient spectrum design and sharing, which is essential for meeting the stringent demands of vehicular communication. V2X communications encompass a broad array of technologies aimed at improving traffic safety, efficiency, and enabling automated driving and infotainment through Intelligent Transportation Systems. V2X communication includes, but is not limited to, V2V, Vehicle-to-Network (V2N), Vehicle-to-Pedestrian (V2P), and Vehicle-to-Infrastructure (V2I) interactions. Significant advancements in V2X standardization have been made by various bodies. In the US, the IEEE/SAE DSRC standards were established in 2010 [5], focusing on short-range communications primarily for V2V applications. In Europe, the ETSI/CEN introduced the Cooperative-ITS (C-ITS) Release 1 in 2013 [6]. Both of these frameworks utilize the IEEE 802.11p standard for their physical and data

link layers, catering to the needs of short-range V2V communications.
Parallel to earlier V2X efforts, the 3GPP introduced Cellular-V2X (C-V2X) in LTE Release 14 in early 2017 [7]. C-V2X features a dual approach: it supports short-range direct D2D communications via a Sidelink/PC5 air interface, and wide-area V2N communications that link vehicles to cellular base stations(eNB). The development of C-V2X continues to progress, with significant enhancements incorporated into 5G-NR, particularly from Release 17 onwards. These enhancements focus on expanding V2X capabilities to support emerging use cases like automated driving, substantially improving both the efficiency and reliability of direct vehicle communications in modern ITS applications.

The necessity of employing direct D2D communication, the primary approach in C-V2X, is increasingly recognized across various domains for its role in current V2X applications. Utilizing a direct, fully functional configuration over the 5G-NR PC5 link significantly reduces latency and communication complexity, while providing dynamic control in vehicular scenarios. This enhanced control is crucial for real-time responses needed in safety-critical applications such as collision avoidance and traffic flow optimization. Furthermore, D2D communication allows for efficient bandwidth utilization, which is vital in multiple services required environment, or when high-volume data transmissions is high. These capabilities are crucial for enabling seamless communication among autonomous vehicles and infrastructure, fostering a smarter and more integrated transportation system.
However, as highlighted in the work of [8], there is currently no clear scheme for achieving deterministic transmission of vehicle control signals over the PC5 link, which is essential for realizing TSN in 5G V2X. Consequently, the existing 5G+TSN technology cannot be directly applied to 5G V2X, and further advancements in PC5 Sidelink communication are necessary.
Despite the critical importance of these requirements, there is a noticeable gap in comprehensive studies focused on enhancing the quality of direct communication within vehicular networks. Most existing research has predominantly focused on centralized communication managed through gNB base stations, where efficient resource allocation is achieved across various scenarios. However, efficient direct Sidelink management through a distributed scenario has yet to be thoroughly analyzed. Furthermore, achieving high reliability and low latency in this decentralized architecture remains unclear. Additionally, in V2X communication, different services require varying levels of QoS. The challenge of simultaneously supporting these diverse service requirements remains an open question, underscoring the need for further investigation into decentralized communication solutions that can effectively handle multiple service demands in direct vehicular environments.
To this aim, a primary objective of this thesis is to thoroughly analyze the current state of D2D communication within the 5G-NR framework and identify potential improvements that could enhance the quality of service. This analysis aims to pinpoint practical enhancements that can be realized under the existing standards to better support the dynamic and demanding nature of V2X communication. Moreover, how to effectively integrate existing 3GPP standards within 5G-NR to support these dynamic service requirements spontaneously remains an open question. This necessitates the design of a new architecture or methodology in resource sharing tailored to the diverse different service requirements in vehicular communication.

The remainder of this chapter provides a concise overview of research on 5G-NR direct communication, followed by a high-level description of the requirements for dependable networks across various applications. Additionally, this chapter defines the research problem addressed in this thesis and details the research methodology employed. It also highlights the contributions made by this work, lists related publications, and outlines the organization of the subsequent chapters of this thesis.

1.2 Research Content and Background

1.2.1 5G-NR Direct Communication Aspect

Building on the foundation laid in the previous section on the advantages of direct D2D communication, we start from examine the specific technologies that facilitate such interactions in vehicular environments. The first technology focus on IEEE 802.11p/ITS-G5, which has set the standard for immediate V2V communications, while the following C-V2X represents an evolution of this technology, starting with LTE-V2X in 3GPP Release 14 and further refined under 5G-NR in Release 16. We will now discuss the physical modulation and MAC scheduling mechanisms that underpin these technologies, crucial for ensuring the high-speed, reliable connections needed for contemporary V2X communication.

ITS-G5, based on IEEE 802.11p [9], uses orthogonal frequency division multiplexing (OFDM) and carrier sensing multiple access with collision avoidance (CSMA/CA) for its PHY and MAC layers, respectively. This asynchronous ad-hoc protocol requires vehicles to sense the channel before transmitting, pausing as needed to mitigate collisions. Additionally, ITS-G5 supports broadcasting messages using full channel bandwidth with a choice of eight modulation and coding schemes (MCS).

Simultaneously, C-V2X Sidelink communication, introduced by 3GPP in Release 14 [7] for LTE-V2X and evolved in Release 16 for 5G-NR [10], operates through the PC5 interface to manage direct vehicle-to-vehicle (V2V) communications. Figure. 1.1 illustrates the fundamental concept of 5G Sidelink communication as proposed by Qualcomm [11].

LTE-V2X uses SC-FDMA for Sidelink communication, while 5G-NR Sidelink adopts Orthogonal Frequency-Division Multiple Access (OFDMA), enhancing resource allocation flexibility and communication efficiency. 5G-NR Sidelink introduces advanced resource allocation techniques with four distinct scheduling modes, these mode support allows for more dynamic resource allocation strategies and greater flexibility with sub-modes under mode 2, offering an improvement over the more rigid mode 3 and mode 4 of 4G-LTE. We will explore these modes in detail in the following section. Additionally, 5G-NR provides a range of numerologies, enhancing transmission granularity and optimizing performance for varying scenarios. Notably, the enhanced flexibility in coding rates adapts well to diverse communication needs. 5G technology, underpinned by its three main pillars—enhanced Mobile Broadband (eMBB), massive Machine Type Communications (mMTC), and URLLC—is revolutionary for V2X applications [12]., particularly in delivering ultra-low latency, high data rates, and massive connectivity.

Qualcomm is at the forefront of innovation for 5G Advanced and beyond, proposing a promising future for 5G development alongside parallel propositions from 3GPP Rel.18 [13]. 5G-NR aims to deliver higher capacity, improved communication reliability, and significantly reduced latency. These objectives clearly surpass the current capabilities

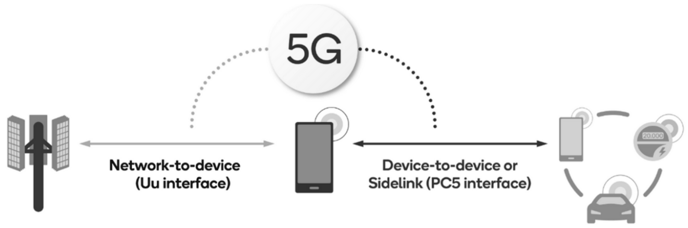

Figure 1.1: 5G System Sidelink is a core technology [11]

of ITS-G5. However, the specifics of how these criteria will be realized through Sidelink technology remain unclear.
To ensure dependable 5G-NR D2D communication, several strategies can be employed, focusing on optimizing transmission intervals and enhancing transmission reliability. Manipulation of various 5G-NR parameters, particularly at the MAC layer scheduler and the physical layer's resource block settings, is crucial. These adjustments facilitate shorter transmission intervals and direct, rapid transmissions. Detailed examination of these settings will be provided in the subsequent section.
Another critical approach to improve transmission reliability is to ensure each transmission is successful and minimally interfered with by others, protected resources exclusively for D2D communication are necessary. Traditional channel sharing in 5G-NR, although useful, does not suit dynamic V2X scenarios well due to its static nature.
Network slicing emerges as a potent solution here, offering dynamic, protected resources tailored to specific service needs. This feature of 5G-NR allows for flexible manipulation of lower-layer settings to meet varying requirements. Implementing network slicing directly over D2D communication in 5G-NR for V2X scenarios can significantly enhance performance, making it a promising approach to address the complexities of modern vehicular communications.
By comparing to the multi-channel access methodology in 5G-NR, network slicing offers certain advantages: 1) Network slicing supports more dynamic resource usage, as slices can be created and released according to the service state. 2) With multi-channel access, each service must be verified and switched to the correct channel, which can be challenging when meeting low latency requirements. In contrast, services can directly connect to the target slice; 3) Effective utilization of network slicing will significantly improve the performance and reliability of V2X communication systems by ensuring that each application receives the appropriate resources and prioritization.

1.2.2 V2X Application Aspect

The objectives of V2X communication is to increase road safety, improve transportation efficiency, improve ride experience and provide additional services. The standardization of these application is primarily addressed in the 3GPP Releases for V2X (starting from Release 14 onwards for LTE-V2X and continuing into 5G-NR V2X in Release 16 and beyond). Additionally, ETSI has published various specifications and reports under ITS (Intelligent Transportation Systems) [6], which outline the requirements and use cases for V2X communications. We'll further investigate into these related standards in the following sections.
The set of applications have been envisioned dividing from day-1 to day-2 applications as

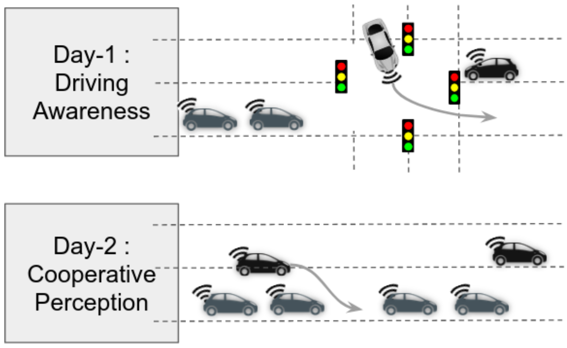

Figure 1.2: Examples of V2X Applications

shown in Fig. 1.2. For day-1 applications in V2X systems, these functionalities represent the initial deployment phase and are essential for basic safety and traffic efficiency. As illustrated in Fig. 1.2 for day-1, typical applications involves message exchanges including Cooperative Awareness Messages (CAM) and Decentralized Environmental Notification Messages (DENM) [14, 15]. CAMs provide ongoing updates about a vehicle's position and movement, enhancing situational awareness among nearby vehicles. DENMs are triggered during potential hazards or accidents, alerting other drivers to changes in road conditions or emergencies. Together, these applications facilitate continuous information exchange, enabling vehicles to maintain safety and efficiently navigate the roads. The further details of these messages functionality and mechanism, such as message rate and message size are explained in following Chapter 2.

Day-2 applications in V2X systems extend the capabilities established by day-1, integrating more sophisticated technologies and functionalities that demand enhanced communication and sensor interoperability. As depicted in Fig. 1.2 for a cooperative driving scenario, these applications leverage shared sensor data and other perception information to enable vehicles to collaboratively adjust speed and direction based on real-time environmental conditions. For instance, during a lane change or when a vehicle intends to join a platoon, day-2 functionalities facilitate coordinated maneuvers among multiple vehicles, enhancing traffic flow and vehicle safety through advanced cooperative driving techniques.

There is also a rising demand for advanced vehicular applications like vehicular platooning and autonomous driving, various works [16, 12] have pointed out these applications impose stringent requirements on communication systems in regards to low latency and high reliability. These applications need to swiftly adapt to dynamic, high-mobility environments and respond promptly in emergency situations to ensure correct vehicle responses. Furthermore, the complexity of these applications is increasing as they begin to incorporate AI-driven scenarios, such as work from Barbieri et al. [17] analyzed the demanding requirements in continuous data exchanges among local vehicles for decentralized federated learning. Future developments might also involve the direct transmission and reception of AI models among vehicles within communication zones. This evolving landscape necessitates that V2X communication systems effectively manage a variety of data rates and message sizes, accommodating the diverse and dynamic nature of traffic types and conditions.

In general day-1 applications generally align with the capabilities of standard 5G-NR communication, where requirements like the transmission of CAM with typically delay under

100 ms and reliability of 90-99% for packets around 300 bytes at a rate of 10Hz, are capable to be met. However, day-2 and other advanced applications pose greater challenges, demanding latencies under 10 ms and reliability rates between 99.99-99.999%—requirements that are difficult to achieve with standardized 5G-NR settings due to their role in complex vehicular operations that require enhanced control.
Additionally, 5G-NR Sidelink allocates between 10 and 20 MHz of spectrum at 5.9 GHz for C-ITS safety-related communication [18]. This bandwidth is proving already to be insufficient to support all day-1 basic V2X messages effectively, while also needing to accommodate advanced day-2 applications. These applications must coexist seamlessly with day-1 and day-2 functionalities, maintaining operational harmony and ensuring the integrity of basic vehicular communications.
This scarcity of spectrum and the current limited methodology for resource allocation scheme highlight the necessity to develop a more dynamic and efficient architecture. Such an architecture should support varying levels of QoS and adapt resource allocation dynamically to handle the complex and dense requirements of V2X communication.

1.2.3 5G-NR Resource Allocation Methodology

In the 5G-NR system, channel resources dedicated for direct Sidelink communication are limited, ETSI TR 103 853 [18] specified with only 10 to 20 MHz of spectrum at 5.9 GHz specifically designated for C-ITS safety-related communication. Despite this, Sidelink is intended to support ubiquitous connectivity for a large number of UEs using these scarce spectrum resources. Consequently, developing an efficient method to dynamically allocate resources across various applications is essential for enhancing the system's capacity to support services with higher requirements. This strategic allocation is crucial to maximizing the potential of limited Sidelink resources while ensuring robust safety communications and broader connectivity.
Numerous studies have focused on efficiently and dynamically assigning resources to various users within 5G-NR communication frameworks. For instance, Lucas-Estañ et al. [19] proposed a sensing-based grant-free scheduling for vehicles within a group, with UL/DL assistance they realised a prominent URLLC service for small packets. In regards of 5G-NR V2X. Feng et al. [20] suggests multiple methods of centralised Cloud management, such as Mobile Edge Computing (MEC), or assignment by road-side units (RSUs). Another study by Ge et al. [21] proposes a monte-carlo approach to tackle a combined optimization of reliability and latency for URLLC V2X on the millimeter wave band (FR2). These studies do not, however, consider the use of Sidelink (SL) communication or the sub-6GHz band (FR1), including the C-ITS band at 5.9GHz.
The ETSI initially developed Decentralized Congestion Control (DCC) for ITS-G5, which has since been adapted for C-V2X [22]. This reactive DCC mechanism operates based on a state machine correlated with specific Channel Busy Ratio (CBR) ranges. The system adjusts transmission rates by introducing delays between consecutive packets, based on the CBR, to mitigate potential congestion. However, this approach necessitates a significant listening period during communication, making it challenging to satisfy services with stringent requirements. Additionally, the inherent delay compensation is an obstacle in achieving low latency demands, which are crucial for time-sensitive applications.
Given the limited spectrum allocated for V2X Sidelink communication and the varied service requirements of diverse V2X applications, network slicing emerges as an essential

strategy. It enables the system to dynamically partition resources into distinct, protected groups, each optimized to support specific service needs. However, most existing research on network slicing has focused on implementation through higher infrastructure layers and core network modifications[23, 24, 25]. There is limited research on implementing a pure Sidelink-based network slicing architecture [26], particularly lacking is the exploration of how to design these slices to effectively meet different QoS requirements.

1.3 Problem Statement

D2D communication, known as Sidelink in 5G-NR, has increasingly been recognized and standardized across various scenarios in V2X communications. Despite this progress, based on Section 1.2, several unresolved issues remain concerning the realization of reliable and efficient 5G Sidelink communication tailored specifically for V2X applications. These challenges present key research questions that this thesis aims to address:

- Can 5G-NR Sidelink technology support URLLC? If so, what are the optimal methods for implementation?

Despite significant industrial and 3GPP interest in advancing 5G Sidelink technology, research into developing a more dependable network directly over 5G-NR Sidelink remains limited. Similar key parameters from vertical UL/DL communication settings coexist in 5G-NR Sidelink, presenting the potential to deliver high-quality services comparable to URLLC currently provided over UL/DL. However, to fully achieve this potential, certain parameters, such as the Modulation and Coding Scheme (MCS) and numerology, which are typically preset, need to be carefully adjusted. These adjustments are crucial as they are not typically adaptable in real-time to varying communication conditions. Identifying optimal values for these parameters is essential for laying a strong foundation that ensures the 5G-NR system performs optimally across diverse scenarios.
Furthermore, the challenge extends beyond merely selecting the appropriate parameter settings; it also involves a meticulous design of the network architecture to meet these stringent requirements. This includes deciding which vehicles require URLLC services and how to safeguard the integrity of general V2X communications while accommodating these specialized needs. Each aspect requires careful consideration and study to ensure the successful deployment of dependable V2X communication.
Another critical approach to achieving a dependable network via Sidelink involves network slicing. However, this raises a pertinent question:

- Is direct network slicing feasible within the 5G-NR Sidelink framework, and how can these slices be effectively safeguarded?

As the current implementation of network slicing in 5G-NR primarily revolves around uplink/downlink (UL/DL) paths facilitated by gNB and core network infrastructures, there is a noticeable trend towards making these processes more efficient and simplified [27, 28]. The next developmental step requires directly applying network slicing over 5G-NR Sidelink V2X to achieve lower latency and simplify configuration management. However, efficient adaptation of existing standards and protocols to implement network slicing on 5G-NR Sidelink remains largely unexplored. Addressing this gap is a crucial step in advancing 5G-NR V2X capabilities.

Additionally, providing tailored network slicing for various V2X scenarios requires meticulous resource allocation among different slices. Each slice must be customized to meet specific QoS demands of V2X applications, particularly focusing on the distribution and management of resources. URLLC services, which cater to high-priority, high-demand applications, should also be restricted to a limited number of users within targeted service slices. Careful selection and optimization of network parameters within these slices are essential to fulfill the stringent requirements of URLLC services, ensuring efficiency and reliability in V2X communications.
For the actual application of URLLC services in V2X, the next question arises:

- What impacts do Sidelink slices have on Connected and Automated Mobility (CCAM) performance, specifically within the context of vehicular platooning? What benefits does this architecture offer?

While URLLC services significantly enhance the quality of service for V2X applications, understanding their specific impacts on vehicular performance across different scenarios remains crucial. First, it is essential to identify key V2X applications that benefit from URLLC, such as vehicular platooning, and to characterize these applications in terms of the number of vehicles involved, communication density, mobility control, and the use of URLLC services to enhance performance. Additionally, performance metrics for vehicular mobility are yet to be standardized. Comprehensive studies are required to establish performance criteria and define driving limits that align with the enhanced capabilities provided by URLLC.

1.4 Research Methodology and Designs

This section outlines our approach to addressing and resolving the problems previously mentioned, and it provides insight into the rationale behind our design choices.
Firstly, in respect of supporting dependable URLLC over 5G-NR Sidelink communication, we formulate the first few steps as following :
Step 1: To improve latency, we leverage two advanced 5G-NR Sidelink parameters: flexible numerology and enhanced Modulation and Coding Schemes (MCS). We begin by assessing the communication performance across a broad range of MCS values to understand their impact under different traffic densities. This analysis will help us identify the MCS setting that provides the best adaptation to the most diverse scenarios. Similarly, we explore how different numerologies affect performance, aiming to pinpoint the most effective MCS values for varying numerologies and communication densities. This comprehensive evaluation is critical for optimizing resource utilization and enhancing network efficiency in dynamic vehicular environments.
Step 2: To enhance reliability, we employ a new MAC layer mode 2 scheduler tailored for URLLC requirements. This scheduler, integral to the 5G-NR Sidelink architecture, is designed to align with the optimal parameter settings identified earlier. By integrating these elements, we aim to evaluate whether the new 5G-NR Sidelink architecture can reliably support URLLC services across various traffic scenarios.

Now we address the second problem outlined in section 1.3 as designing and managing slice allocation over direct 5G-NR Sidelink PC5 connections:

Step 3: To implement network slicing over the 5G-NR PC5 link, it is essential first step to develop an orchestration mechanism capable of configuring and managing slices directly through the 5G-NR Sidelink. Additionally, defining the slices and establishing effective communication for slice management are critical steps that need further development.
Step 4: After establishing the network slicing architecture, the subsequent crucial step is the meticulous design of slice parameters tailored to specific requirements, especially concerning resource allocation and MAC and Physical layer settings. Additionally, analyzing the impacts among different slices is essential for ensuring optimal network performance.

Finally, we analyze the impact of the newly designed slices on Connected and Automated Mobility (CCAM) over 5G-NR as the last problem listed in section 1.3:
Step 5: To comprehensively evaluate the enhancements provided by a dependable network within general V2X communication, we focus on a critical use case—vehicular platooning. This involves understanding the control and management mechanisms applied to vehicular platooning and assessing the impact of a protected, dependable network slice on this application. We conduct simulations based on our proposed architecture, that analyze the specific improvements in vehicular mobility performance attributable to the dependable network. Additionally, we will develop metrics to precisely measure these improvements, ensuring a thorough analysis of the network's effectiveness in real-world scenarios.

1.5 Publications and Contributions

The contributions of this doctoral work to the literature are as follows:

- This study examines the key parameter of Modulation and Coding Scheme (MCS). By analyzing MCS across various traffic scenarios, we identified optimal data rates to enhance 5G-NR Sidelink performance

  Publication : J. Yan and J. Härri, "MCS Analysis for 5G-NR V2X Sidelink Broadcast Communication," 2022 IEEE Intelligent Vehicles Symposium (IV), Aachen, Germany, 2022. [29]

- A novel architecture proposed in realizing URLLC over 5G-NR Sidelink, by integrates physical layer rearrangement, MAC layer scheduler optimizations, and an admission control mechanism.

  Publication : J. Yan and J. Härri, "On the Feasibility of URLLC for 5G-NR V2X Sidelink Communication at 5.9 GHz," GLOBECOM 2022 - 2022 IEEE Global Communications Conference, Rio de Janeiro, Brazil, 2022. [30]

- A framework for vehicular platooning over 5G-NR Sidelink is established by adapting 5G ProSe services for platoon management and slice configuration. Through adjusting 5G-NR parameters the system delivered URLLC services within a platoon slice.

  Publication : J. Yan and J. Härri, "Towards 5G-NR ProSe-Based Platoon Services Supporting URLL Vehicular Communication," ICC 2024 - IEEE International Conference on Communications, Denver, CO, USA, 2024. [31]

- The impact of 5G-NR Sidelink communication qualities on vehicular platooning performance is analysed. A matrix for evaluating platooning mobility proposed and how enhanced communication improves specific aspects on platoon behavior are investigated.

  Publication : under submission to journal "IEEE Transactions on Intelligent Vehicles (T-IV)"

- A newly proposed platoon architecture with mobility dynamics, a dual-slice design, URLLC service support, under realistic communication scenarios. The benefits of URLLC for vehicular platooning revealed the system enhancements in performance.

  Publication : under submission to journal "IEEE Transactions on Mobile Computing"

- A study on supporting URLLC services for multiple clusters in decentralized Sidelink environments. A decentralized cluster formation methodology proposed, which effectively limits the number of devices to match available URLLC resources in 5G-NR SL.

  Publication : under submission to Conference to be decided.

1.6 Structure of the Thesis

The main body of this thesis is organized as follows :
Chapter 2 presents the evolution of D2D communication within the 5G-NR framework, detailing the relevant standards and protocols that have developed over the years. It introduces a crucial aspect of 5G-NR—network slicing, which is essential for providing dependable networks in V2X scenarios, thereby highlighting the primary focus of this study. Additionally, this chapter outlines the simulation platforms pertinent to 5G-NR D2D communication, describing the fundamental capabilities of each to provide a comprehensive overview of the tools available for this research.
Chapter 3 proposes an architecture designed to achieve a dependable network directly over 5G-NR D2D communication, by focusing on enhancing high reliability and low latency. The chapter explores how various 5G-NR parameters influence overall network performance, with simulations conducted using the NS3 simulator to validate theoretical findings against practical results. This rigorous analysis helps clarify how different configurations impact network dependability.
Chapter 4 concentrates on V2X communication protocols and service requirements, introducing the concept of network slicing to support diverse V2X services. It details the methodology for implementing network slicing directly over Sidelink communication using ProSe standards, followed by an evaluation of the new architecture's performance through simulation.
Chapter 5 examines a specific vehicular use case—vehicular platooning. This chapter begins with an overview of vehicular control mechanisms and discusses communication aspects vital for implementing vehicular platooning. By comparing existing platooning projects, a new architecture based on proposals from Chapter 3 is suggested. The potential of this dependable network, supported by network slicing, is then assessed using both analytical models and simulated scenarios to analyze the outcomes.

Finally, Chapter 6: "Conclusion and Perspectives" concludes this work, some current ongoing works are listed out and also opens to some possible future extensions of the concepts we introduced with this thesis.

Chapter 2
State of the Art

In this chapter, we investigate the current state-of-the-art on dependable 5G-NR Sidelink communication related to the described methodology in Chapter 1. We begin with an in-depth overview of the current state of art on 3GPP 5G-NR, then 3GPP 5G-NR Sidelink, both from a standardization as well as scientific domains. To achieve the reliability and QoS necessary for dependable communication, we extend the state-of-art study to 5G Network Slicing, both related to 5G-NR and 5G-NR Sidelink domains.
Most of the current 5G-NR Sidelink applications being related to V2X use cases, we review the V2X standards and protocols defined in Europe by the ETSI ITS, covering spectrum, architecture, protocols and messages.
We finally provide an overview of the application requirements matching 5G-NR capabilities in terms of dependable wireless communications, and identify challenging gaps that will be investigated in this work.
We conclude this chapter with a state-of-art review of the state-of-art simulators/emulators available to apply the methodology described in Chapter 1.

2.1 5G-NR Communication Overview

2.1.1 Introduction to 5G-NR Communications

Basics of 5G-NR

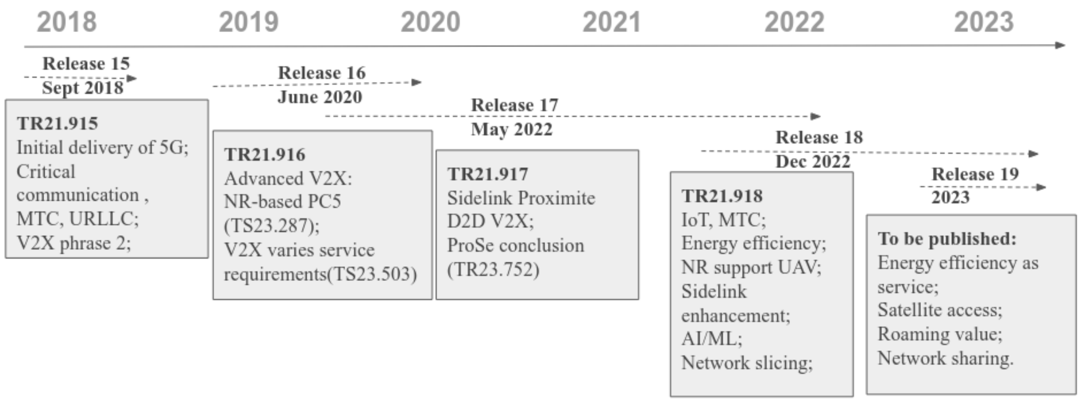

Figure 2.1: 3GPP 5G Releases over the years

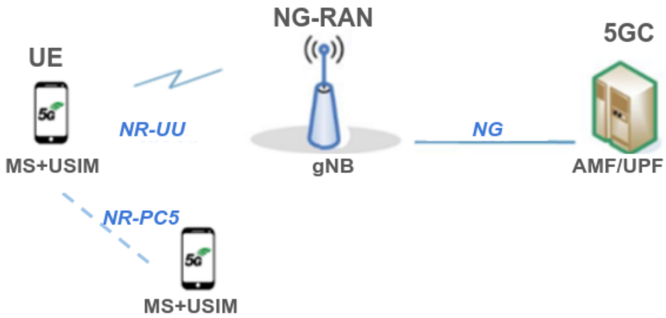

Figure 2.2: 5G-NR Communication Architecture[33]

5G New Radio (NR) was initially introduced by the 3rd Generation Partnership Project (3GPP) in Release 15 [32], featuring a Non-Standalone (NSA) architecture that leverages existing 4G LTE infrastructure. As an iterative development, 5G-NR has evolved through subsequent 3GPP releases, with significant enhancements and milestones documented in Fig. 2.1. This progression incorporates cutting-edge technologies selected from numerous proposals by 3GPP members, setting the global standard for next-generation wireless communication.
The overall architecture of 5G is shown in Fig. 2.2. 5G systematically uses the similar elements as previous 4G LTE: a User Equipment (UE) which itself composed of a mobile station with unique identify, the next generation Radio Access Network (NG-RAN) and the Core Network (5GC). The main entity of the NG-RAN is the gNB, which represents the base station in 5G-NR. The radio interface NR-UU representing the link between UE to gNB, while NR-PC5 representing the direct link, namely "Sidelink" among UEs. The Sidelink communication in 5G-NR, facilitated through the PC5 interface, offers direct D2D connections among UEs, bypassing the gNB and 5GC infrastructure as depicted the figure. This contrasts with UL/DL communications, which rely on transmission through the cellular network infrastructure, involving more complex routing and potentially increased latency.
3GPP definition extends beyond the air interface; it encompasses all the protocols and network interfaces that facilitate comprehensive mobile system functionalities such as call and session control, mobility management, and service provisioning. Thanks to this approach 3GPP networks can operate in an inter-vendor and inter-operator context, this can potentially guiding further development of the 5G-NR system to meet a broader and more complex range of service demands.
To further understand the data flow and control signalling between UE and the network, we illustrate the protocol stack structure in Fig. 2.3. 5G-NR User plane contains the same RAN layers as LTE and has introduced a new layer named as SDAP (Service Data Adaptation Protocol). Meanwhile for the control plane of 5G-NR is identical to LTE, here MME(Mobility Management Entity) equivalent node named as AMF (Access and Management Mobility Function).
The protocol stack in the RAN layers consist of: **Radio Resource Control (RRC)**, which manages control plane signaling between the User Equipment (UE) and the network; **Packet Data Convergence Protocol (PDCP)** provides essential services including header compression, integrity protection, and ciphering of user data to ensure secure and efficient data transfer; **Radio Link Control (RLC)** handling the segmentation and

reassembly of packets to match the size of transport blocks managed by lower layers. It ensures reliable data transmission through error correction via retransmission mechanisms. Then its comes to the key layers which this work will primarily focus on: the Physical (PHY) and Medium Access Control (MAC) respectively.
The **Medium Access Control** layer plays a critical role in the 5G architecture. It serves as the interface to the physical layer, facilitating the mapping of logical to transport channels. It plays a crucial role in managing dynamic scheduling among UEs, which allows for flexible resource allocation across multiple users. This layer is pivotal in prioritizing communication requests and efficiently distributing network resources to ensure optimal performance.
The **physical layer** is deeply integrated with MAC, where adjustments in the PHY can significantly influence overall network performance. Key features of the PHY include modulation schemes, the use of numerologies for flexible subcarrier spacing, and advanced antenna technologies for massive MIMO systems. These features can be tuned to optimize the QoS, especially in scenarios demanding high reliability and low latency, such as URLLC applications.
These layers work together to facilitate efficient, secure communication that supports a variety of mobile and fixed devices across vast and versatile network architectures, crucial for realizing the diverse applications and services envisioned for 5G.

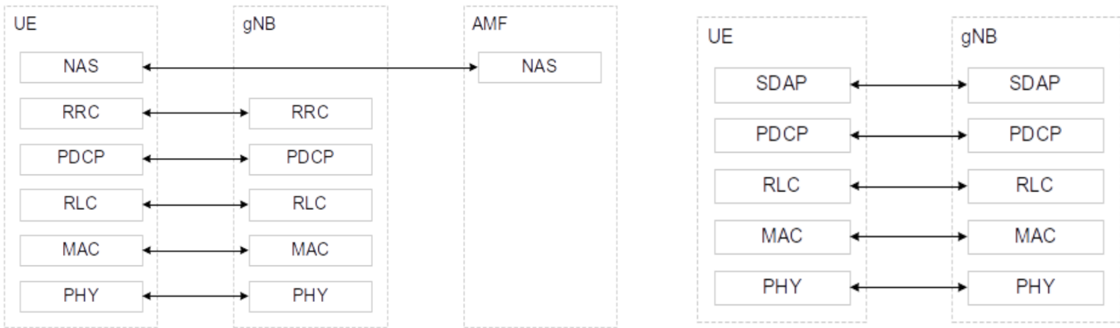

(a) Control Plane Protocol Stack [34] (b) User Plane Protocol Stack [34]

Figure 2.3: 5G System Protocol Stack

Services Catalogues in 5G-NR Communication

5G technology extends its reach to a broader audience and is targeted for deployment across all industry sectors, particularly for time-critical applications. In 5G-NR, to accommodate the diverse demands of industrial and real-world applications, three primary service catalogues are proposed. This segmentation ensures that different services are accurately categorized, allowing for a more focused approach in delivering them via 5G-NR communication. As illustrated in Figure. 2.4, the three main service categories are eMBB, mMTC, and URLLC.Each category is designed to target specific performance characteristics and application scenarios. Additionally, this emphasizes the potential need and role of 5G-NR communication, examining both Uplink/Downlink (UL/DL) and Sidelink (SL).
Enhanced Mobile Broadband (eMBB) caters to delivering high data rates over extensive coverage areas to support applications that require intensive bandwidth, such as

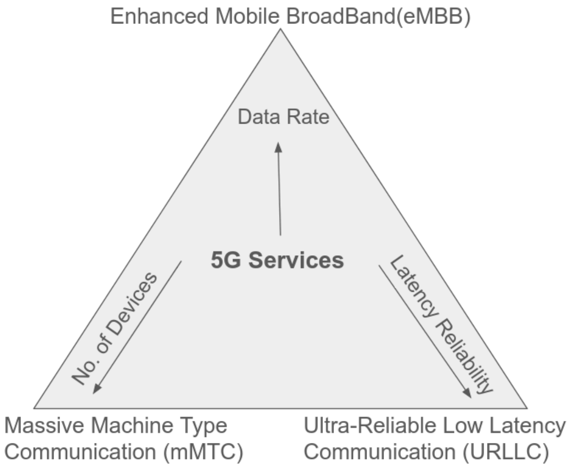

Figure 2.4: 5G-NR Services Catalogues

high-definition video streaming and virtual reality. It is designed to achieve high throughput, with capabilities for peak data rates of up to 20 Gbps. Typically, eMBB relies on Uplink/Downlink communications. However, incorporating Direct D2D Sidelink communications can significantly enhance user experiences in densely populated environments by enabling devices to communicate directly without the intermediary of the core network.

Massive Machine Type Communications (mMTC) is engineered to support the connectivity needs of a large array of devices that transmit low complexity, small, and infrequent data packets. mMTC is typically employed in scenarios that do not require high mobility support, making it ideal for static or low-mobility devices such as sensors and actuators in industrial IoT environments. The integration of Sidelink communications can further enhance mMTC capabilities by allowing direct connections between devices, which could lead to reduced latency, lower power consumption, and increased overall system reliability.

Ultra Reliable Low Latency Communications (URLLC) at the meanwhile, as another key catalogue promises a significant innovation for 5G-NR, especially in pioneering technological domains. Since its initial definition in 3GPP Release 15, URLLC has continuously evolved, as detailed in Table 2.1 across subsequent releases, underscoring its growing importance and implementation. URLLC is designed to cater to applications demanding immediate response times and utmost reliability, where even minor delays or discrepancies could have substantial implications. It aims to deliver sub-millisecond latency and error rates as low as 10^{-5}, specifications that exceed the capabilities of conventional network architectures.

Among the three service categories, URLLC currently stands out as the key point for industrial and real-time applications. It offers significantly improved services compared to previous generations, such as LTE, marking a pivotal breakthrough for 5G-NR in meeting the demands of today's resource-intensive communication needs. This is particularly relevant with the recent surge in AI and other advanced technologies, which require more stringent performance standards. Consequently, this thesis concentrates on URLLC services within 5G-NR, characterizing it as providing a 'dependable network' to the modern communication systems.

This diversity of requirements, associated to the different categories of usage described

above, enables the 5G system (5GS) to be useful to a new set of markets aka. ”verticals”, including: automotive, rail & maritime communications; transport and logistics; discrete automation; electricity distribution; public Safety; health and wellness; smart cities; media and entertainment.
In 3GPP Rel.16 [35], it highlights vertical use cases across various industries that are requiring URLLC, such as : smart cities; e-Health; Rail-bound mass transit etc. These vertical use cases identify specific 5G service requirements, which often demand both low latency and high reliability to ensure efficient and secure operations in these critical sectors. Specifically in industrial sectors, they are increasingly reliant on 5G-NR to facilitate secure and reliable wireless connections for various applications, from 3GPP Rel.17 [36] the standardization has started to focus on applying URLLC in supporting of enhanced industrial IoT. To supplant traditional wired networks, industrial wireless solutions must achieve low latency, high security, and reliability, along with ubiquitous connectivity. These critical requirements underscore the importance of URLLC within the 5GNR framework.
In summary, 5G-NR is characterized by three primary service categories, each tailored to meet specific user needs and application requirements. The development of 5G-NR in both Uplink/Downlink (UL/DL) and Sidelink (SL) adaptation is analyzed, highlighting the distinct advantages of SL in fulfilling these service requests. Furthermore, the focus is drawn to URLLC services, which promise to deliver breakthrough high QoS required by a variety of cutting-edge applications. The necessity of providing a dependable network to support the evolving landscape of application development is critical.

Table 2.1: 3GPP Releases related with URLLC Aspect

Rel No.	Time	No. of Doc	Details
Rel.15 [32]	2019	TS 22.261	The first definition of URLLC among other services catalogues and its requirements are listed.
Rel.16 [37]	2021	TR 21.916	Introduction of retransmission to gurantee high-reliability; QoS Monitoring, Dynamic division of Packet Delay Budge; new DCI formats, Enhanced PDCCH monitoring capability, Sub-slot based HARQ-ACK feedback.
Rel.17[36]	2022	TR 21.917	Physical Layer feedback enhancements for HARQ-ACK and CSI reporting; Intra-UE multiplexing and prioritization of traffic with different priority.

2.1.2 5G-NR Sidelink Communication

This section will begin by detailing the fundamental aspects of 5G D2D design, ranging from the configuration of the physical layer to the diverse Medium Access Control layer scheduling options available for Sidelink. Additionally, various service catalogs in 5G-NR will be explored, and the initial potential of implementing network slicing over Sidelink will be analyzed, laying the groundwork for discussing its impacts on network functionality and service delivery.

Architecture Overview of 5G-NR Sidelink

As highlighted in the previous section, 5G New Radio (NR) supports two modes for V2X communications as described in ETSI report [33]: Uu links and direct PC5 links. This section explores into the technical background of the direct connections among UEs

facilitated through PC5 links. The ETSI TR 137 985 [10] defines PC5 interface on 5G devices includes several key components essential for direct D2D communications:
PC5-S (Signaling Protocol Stack): Used for control plane signaling, it manages tasks like establishing, maintaining, and terminating secure direct links between two UEs.
PC5-C (Control Plane): Once a connection is established, UEs exchange information such as capability levels, configurations, and measurement reports through RRC messages.
PC5-U (User Plane): Handles the transmission of data directly between UEs and supports multiple logical channels, each identified by a Logical Channel ID (LCID) within a specific context of Source Layer-2 ID and ProSe Layer-2 Group ID. This enables efficient data routing and management of direct communications between devices

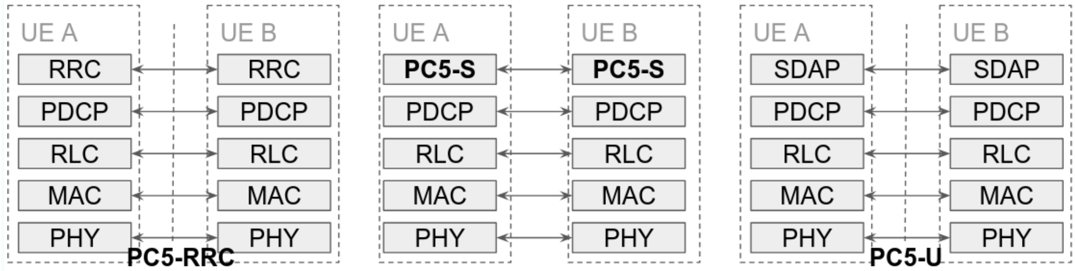

Figure 2.5: 5G-NR PC-5 protocol stacks [10]

Direct D2D communication, also known as Sidelink(SL) or PC5 link in 5G New Radio (NR), enables devices to communicate directly without relying on network infrastructure such as base stations and network servers. In general, wireless devices connected through centralized network cores, with data traffic routing through gNBs to upper infrastructure layers to ensure connectivity, as depicted in Figure. 2.2. However, with the implementation of D2D PC5 communication, devices can establish direct connections among themselves, bypassing these central components. This direct connectivity is crucial for scenarios that demand immediate, low-latency communication. In detail, the advantages that Sidelink communication brings to the current 5G-NR system are as follows:
Improved Latency and Reliability: The primary benefits of D2D communication include reduced latency and enhanced reliability, which are crucial for establishing dependable networks by minimizing the distance data travels. Sidelink facilitates efficient local broadcasting, ideal for scenarios such as mass event broadcasts or quick information dissemination among nearby devices without burdening the entire network. According to the Release 17 work item meeting [38], enhancements in 5G-NR's Sidelink are aimed at supporting URLLC-type use cases across broader scenarios by improving reliability and reducing latency. Challenges remain in achieving these goals under certain conditions, such as busy channels, where system-level performance can be compromised. Thus, developing solutions to enhance reliability and reduce latency is essential to maintain high performance in demanding communication environments.
Enhanced Network Efficiency:D2D communication significantly enhances efficiency, particularly in terms of energy and resource utilization. The Release 17 work item [38] highlights that in 5G Sidelink networks, devices with battery constraints can operate in a power-efficient manner through sidelink communication. Supporting this, a survey by Waqas et al. [39] underscores the potential for energy savings with D2D communication. This study reviews various efforts that employ dynamic scheduling and routing path opti-

mization to demonstrate how D2D can achieve superior energy and bandwidth efficiency compared to conventional uplink/downlink (UL/DL) approaches.

Increased System Capacity: D2D communication notably enhances spatial resource utilization, substantially increasing overall network capacity. Research by Waqas et al. [39] also outlines mechanisms to improve D2D communication. These include using advanced dynamic graph theory for adaptive management of time-varying communication opportunities and implementing relay-aided multi-hop techniques to support connectivity for devices with poor direct links. These strategies significantly enhance spectrum and energy efficiency within D2D frameworks.

Enhanced Security and Privacy: In 3GPP Release 18 [40], security protocols specific to Sidelink Communication for the 5G-NR network are detailed. These protocols ensure security during UE discovery and authentication processes, particularly for SL ranging and positioning service requests. Additionally, these procedures are managed through ProSe (Proximity Services) standardization, which operates based on service announcement-based requests.

Combining in Section. 2.1.1 the direct Sidelink communications can play a critical role in the demanding requirements on realizing URLLC over 5G-NR.By using Sidelink, URLLC can facilitate direct paths between devices, bypassing network infrastructure to minimize delays and increase reliability.

The advantages of Sidelink are particularly prominent in the context of autonomous vehicular communications (V2X), a key industrial focus for future technology development. Innovations such as federated learning and AI are increasingly integrated into V2X environments, necessitating low-latency vehicle-to-vehicle (V2V) and vehicle-to-infrastructure (V2I) communications. These communications are crucial to support cutting-edge technologies, and a more detailed examination of current research developments will be presented in Section 2.1.2.

To maintain clarity and coherence in this thesis, the focus is specifically on V2V communication applications of D2D interactions, recognizing their critical role in advancing intelligent transportation systems. V2V communication is essential for its high reliability and rapid data exchange, which directly impact road safety and traffic efficiency. The integration of D2D communication in V2X scenarios offers substantial benefits, enhancing real-time responsiveness necessary for dynamic vehicular environments.

Garcia et al. [41] have provided a comprehensive study on 5G-NR Sidelink communication, highlighting that most V2X services and applications for intelligent vehicles are predicated on a broadcast communication paradigm, which incorporates *ad hoc* resource allocations to meet both research and industrial demands. Building on this insight, this thesis further explores the implications and efficiencies of broadcasting within V2X communication scenarios. We specifically examine how Sidelink enhances these applications by enabling more effective and reliable broadcast communications, critical for advancing intelligent transportation systems and supporting real-time vehicular network interactions.

5G-NR V2X Specification Overview

5G-NR direct Sidelink (SL) communication, originally defined in 3GPP since LTE Release 12 for Proximity Services (ProSe), Sidelink communication has evolved significantly to meet the advanced requirements of these days technologies.

The evolution of Sidelink Communication in 3GPP Standards starts from LTE Release 12, which Sidelink was first introduced to support Proximity Services (ProSe). The later releases related to 5G-NR Sidelink communication are listed in Table. 2.2, particular in focus on Vehicle-to-Everything (V2X) communication. In 5G-NR Release 16 [10], Sidelink was specified for 5G-NR to support Vehicle-to-Everything (V2X) communication, this included initial enhancements to support basic V2X scenarios with improved latency and reliability. In Release 17 [36], further improvements were made to sidelink communication, focusing on expanding coverage areas and enhancing the reliability of V2X communication. And in recent release 18 [13], it continued to build on the previous enhancements by introducing features aimed at further reducing latency, improving power efficiency, and supporting more complex V2X and ProSe scenarios. These enhancements included better resource allocation mechanisms, advanced interference management, and more robust error correction techniques.

Table 2.2: 3GPP Releases related with 5G-NR Sidelink V2X Aspect

Rel No.	**Time**	**No. of Doc**	**Details**
Rel-16 [10]	2021.6	TR 137 985	5G V2X on NR Sidelink : 1)Physical Channel : SL channel description and signals definition; 2) Resource allocation : mode 1&2; 3)HARQ feedback, CSI, PC5-RRC definition; 4) Sidelink congestion control; 5) V2X SL high layer protocols.
Rel-17 [36]	2022.07	TS 123 304	Proximity Services on NR Sidelink: high level functions and features; detailed procedures and messages definition for ProSe standards, such as direct-link discovery, link-establishment etc.
Rel-18 [13]	2024.08	TR 21.918	5G-NR SL enhancements for eV2X: improved NR positioning; NR SL relaying; Relaying enhancements for ProSe 5GS protocols; enabling ProSe path switching between PC5 and Uu.

Regarding the physical layer layout and protocol definition in 5G-NR SL V2X, as specified in 3GPP Release 16 [10], the physical resources are inherited directly from 5G-NR and span both time and frequency domains. Within the frequency domain, the available bandwidth is segmented into 15kHz Physical Resource Blocks (PRB), facilitating efficient spectrum utilization. In the time domain, the network operates on a frame structure where a 10 ms frame is systematically divided into 10 sub-frames. These sub-frames are further subdivided into numerous mini-slots based on the numerology setting, enhancing the granularity and flexibility of data transmission scheduling.

Unlike the LTE system, which utilizes fixed sub-carrier spacing, 5G-NR introduces a highly flexible frame configuration. This flexibility is primarily enabled through the implementation of variable transmission time intervals (TTI), synonymous with the *mini-slots.* durations. These TTIs can be significantly reduced—from the standard 1 ms in numerology-0, which is typical in LTE, down to as short as 0.125 ms in numerology-3. This reduction in TTI not only allows for quicker data transmission but also supports the ultra-reliable and low-latency communication requirements crucial for advanced V2X applications.

The variation in the number of slots available per sub-frame according to the chosen numerology is illustrated in Fig. 2.6, highlighting the adaptability of the 5G-NR SL to efficiently manage both time-sensitive and data-intensive applications. This level of resource management and allocation flexibility is what sets 5G-NR apart in the realm of

next-generation wireless communication technologies, particularly in enhancing the capabilities of vehicle-to-everything communications.
The methodology of resource allocation has always been a cornerstone in enhancing the performance of wireless communications, particularly in direct D2D scenarios. Yu et al. [42] investigate into this by analyzing orthogonal and non-orthogonal resource-sharing modes,their study primarily focuses on optimizing the sum rate through strategic power control and resource allocation, taking into account constraints on spectral efficiency and maximum power or energy limitations.
In the realm of 5G-NR, the MAC layer scheduler emerges as a pivotal element in resource sharing, influencing the overall system performance significantly. Various studies, including those works in [43] and [44],have explored different scheduling modes within 5G-NR, assessing their effectiveness across diverse scenarios. These investigations underscore the scheduler's critical role in managing the complex dynamics of resource allocation to meet the varying demands of network traffic. We therefore in the following part target to thoroughly examine the current standardization efforts concerning MAC scheduling, with a particular focus on its application in Sidelink communication.

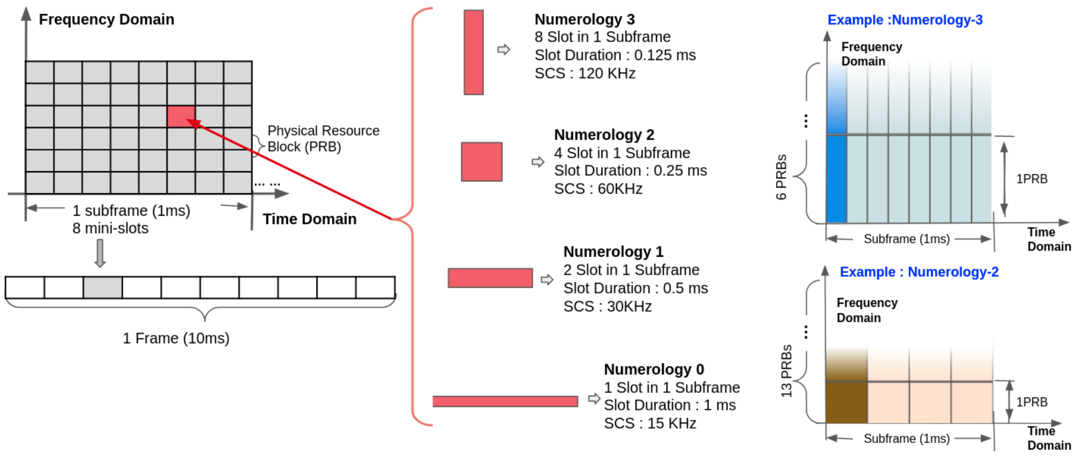

Figure 2.6: 5G-NR Sidelink Physical Structure

Regarding to MAC layer schedulers, Release 16 [10] introduces two modes (modes 1 and 2) for sub-channel selection in NR V2X Sidelink communications via the NR V2X PC5 interface. These modes correspond to LTE V2X modes 3 and 4. Unlike LTE V2X, which is limited to broadcast Sidelink communications, NR V2X expands its capabilities to include not only broadcast but also groupcast and unicast communications. Nonetheless, for simplicity and clarity in this study, our focus will predominantly be on V2X broadcast scenarios.
Mode 1 : Mode 1 in 5G-NR V2X Sidelink operates similarly to Mode 3 in LTE V2X, where the gNB centrally manages the Sidelink radio resources for vehicle-to-vehicle (V2V) communications via the NR Uu interface. In this mode, dynamic grant scheduling is employed: UEs initiate a scheduling request for each Transport Block (TB). In response, the gNB issues Downlink Control Information (DCI) that specifies the precise resources—slot and subchannel information—for transmitting a TB and allows for up to two potential re-transmissions of that TB. Additionally, UEs are required to inform neighboring UEs of their resource usage to mitigate potential collisions with transmissions scheduled under

Mode 2.

This reliance on gNB coverage can pose challenges in V2X scenarios characterized by high mobility, where seamless connectivity and low latency are critical. The uplink/downlink (UP/DL) grant mechanism inherent in Mode 1 can also introduce additional latency. Consequently, to enhance reliability and reduce delays in dynamic V2X environments, Mode 2, which operates directly over the PC5 interface and does not depend on gNB coverage, presents a more adaptable and dependable approach.

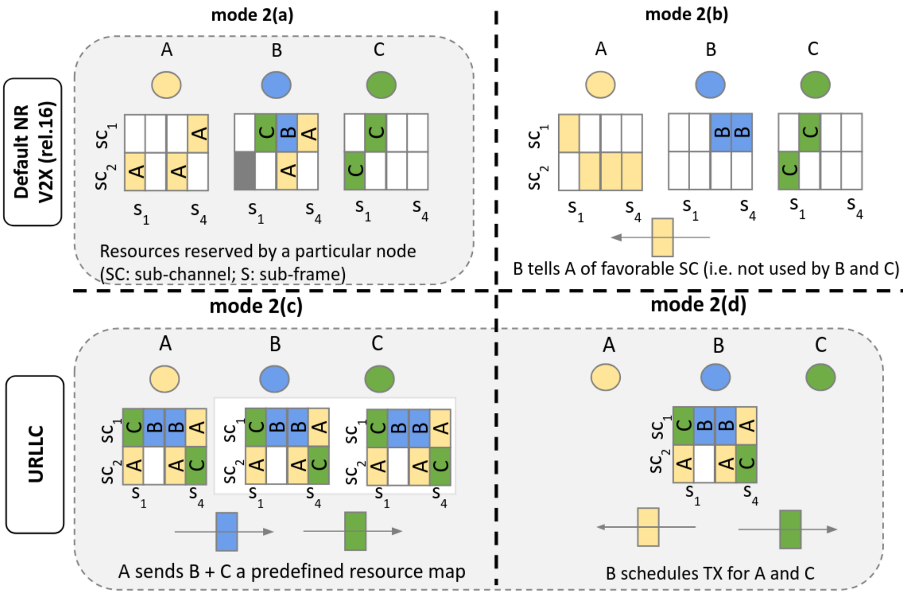

Figure 2.7: 5G-NR Mode 2 schedulers

Mode 2 :

While mode 1 relies on network infrastructure for scheduling, mode 2 operates in an ad-hoc manner, making it suitable for scenarios where infrastructure support is limited or unavailable. Mode 2 is further enhanced with four sub-modes, each offering different mechanisms for resource allocation(as depicted in Fig. 2.7):

Mode 2(a) - Autonomous Resource Selection:

In this sub-mode, each vehicle selects its resources autonomously using a semi-persistent sensing-based scheduling approach. Vehicles periodically sense the radio environment to identify and select available resources for their transmissions. This decentralized method allows for flexible and dynamic resource allocation without relying on central coordination. However, it does not provide any delay bound, making it less suitable for applications requiring strict latency guarantees.

Mode 2(b) - Cooperative Distributed Scheduling:

This sub-mode involves a cooperative approach where User Equipment (UEs) assist each other in resource selection. Vehicles share their resource selection windows with neighboring vehicles, helping to mitigate near-far effects and improve overall reliability. Although this method enhances reliability through cooperation, it still lacks a defined delay bound, which limits its applicability for URLLC scenarios.

Mode 2(c) - Resource Assignment by a Vehicle:

In this sub-mode, a specific vehicle is responsible for assigning resources to other vehicles based on pre-defined transmission patterns. This centralized control within the ad-hoc environment enables more deterministic scheduling, as the vehicle managing the resources can ensure that allocated time slots and frequencies avoid conflicts and meet transmission requirements. This mode is particularly useful for applications needing predictable performance and latency, such as URLLC.

Mode 2(d) - Scheduling by a Vehicle for Neighbors:

Similar to mode 2(c), this sub-mode involves a vehicle scheduling sidelink transmissions for its neighboring vehicles. However, the focus here is on dynamic adaptation to current network conditions and real-time requirements. The scheduling vehicle monitors the transmission needs of its neighbors and allocates resources accordingly. This mode offers a high degree of control and can provide deterministic scheduling, making it a prime candidate for high stringent request applications due to its ability to guarantee low latency and high reliability.

The resource allocation methodology in 5G-NR Sidelink (SL) is depicted in Fig. 2.8, illustrating the procedures on the physical layer for selecting resources during transmissions. For modes 2(a) and 2(b), which utilize a sensing-based resource selection procedure, the UE first undergoes a *sensing window*. This is a specific duration where the UE listens to the channel to gather information about its current state. Based on this data, the UE then decides on the appropriate resources during what is known as the *resource selection window*. This window is constrained within a predefined interval, allowing for dynamic adaptation based on real-time channel conditions.

Conversely, modes 2(c) and 2(d) employ a strategy where resource allocation patterns are predetermined and assigned to UEs at the outset. These modes do not require a *sensing window*, enabling immediate resource selection within the *selection window*. This streamlined approach is particularly advantageous for achieving lower latency, which is crucial for dependable network communication over direct PC5 links, catering efficiently to scenarios demanding urgent data transmission with minimal delay.

Figure 2.8: 5G-NR Mode 2 schedulers

Meanwhile, enabling 5G-NR direct Sidelink communication in supporting the primary service catalogs for eMBB, URLLC, and mMTC not only a natural evolution of the standard network architectures but also enhances them. For instance, URLLC and specific mMTC scenarios could benefit from a direct communication over the PC5 interface between two users. By leveraging these advanced communication techniques and aligning them with the varied service requirements, 5G-NR SL emerges as a robust and flexible network. However, the specific 5G-NR SL applications across different services, particularly how SL features can address the rigorous requirements of URLLC, remain widely under-investigated yet the subject of this work.

Related Works for 5G-NR Sidelink

This section reviews relevant studies that contribute to our understanding of 5G-NR Sidelink communication, focusing particularly on the adaptation of communication parameters to improve vehicular communication systems.

For C-V2X, Sidelink communication, initially explored in 4G-LTE by Molina-Masegosa et al. [45], focused on Mode 4 scheduling parameters across various channel loads and traffic scenarios. They proposed using an exponential sensing window to enhance overall performance.

Campolo et al. [44] has investigated the focus on the sidelink resource scheduling methodologies, specifically comparing Sensing Based Semi-Persistent Scheduling (SB-SPS) and pre-allocated pattern mechanisms. The findings suggest that SB-SPS scheduling tends to outperform dynamic scheduling in highly dense traffic scenarios. However, this advantage diminishes as traffic intensity returns to normal levels. Both scheduling approaches demonstrate comparable performance in aperiodic traffic patterns, with dynamic scheduling showing a potential for greater benefits from retransmission compared to SB-SPS.

Campolo et al. [46] has also explored the impact of flexible numerology in New Radio (NR), focusing on how the scalable Transmission Time Interval (TTI) durations and sub-carrier spacing (SCS) influence Cellular-Vehicle to Everything (C-V2X) autonomous access mode 4. This study reveals how TTI and SCS adjustments can optimize resource allocation, enhancing V2X communications' efficiency and reliability.

Complementing this, the work by Hamidreza Bagheri et al. [47] investigates into key features of 5G-NR V2X, emphasizing cooperative and autonomous driving's requirements. It highlights the essential use cases enabled by 5G-NR, such as how its advanced capabilities support the complex needs of modern vehicular communications.

Muhammad et al. [48] provide an in-depth investigation of 5G-NR's structural advancements, specifically for vehicle-to-vehicle (V2V) applications. Their research underscores the enhancements 5G-NR brings to V2V communication, including improved security measures over the PC5 V2V communication link.

In terms of service catalogues, particularly URLLC, V2X services under URLLC exhibit stringent requirements for reliability and low latency. Current 3GPP Release 16 specifies 5G-NR V2X SL mode 2 designed to accommodate any Vehicle User Equipment (VUE), but performance degradation is noted with an increase in VUE numbers, indicating a need for robust admission control to maintain URLLC's QoS [41].

Shashika et al.[49] and Ginige et al.[50] discuss optimization strategies for admission control, emphasizing the necessity to manage user admissions effectively to maintain the balance between enhanced Mobile Broadband (eMBB) and URLLC requirements in 5G-NR. This balancing act is crucial for scheduling resources effectively across different user demands in V2X communication.

2.2 5G Network Slicing

2.2.1 Background on 5G Network Slicing

Network slicing enabling the creation and management of customized networks to meet specific service requirements demanded by future applications, services, and business verticals. The network slicing process begins with the Network Slice Selection Assistance Information (NSSAI), which categorizes the network functions into specific slices such as eMBB, URLLC, or MTC based on the service type. This initial step is crucial as it aligns with 5G standardization efforts that define distinct slices and their Service Level Agreements (SLAs), the SLAs cover various metrics such as bandwidth, latency, reliability, availability, and others.

Once the NSSAI is defined and SLAs are set, the network can instantiate the appropriate slices. As shown in Figure. 2.9, the slicing involves segmentation and configuring network resources and functions across the Core Network (CN) and Radio Access Network (RAN) to meet the specified SLAs. In particular RAN must adhere to slicing principles, including fulfilling QoS requirements and ensuring resource isolation. This integration ensures that each user equipment (UE) has a dedicated Packet Data Unit (PDU) session for each slice, effectively mapping these sessions to radio bearers through the Service Data Adaptation Protocol (SDAP) layer. This structured approach enables the RAN to support the diverse and dynamic needs of modern digital ecosystems efficiently.

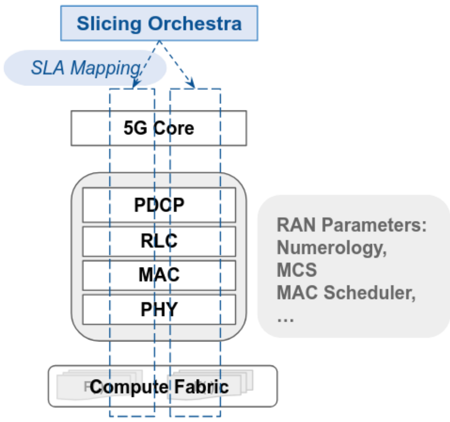

Figure 2.9: Network Slicing Concept

Network Slice Related Standardization

The evolution of 3GPP standardization concerning network slicing over the years is outlined in Table 4.2, the contents of this table are based on a technical report from 3GPP [51]. In details, Release 15 introduced the foundational concepts of network slicing in the 5G system (5GS), enabling the creation of multiple virtual networks over a shared infrastructure, each tailored to specific service requirements. This release defined NSSAI and mechanisms for slice selection. Release 16 enhanced inter-working between 4G and 5G core networks, introducing slice-specific authentication and authorization for secure access. Release 17 advanced network slicing by enabling the Radio Access Network (RAN)

Table 2.3: 3GPP Releases related with Network Slicing Aspect [51]

Rel No.	No. of Doc	Details
Rel.15	TS 28.530	Basic network slice life-cycle management features are supported; introduction of network slice related concepts, provisioning management, performance monitoring.
Rel.16	TS 28.541; TS 28.535; TR 28.836	Service Level Agreement (SLA) attributes and the concept of closed loop automation are introduced.
Rel.17	TS 28.557; TS 28.554	Management of non-public networks; multiple SLA requirements supported; network slicing related Energy Efficiency (EE) KPIs and SLA enhancement is also included.
Rel.18	TR 28.829; TR 28.824	Discussion on improving efficiency for asynchronous operations; support energy utilities service providers; intent-driven network slicing management is initiated.

to broadcast slice information, supporting slice-specific random access and service continuity, ensuring consistent user experiences and paving the way for dynamic slice management and optimization. The recent Release 18 emphasizes enhancing slicing capabilities to meet the KPIs required by emerging V2X applications, also this version include the ability to create customized network slices with specific QoS parameters and traffic routing policies, this aspect can be applied to improve the performance and reliability of URLLC application. For more detailed information regarding each development aspect, a recent 3GPP report [51] provides in-depth explanations and lists the specific standardization releases. Please refer to the report for further details.

Network Slice Key Elements and Definition

A network slice encompasses the entire pathway from an end device to an application, incorporating all the necessary network functions and domains along the way, including both the Radio Access Network (RAN) and Core Network segments. Consequently, we examine these two critical aspects to gain deeper insights into the current developments in network slicing.

The first key domain is **Core network slicing**, as the anchor for 5G network slices. This domain 5G involves creating multiple virtual networks over a common physical infrastructure, each customized to meet specific service requirements. The key components in realizing core network slicing include Network Slice Selection Assistance Information (NSSAI), which helps in identifying and selecting the appropriate network slice for each service, ensuring that the service requirements are met; Network Functions Virtualization (NFV) by virtualizing network functions, core slicing enables the creation of customized network slices with specific functionalities and performance characteristics; and also Software-Defined Networking (SDN) which provides a centralized control plane that can dynamically manage and optimize the network resources allocated to each slice.

Then comes to the second key domain as **RAN Slicing**. Nokia [52] has pointed out RAN performance is usually the gating factor for user experience in terms of throughput, latency and reliability. Therefore, RAN network slicing is a critical part of end-to-end network slices. Slice-specific resource allocation, scheduling, and admission control enable differentiated traffic handling and isolation. Meanwhile, a key architecture as Open RAN (O-RAN) offers a tailored approach to designing and implementing the RAN for various network slices, aligned with the 3GPP's architectural framework. A central element in this framework is the RAN Intelligent Controller (RIC), which facilitates real-time analytics, control, and optimization of the RAN. The RIC supports applications that range from non-real-time to near-real-time operations. According to the O-RAN specifications [53], the implementation of network slicing allows operators to manage spectrum resource allocation more efficiently and dynamically. This adaptability optimizes spectrum use, adjusting to fluctuating usage patterns and enhancing overall network performance.

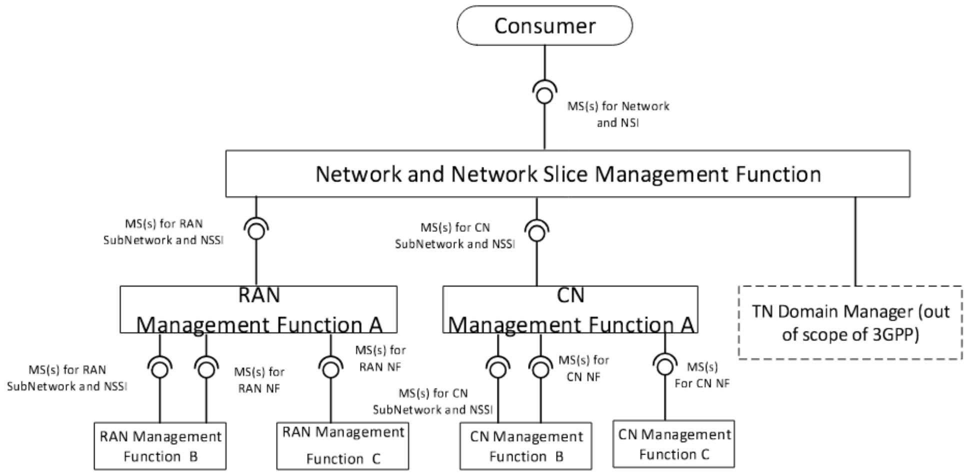

Figure 2.10: Network Slicing Example [54]

Fig. 2.10 illustrate an example from ETSI TS 128 533 [54] for network slicing from the management service(MS) point of view. In this deployment scenario, the Network and Network Slice Management Function provides management for network slices, covering the RAN, CN, and Transport Network(TN) segments. The RAN Management Function is divided into several components that handle RAN SubNetworks or Network Slice Subnet Instances (NSSIs) and RAN Network Functions (NFs), with each component potentially consuming services from the others. Similar architecture applied for the CN Management Function management, coordinating to provide and consume services as needed to enable comprehensive slice management across RAN and Core networks.

A recent Qualcomm document [26] outlined key elements essential for configuring a slice: Firstly, the **service type identifier** helps to initially mapping the slice to specific service requirements. Similarly, **QoS parameters**, often represented by QCI (QoS Class Identifier) values, further refine the definition by linking the slice to the required QoS level. This ensures that the service demands are met with the appropriate performance standards.

Additionally, **resources**, referring to the physical layer resource blocks, defines the dedicated or protected resources for each slice. Specifically, detailed physical parameters such as the applied **MCS (Modulation and Coding Scheme)** value, **numerology**, and other relevant settings should be clearly defined to ensure that all users within the slice are synchronized. This guarantees that each slice receives exclusive resources, enhancing reliability and preventing interference between slices.

Moreover, the **MAC layer scheduler** must also be specified within the slice. Given the variety of MAC schedulers available for 5G-NR communication, it is essential to have a clear understanding of the scheduler applied within the current slice, particularly for

new users. This ensures seamless access and communication, safeguarding the future performance and reliability of the slice.
This slice description will be used and extended in the following work to defined 5G-NR Sidelink Slicing on the PC5 interface.

2.2.2 5G-NR Sidelink Network Slicing

In the context of supporting direct sidelink network slicing, since the communication bypasses the core network and occurs directly between devices (UE to UE), the network slicing design would largely focus on allocating and managing the RAN resources efficiently. The RAN network slicing faces significant challenges when adapted to decentralized scenarios such as ad-hoc networks, which are common in V2X communications. The core issue lies in its reliance on centralized controllers to manage network resources, which contrasts with the needs for dynamic, decentralized control in V2X environments. Additionally, O-RAN [53] struggles with effective group management, essential for creating dependable networks aimed at a limited user base. Therefore, developing a method for applying network slicing more directly through decentralized management becomes crucial for achieving dependable 5G-NR communication. The design of Sidelink-based network slicing should therefore focus on the following key aspects:
Configuration Realization Over Sidelink: As highlighted in previous section, establishing network slicing begins with a consistent configuration that can be systematically referenced across various management layers. It is crucial to develop a correct methodology that enables effective management of network slicing configurations and related procedures, ensuring comprehensibility from the application layer down to the physical layer.
Service Translation into Slices: To uniformly translate services into slices among different UEs, the slice design must be meticulously designed. Key elements such as the service type identifier, numerology, MCS, and resource allocation need to be carefully considered and implemented to ensure effective service delivery.
Admission Control: It is important to consider the different acceptance rates within various slices, tailored to the specific needs of different services. Developing appropriate communication protocols to manage admission control is essential to maintaining the integrity and efficiency of each slice.
Optimizing network slicing for D2D scenarios within V2X applications involves configuring slices that can dynamically allocate resources based on real-time demands and traffic conditions. This could mean prioritizing bandwidth and reducing latency for slices handling emergency vehicle communications during peak traffic times, while other less critical slices, such as those handling infotainment transmissions, might be allocated less bandwidth. This dynamic allocation not only enhances the efficiency of network resource usage but also ensures that critical communications can maintain a high level of performance without interruption.
Furthermore, by implementing advanced management and orchestration capabilities, network operators can automate the process of slice life-cycle management. This includes the creation, scaling, and termination of slices according to the changing needs of the network and its users. Such flexibility is pivotal in D2D communications where the network conditions and user requirements can vary significantly and frequently.

In [26], Qualcomm provides some preliminary insights into designing network slicing over sidelink communication. This patent report has pointed out several advantages that can be brought by direct sidelink slicing, such as the slicing sidelink channel resources can enhance resource utilization and spectral efficiency. This approach allows for dynamic reallocation of resources based on service usage within specific areas, improving network performance. For instance, resources not needed for inactive services can be redirected to active ones, ensuring that specific communication requirements are met efficiently and performance for critical services is optimized.
Also for sidelink resource slicing on a 5G-NR interface involves both static and dynamic allocation methods to optimize resource usage for different service types. Static slicing assigns resource slices based on predefined requirements of various services, enhancing performance through efficient resource distribution. Dynamic slicing adjusts resource slices in real time, responding to fluctuating service demands within different areas or among devices using D2D communications. This flexibility in resource management significantly boosts network efficiency and adapts seamlessly to changing conditions.
Sidelink PC5 slicing stands out as a promising solution for future D2D communications, offering reliable and secure networking tailored for a variety of applications. Despite its potential, there is a noticeable lack of extensive research or established standards in this area. However, to the best of our knowledge, no comprehensive research analysis has yet been conducted in this field. This gap underscores the significant potential for development in sidelink slicing, positioning it as an approach that could lead to innovative enhancements in the performance of 5G-NR D2D communication.

2.2.3 Related Works for 5G-NR Network Slicing

Work from Li et al. [55] has pointed out the Internet of Things (IoT) encompasses a diverse array of devices ranging from electronic devices and mobile devices to industrial equipment. Each entity within the IoT ecosystem possesses distinct capabilities in terms of communication, networking, data processing, storage, and transmission power. This diversity breeds heterogeneous networks where each component may have unique QoS requirements, including performance, energy efficiency, and security.
Given these varied demands, network slicing emerges as a vital strategy to meet the specific needs of different IoT applications effectively. Implementing direct sidelink slicing within 5G networks further enhances this approach by facilitating tailored service provisions directly between devices, bypassing typical network paths. This direct method not only streamlines communication but also optimizes resource usage and security, making it indispensable for the robust and efficient functioning of IoT networks.
Most existing research on network slicing primarily focuses on the core network. A recent contribution by Ciprian et al. [27] centers on network slicing specifically for V2X communication in 5G-NR, where they propose a framework designed for a dedicated V2X slice that accommodates the coexistence of other traffic types. Additionally, they have developed a suite of algorithms for base stations and UEs, featuring flexible parameter settings and implemented in Python.
Previous work by Lekidis et al.[25] suggested a framework for platoon network slicing that combines V2V and V2I control, facilitated by higher-level Roadside Unit (RSU) assistance. However, the specifics of URLLC slice design and slice segmentation remain unclear. Chang et al.[56] explored dynamic resource reservation for CACC platooning and

emergency situations, but offered limited insight into the physical layer implementation of network slicing.
Ge's study [21] highlights the limited research on applying URLLC services to V2X communication and proposes a comprehensive network slicing approach that encompasses resource, service, and function slicing, implemented via Road-Side Units.
Hamza et al. [24] demonstrates that configuring network slices for autonomous driving and infotainment services significantly enhances performance and throughput compared to direct Road-Side Unit (RSU) communication, with further improvements observed when combining network slicing with relaying, despite increased interference challenges.
The aforementioned related works show that the majority of the current networking slicing assisting V2X stringent requests study are mainly executed through the UL/DL configuration. Regarding to a more purified sidelink management and configuration for network slicing, except the aforementioned patent from Qualcomm [26],

2.3 V2X Standardization Protocols and Architectures

To develop a suitable architecture for 5G-NR Sidelink that supports multiple applications in V2X communication, it is essential to thoroughly analyze current developments in V2X protocols. As V2X communication is pivotal in Intelligent Transport Systems (ITS), enabling dynamic interactions between vehicles and their environment to enhance road safety and traffic efficiency. This section, focusing on ITS spectrum design and standardization protocols, build on the foundations of V2X protocols and architectures, exploring how they are implemented within the broader ITS framework to support advanced transportation technologies

2.3.1 ITS Spectrum for 5G-NR Sidelink Communication

ETSI TR 103 853 [18] specifies dedicated frequency bands for Intelligent Transport Systems (ITS) in Europe to enhance road safety and traffic efficiency. It allocates the 5,875 MHz to 5,935 MHz band for safety-related ITS applications, supporting the EU eSafety initiative, which aims to reduce road fatalities and improve traffic management through Intelligent Vehicle Safety Systems. This allocation ensures that road ITS applications are prioritized below 5,915 MHz, with Urban Rail ITS applications sharing this frequency, as depicted in Figure. 2.13, to protect prioritized services.
For NR-V2X sidelink communication, based on the technical specifications of 3GPP, is supporting channel bandwidths of 10 MHz, 20 MHz, 30 MHz, and 40 MHz, in band n47(equivalent to the 5,9 GHz ITS band). ETSI TR 103 853 [18] also reflects concerns from ETSI Members about expanding even the current 10 MHz bandwidth. This expansion could lead to inefficient use of this exclusive channel and potential interference with other services, as illustrated in Figure. 2.13, challenging the coexistence of multiple applications within the same spectrum.
Consequently, optimizing the limited bandwidth allocated for ITS applications is crucial. The system must support a variety of ITS services, each with unique requirements, within a framework of protected resources. Given the limited researches on direct 5G sidelink communication, developing a fully functional architecture that meets these needs purely via the PC5 link represents a novel and demanding challenge. Addressing these dual

objectives requires a sophisticated architectural approach. This chapter establishes the foundation for such a proposal, investigating deeply into its development in subsequent sections, and highlighting our commitment to tackling this complex issue.

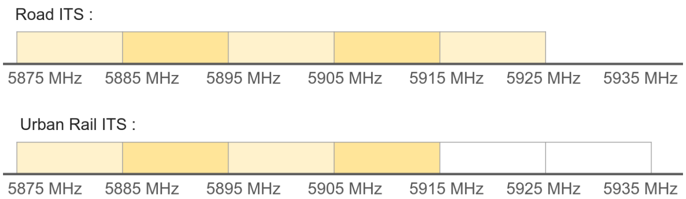

Figure 2.11: ETSI C-ITS Spectrum Allocation [57]

2.3.2 ETSI C-ITS Architecture

The ETSI proposed C-ITS architecture is shown in Figure. 2.12. This figure illustrates the ETSI ITS protocol stack. As shown, the stack follows the traditional OSI layered approach, the ETSI ITS stack contains Access, Network and Transport, Facilities, and Application layers.

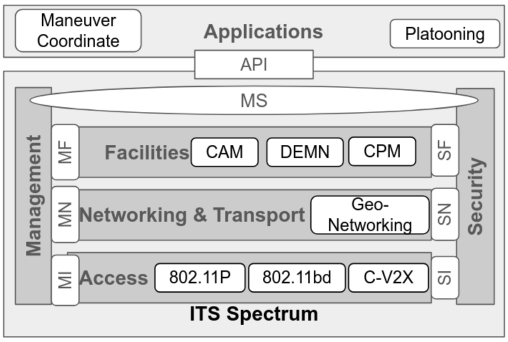

Figure 2.12: ETSI C-ITS Architecture with 5G-NR Communication

From the top down, the stack begins with the Application Layer, hosting diverse applications ranging from safety to infotainment, all of which depend on the data managed by the layers below. The Facilities Layer orchestrates services that these applications utilize, such as cooperative awareness, and other safety related services. The following Network and Transport Layers are responsible for the efficient and reliable routing of data across the network, ensuring seamless connectivity. At the foundational level, the Access Layer ensures robust wireless communication among vehicles, aligning with the 5G-NR standards specified for Radio Access Network (RAN) functionalities. This layer, as detailed in the referenced RAN architecture as introduced in previous section. 2.1.1, includes critical communication components such as the MAC and PHY layers, which are pivotal for the direct transmission and reception of data in vehicular environments.
In this study, we adopt a 5G-NR based methodology for the RAN within the ETSI ITS protocol stack. This framework is instrumental in managing the diverse requirements of various V2X applications by integrating them into a cohesive, functional stack.
The 5G-NR technology, as documented in various studies [58], significantly enhances capacity and efficiency, particularly when integrated into the access layer. This integration

is crucial in supporting the spectrum of V2X communications, ranging from safety-critical messaging to high-bandwidth applications. By optimizing resource allocation, 5G-NR ensures that all applications function within a robust and adaptive communication environment, keeping pace with the latest standards and technological advances. This makes it an essential component for meeting the diverse demands of V2X communication.

2.3.3 ETSI V2X Message Services

Regarding to the communication messages, for Cooperative Intelligent Transport System (C-ITS), ETSI in charge of V2X communication standards has completed a full set of specification for applications.

Day-1 Phase

In this initial phase, applications exchange vehicle state information (such as position and speed) and share alerts about dangerous situations. These applications mainly focus on providing driver information and warnings. The following listed the main messages destination from the ETSI standardization for basics applications for vehicular communications. Additionally, these functions are specifically managed by the Facilities Layer within the ETSI C-ITS architecture, as depicted in Fig. 2.12. This layer ensures that messages are properly structured, interpreted, and relayed, supporting the applications that depend on them. These service messages include, but are not limited to:
Cooperative Awareness Message (CAM) The CAM message, which is equivalent to the Basic Safety Messages (BSMs) in American standards, is in charge of the information exchange for cooperative awareness(CA) in the periodically transmission manner, and this basic service is mandatory for all on-board vehicles ETSI [14]. The CAM contains information about the current position, velocity and expected trajectory of the ego vehicle. As depicted in Figure 2.5, a Cooperative Awareness Message (CAM) is structured into several containers. According to ETSI TS 102 894-2 [2], the ITS PDU header and the data presentation rules in Annex B dictate the format. Every CAM must include the High Frequency (HF) containers, which carry dynamic data such as heading, speed, and basic sensor information. The Basic Container is always present and provides fundamental information such as the type of the originating ITS station and its most recent position. The Low Frequency (LF) container, which is optional, contains data that changes less frequently. For vehicles with special roles like emergency vehicles or roadworks, a Vehicle Container provides specific vehicle data. CAMs, typically broadcasted by mobile nodes at a frequency of 1 to 10 Hz, are triggered by changes in dynamics like speed, direction, or position.
For ITS UEs, CAMs are transmitted between 1 and 10 Hz, triggered by significant changes in dynamics such as speed, direction, or position. A CAM is initiated if the vehicle's heading changes by more than 4 degrees, the position shifts by over 4 meters, the speed alters by more than 0.5 m/s, or if more than 1 second has passed since the last CAM. These triggers ensure timely updates on the vehicle's state, facilitating rapid response to dynamic traffic conditions and system congestion.
Decentralized Environmental Notification Message (DENM) ETSI EN 302 637-3 [15] defines Decentralized Environmental Notification Messages (DENMs) which are mainly used by the Cooperative Road Hazard Warning (RHW) application in order to

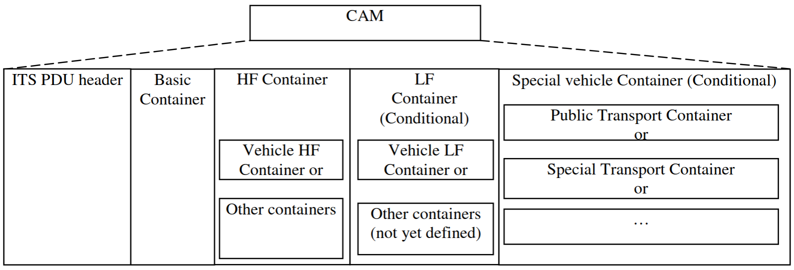

Figure 2.13: Structure of a CAM, source ETSI EN 302 637-2 [14]

alert road users of the detected events. The RHW application is an event-based application composed of multiple use cases.
When an ITS station detects an event related to a Road Hazard Warning (RHW) use case, it immediately broadcasts a Decentralized Environmental Notification Message (DENM) to other ITS stations within the relevant geographical area. The DENM is repeatedly transmitted at a certain frequency for as long as the event persists. The event is considered terminated either when a predefined expiry time is reached or when an ITS station generates a special DENM to indicate that the event has ended.

Day-2 Phase

The second phase, known as "Day-2" applications, focuses on sharing sensor data, specifically the exchange of detected objects in a vehicle's vicinity. These applications enhance situational awareness and enable more advanced cooperative driving functionalities. The primary services selected for this phase include:
Collective Perception Message (CPM) The CPMs, as standardized by ETSI TR 103 562 [59], are transmitted by ITS stations (ITS-Ss) to share information about perceived objects, such as vehicles, pedestrians, and other collision-relevant entities, as well as perception regions indicating unoccupied road areas. This enhances the environmental awareness of CPS-enabled ITS-Stations by providing data on both non-V2X-equipped road users and other important objects, thereby increasing the information sources available for V2X-equipped road users.
A CPM conveys data on observed objects and regions, detailing their status and attributes based on the detection capabilities of the originating ITS-S. This includes timing of detection, position, and potentially other kinematic and attitude details. Additionally, information about the sender's sensors, like types and fields of view, may be provided to enhance data interpretation at the receiving ITS-S.
CPMs are triggered under conditions such as changes in heading by more than 4 degrees, position shifts exceeding 4 meters, speed alterations over 0.5 m/s, or if more than 1 second has elapsed since the last CPM. These criteria ensure updates are timely and relevant, catering to dynamic road conditions.
Maneuver Coordination Message (MCM) The Maneuver Coordination Message (MCM) generated for Maneuver Coordination Service (MCS), which has currently been studied in ETSI TR 103 578 V2.1.1 [60]. The MCM is a critical broadcast tool in C-ITS, facilitating vehicle coordination by broadcasting a vehicle's current and planned maneuvers along with potential alternative trajectories for the next 5 to 10 seconds. These

trajectories aid C-ITS applications in predicting vehicle positions and managing conflicts, enhancing cooperative driving dynamics. Although not yet standardized, in TransAID EU project deliverable [61] it suggests MCMs typically range from 300 bytes for planned trajectories to 600 bytes when including desired trajectories. The frequency of MCM broadcasts varies from 1 to 10 Hz, depending on situational demands, to support timely maneuver coordination among vehicles.

2.4 Challenges in 5G Sidelink Deployment

2.4.1 Advanced V2X Applications Requirements

In line with these advancements, 3GPP TS 22.186 rel.17 [62] has outlined specific requirements to support various CCAM scenarios, particularly focusing on V2X scenarios, as detailed in Table 2.4. Different V2X scenarios necessitate the transmission of messages with varying performance requirements for the 3GPP system. To enhance 3GPP support for V2X, we have identified key service requirements in the following areas: Vehicles Platooning, Advanced Driving, Extended Sensors, and Remote Driving. These areas represent critical applications of V2X, each with unique communication and performance needs that are essential for achieving the overarching goals of enhanced safety, efficiency, and automation in vehicular networks.

Table 2.4: Performance Requirements for different use cases

Catalogue	**Latency (ms)**	**Payload (bytes)**	**Data Rate (Mbps)**	**Reliability (%)**
Vehicle Platooning	10-500	50-6500	50-65	90-99.99
Remote Driving	5	-	-	99.999
Extended sensor	3-100	1600	10-1000	90-99.999
Advanced Driving	3-100	300 - 1200	10-53	90-99.99

Vehicle platooning involves multiple vehicles traveling closely together in a coordinated manner. This requires constant communication and control support to maintain safety and efficiency. Given the proximity of the vehicles, the system must ensure low latency to prevent collisions and ensure synchronous movements. The latency requirements range from 10 to 500 ms, with payload sizes between 50 and 6500 bytes, data rates from 50 to 65 Mbps, and reliability between 90% and 99.99%.
Remote driving enables a human operator to control a vehicle from a distant location. This use case has stringent requirements for communication performance due to the need for real-time control, one thing need to be pointed out is remote driving are mostly realized through UL/DL link, instead of the direct sidelink communication, which is out of the scope of this thesis topic. However still this use-case shows that the latency must be extremely low, around 5 ms, and the reliability must be exceptionally high at 99.999% to ensure safe and responsive driving.
Extended sensor applications involve the sharing of sensor data between vehicles and infrastructure to enhance situational awareness and safety. These applications require variable latency from 3 to 100 ms, payloads of 1600 bytes, data rates between 10 and 1000 Mbps, and high reliability ranging from 90% to 99.999%. The high data rates and reliability ensure that detailed sensor information is transmitted accurately and promptly.

Advanced driving applications support semi-autonomous and autonomous driving functionalities, requiring robust V2X communication. These applications need latency between 3 and 100 ms, payloads ranging from 300 to 1200 bytes, data rates of 10 to 53 Mbps, and reliability between 90% and 99.99%. These parameters ensure that vehicles can make timely and accurate driving decisions.
From a general view we can observe, each of these V2X scenarios has specific performance requirements that must be met to ensure safety, efficiency, and reliability. By focusing on these requirements, we can enhance the 3GPP support for V2X scenarios and leverage the full potential of 5G-NR sidelink communication. The following chapters will illustrate how these characteristics are integrated into our proposed framework and the benefits they bring to V2X communication systems.

2.4.2 Current Challenges in 5G-NR Sidelink Evolution

Despite increasing demands from industrial sectors and ongoing research developments, the progression of 5G-NR Sidelink communication remains constrained. Therefore here we summarize the current state-of-art limitation for Sidelink in Table. 2.5, which compares the existing elements in Sidelink communication with those in Uplink/Downlink (UL/DL), we identify what is present and what is lacking. Although Sidelink shares the same flexibility in adjusting physical layer resources, such as dynamic Transmission Time Interval (TTI) and a variety of available numerologies as UL/DL, detailed in Section 2.1.2, challenges persist. Specifically, Sidelink development lags in addressing the stringent requirements of URLLC within 5G-NR; there are also insufficient studies on implementing network slicing architecture directly over Sidelink.
Therefore, this thesis aims to bridge these gaps, focusing on the under-explored areas of Sidelink development to pave the way for the next stages of 5G-NR Sidelink communication enhancements.

Table 2.5: The current development comparison between NR-UU and NR-PC5

Criteria	**Sidelink**	**UL/DL**
Flexible physical resources layout	✓ [58]	✓ [58]
Dynamic MAC schedulers	✓ [58]	✓ [58]
Network Slicing Mechanism	✗	✓ [63]
Supporting URLLC services	✗	✓ [64]

2.5 Platforms for Vehicular Communication

2.5.1 Simulation Platform

Simulation platforms designed to analyze vehicular performance in wireless communication systems have significantly evolved, with a particular focus on sidelink communication. Several platforms have been developed with special attention to 5G-NR Mode 2. In this section, we introduce several main tools that have been extensively used in recent research. The initial part of our discussion on simulators concentrates on network communication. Subsequently, we explore current projects dedicated to the realization of CCAM (Co-operative, Connected, Automated, and Mobility) simulations, which specifically include vehicular mobility scenarios.

Network Simulator 3(NS-3)

Network Simulator 3 (NS3) is a discrete-event network simulator that serves as a vital tool for both research and educational purposes. LENA (LTE-EPC Network simulAtor) is an extension of NS-3 [65], specifically designed to simulate the Long Term Evolution (LTE) and Evolved Packet Core (EPC) networks. It supports detailed modeling of radio access networks, including aspects like scheduling, mobility, and interference.
Importantly, the recent updates to LENA have expanded its utility by incorporating Sidelink (SL) capabilities, which are essential for direct D2D communications within the 5G New Radio (NR) framework[65]. This enhancement is particularly significant for studies focused on 5G applications, as Sidelink communication is pivotal for supporting efficient, low-latency interactions directly between devices without reliance on network infrastructure. The integration of Sidelink into the NS-3 LENA environment aligns with the latest advancements in 5G-NR, offering a robust simulation tool that mirrors current technology trends and meets the research needs for exploring complex network scenarios. This SL version has mainly focused on NR V2X Mode 2 communication, specifically adapted for Sidelink V2X communication. The sidelink UE data plane has illustrated in figure. 2.14. The integration necessitated updates to the bearer establishment processes and adaptations across the RRC, MAC, and PHY layers. For a detailed account of these implementations, please refer to the work by Zoraze et al.[43].

OMNET+

OMNeT++ is an extensible, modular, component-based C++ simulation library and framework, primarily for building network simulators [67]. The main advantage of the simulation system is that it supports large-scale model building, offers an intuitive programming model, includes a powerful GUI environment, and is open-source. It provides a robust environment for simulating a wide range of networks, from wired and wireless to mobile and sensor networks. OMNeT++'s flexibility and modularity make it a popular choice for researchers and developers in the field of network simulation.

Open Air Interface(OAI)

OpenAirInterface (OAI) is an open source initiative that today provides a 3GPP compliant reference implementations of key elements of 5G RAN and core network that run on general purpose computing platforms [68]. OAI proposed a key project focusing on RAN simulation. For RAN L1-simulation framework, the RFsimulator replaces the radio board by software (TCP/IP) communication in order to make possible all functional tests without a RF board. The OAI gNB and the OAI UE communicate as if there were a RF interface between them, but without any real-time clock constraints. The I/Q samples can be transmitted over a radio channel simulator. For L2-simulation framework, it is designed for scenarios with a high number of UEs by employing the interface defined by the Small Cells Forum (SCF). Then this interface splits the gNB into a MAC entity and a PHY entity for 5G. In OAI, the gNB MAC connects through this created interface to a channel

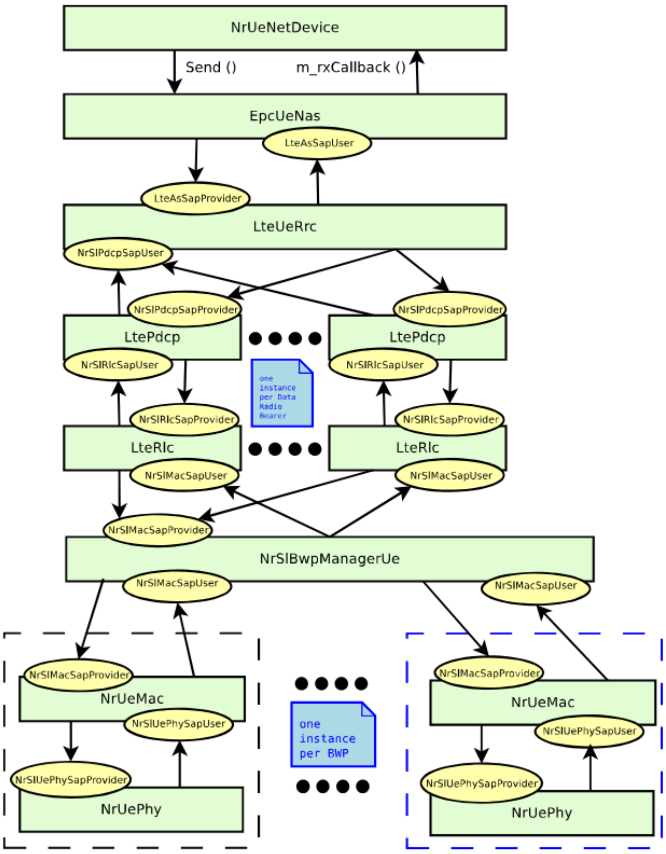

Figure 2.14: NS3 Sidelink UE Data Plane [66]

proxy that simulates the channel and allows to connect many UEs to the MAC stub. Each UE is the simulated OAI UE that connects to the proxy.

2.5.2 Realizing CCAM Simulation

Connected and Automated Mobility (CCAM) simulators are aimed to introduce integral tools for analyzing the complex interactions between vehicle communication systems and dynamic vehicular mobility. These simulators integrate advanced communication models, with realistic traffic simulation platforms. This integration allows researchers and engineers to study and optimize vehicular behavior in a controlled yet realistic virtual environment.

SUMO

Most of the current studies have combined with this main mobility simulator called Simulation of Urban MObility(SUMO) [69]. SUMO is an open source, highly portable, microscopic and continuous traffic simulation package designed to handle large networks. It allows for inter-modal simulation including pedestrians and comes with a large set of tools for scenario creation.
SUMO offers significant flexibility and a range of benefits for traffic simulation. Its dynamic mobility capabilities allow users to tailor scenarios to specific needs, supporting both large

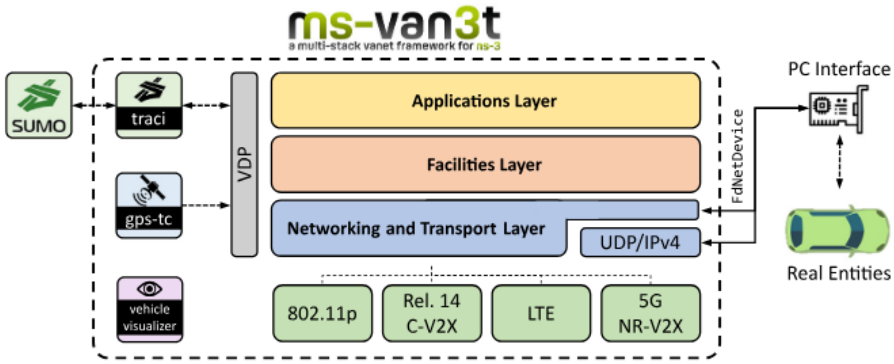

Figure 2.15: Full Architecture of MS-VANET

and small traffic scales and various vehicle types. A key advantage of SUMO is the ease of integration with cellular network simulators through its comprehensive implementation of the Traffic Control Interface (TraCI). This integration facilitates detailed and dynamic vehicular network simulations, enhancing the realism and applicability of studies. Additionally, SUMO's ability to manage complex traffic behaviors and interactions in real-time contributes to its effectiveness in modeling urban traffic systems comprehensively.

MS-VANET

ms-van3t is a simulation platform based on NS-3 and SUMO, tailored for vehicular network research [70]. It integrates vehicular mobility models and network communication protocols, allowing researchers to simulate realistic vehicular communication scenarios. The platform supports the simulation of Vehicle-to-Everything (V2X) communication, which is crucial for the development of Cooperative Intelligent Transport Systems (C-ITS) and Connected and Automated Mobility (CCAM).
MS-VAN3T integrates various software modules through dedicated interfaces to create a robust platform for V2X application testing. It utilizes the aforementioned SUMO platform to dynamically model the positions of nodes, and then combining the NS3, to manage network simulations. MS-VAN3T extends ns-3 capabilities by incorporating 3GPP Release 16 5G-NR-V2X and the ETSI C-ITS stack, along with other innovative features that are easily integrated through libraries facilitated by a user-friendly installation script. The architecture of MS-VAN3T, shown in Fig. 2.15, offers a complete vehicular communication stack, allowing simulated vehicles to be equipped with various access technologies (highlighted in green boxes in the figure). Vehicle mobility within the simulator can be controlled via SUMO for standard simulations or through pre-recorded GNSS traces for specific scenarios. Additionally, MS-VAN3T features a flexible web-based vehicle visualizer that can display vehicles on a map, enhancing the simulation of scenarios based on GNSS traces.

Eclipse MOSAIC

Eclipse MOSAIC is a multi-scale simulation framework in the field of smart and connected mobility [71]. It allows coupling simulators from various domains towards a comprehensive simulation tool. Data exchange and time management is implemented by the Runtime

Infrastructure (RTI), which is the heart of MOSAIC. Simulation models are coupled to the RTI using HLA inspired interfaces; Each simulator is wrapped into a "Federate" object which is linked to an "Ambassador" which is directly coupled with the RTI.
MOSAIC offers a highly adaptable platform that supports a diverse range of applications. On the application layer, it comes equipped with safety and traffic applications, and users also have the flexibility to develop their own service applications. For network simulation, options include NS3, OMNeT++, or MOSAIC's own Network Simulator (SNS). In terms of traffic and vehicle management, MOSAIC operates similarly to MS-VANET, utilizing SUMO-GUI—a detailed and continuous road traffic simulation tool capable of managing extensive road networks.

VEINS

VEINS (Vehicle in Network Simulation) is an open-source framework designed to integrate OMNeT++ and SUMO, creating a comprehensive environment for simulating vehicular communication networks [72]. VEINS leverages OMNeT++'s network simulation capabilities and SUMO's traffic simulation features to provide a realistic simulation of vehicle behavior and network interactions. This integration allows researchers to study the impact of vehicular communication on traffic flow and network performance in a detailed and realistic manner.

2.6 Conclusion

This chapter provided a state-of-art review of the various domains impacted by the methodology described in Chapter 1. We provided an overview of the architecture of 5G-NR as well as the 5G services, in particular URLLC. We then introduced 5G-NR Sidelink providing D2D communication via the PC5 interface, and described the state-of-art of 5G-NR V2X standards and research. We covered the ETSI ITS architecture, which is mandatory to be used for operating 5G-NR V2X in the ITS spectrum in Europe, and presented the various day-1 and day-2 messages required by current and future connected and/or automated vehicles. We extended this study toward standards and research in 5G-NR and 5G-NR V2X towards dependable V2X communications, first by introducing the domain of 5G Network Slicing, as well as key performance indicators (KPIs) of challenging V2X and future CCAM use cases.
From this study, we identified several important gaps that we will address in this work. First, we illustrated that ETSI ITS imposes default parameters to 5G-NR Sidelink, which are not adapted to day-2 or even challenging CCAM use cases requiring dependable communication. Second, while significant research focused on URLLC for 5G-NR or 5G V2X (via gNB), URLLC on 5G-NR SL/V2X over the PC5 interface is globally under investigated. Similarly, we observed that 5G Network (or RAN) slicing has been well studied for 5G-NR or 5G-NR V2X (via gNB), however slicing the PC5 interface remains globally an empty page. Slicing as well as URLLC (or other 5G Services) should also be defined and investigated for 5G-NR SL, considering that future CCAM use cases will require dependable wireless D2D communication.
Filling these gaps is therefore a pioneering work described in the next chapters. In Chapter 3 we will demonstrate that URLLC is possible on 5G-NR Sidelink. Chapter 4 will

present a novel 5G-NR Slidelink architecture providing dependable wireless communication over a PC5 URLLC slice. Finally, Chapter 5 will show the critical benefits of dependable 5G-NR Sidelink communication on a PC5 URLLC slice for vehicular platooning.

Chapter 3
URLLC for 5G-NR Sidelink Communication

This thesis investigates the feasibility of establishing dependable communication via 5G-NR Sidelink. Without loss of generalities, we address URLLC as one form of dependable communication, and we target V2X scenarios representing a major application domain requiring stringent D2D communication over 5G-NR Sidelink.
URLLC service requirements for V2X communication are specified in 3GPP TR 22.804 [35] Rel. 16. For general use cases, a reliability of 10^{-5} within a 1 ms delay for 32-byte packets [73] is expected. For enhanced V2X (eV2X) scenarios over Sidelink, the same reliability of 10^{-5} is expected but with a permissible delay range of 3-10 ms for 300-byte packets.
As described in the previous chapter, most URLLC studies on 5G-NR or 5G-NR V2X focused on UL/DL (Uu vertical interface) considering the assistance of a 5G-NR infrastructure. This study focuses on Sidelink (PC5 horizontal interface) without the assistance of a 5G-NR infrastructure. In this chapter, we investigate URLLC first from *latency* then *reliability* perspectives. As depicted on Fig. 3.1, our methodology is to address URLLC from three key 5G-NR characteristics: numerology, modulation and coding scheme (MCS) and MAC layer scheduling, the first two addressing latency while the latter defining reliability. This chapter therefore address low latency for 5G-NR Sidelink first and then ultra-reliability for 5G-NR SL.

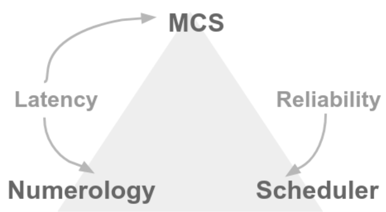

Figure 3.1: 5G-NR Sidelink Proposed Methodology

This work is the first to define and demonstrate the feasibility of achieving URLLC on 5G-NR SL. To that purpose, we rely on a higher numerology allowing shorter slot durations, a higher modulation reducing the channel air time and a deterministic scheduler orchestrated by a decentralized admission control mechanism. While stringent V2X channel conditions may significantly impact URLLC, we leave physical layer features such as

MIMO or beamforming as well as robust coding to future work.

3.1 Minimizing Latency in 5G-NR Sidelink Communication

According to 3GPP TR 38.913 rel.17 [73], the 5G-NR V2X URLLC is expected to achieve latency below 10 ms. Ali et al. [66] assessed latency over 5G-NR Sidelink and demonstrated that the current standard parameter settings in 5G-NR Sidelink struggle to meet such 10 ms latency limit. The approach introduced below involves optimizing the arrangement of physical resources within 5G-NR to enhance network response times and comply with these rigorous latency requirements.
As previously indicated, latency may be influenced through a combination of NR numerology and physical layer modulation and coding (MCS). According to Rel.16 [10], 5G-NR V2X uses a default NR numerology 0 and MCS 14. This section challenges these assumptions considering that the study only addressed *Day 1* messages. We first identify a higher optimal default MCS, then go beyond state-of-art and 3GPP standard to propose a higher NR numerology providing 0.125ms slot duration. Considering that NR numerology impacts MCS studies, we first address numerology then MCS.

3.1.1 Physical Rearrangement in 5G-NR Sidelink

The two primary parameters that can help to reduce latency in 5G-NR over Sidelink through physical layer setting are numerology and MCS.

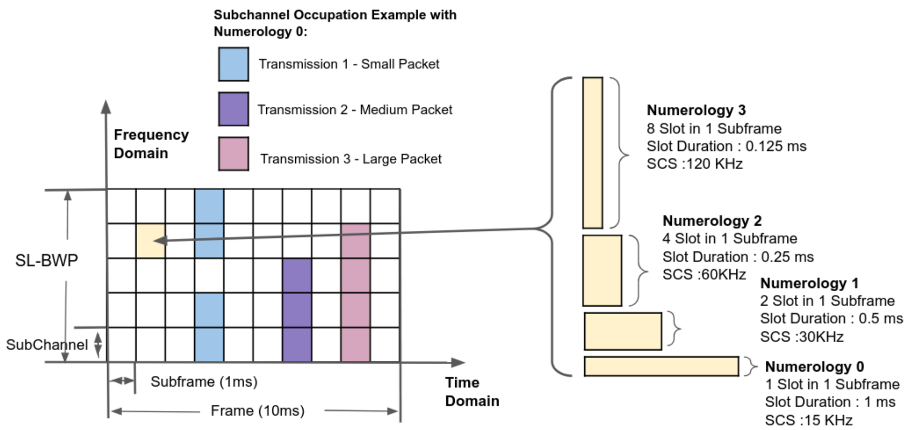

Figure 3.2: 5G-NR Sidelink Physical Structure

For **numerology**, 5G-NR introduces *mini-slots* to enable $< 1ms$ transmit delays. Keeping the number of resources per slot equal, a smaller slot proportionally increases the number of PRBs as depicted on Fig. 3.2, in combination of detailed setting info in Table. 3.1. Four numerology types (0-3) correspond to different configurations of mini-slot vs. PRB configurations, slot time duration consequently varies among 1 ms, 0.5 ms, 0.25 ms and 0.125 ms with respect of increasing numerology.
It is observed that higher numerologies use increased subcarrier spacing to expand on the frequency domain, which effectively reduces the duration of a *mini-slot* on the time domain. This adjustment helps shorten the duration per reservation, making higher numerology

especially advantageous for applications requiring URLLC. Consequently, our initial proposal recommends adopting higher numerology, specifically numerology-3, allowing for 8 different slots within a 1 ms interval for diverse user assignments.
In frequency domain, a certain size of bandwidth part (BWL) is assigned for sidelink communication, within which a group of sub-channels are assigned, one sub-channel may contains 10, 12, 15, 20, 25, 50, 75, or 100 Physical Resource Blocks(PRBs). A sub-channel represents the smallest unit that can be assigned to one or several UEs in a half-duplex manner.
However, higher numerology can increase the potential for adjacent channel interference due to smaller subcarrier spacing. Additionally, the increased complexity of signal processing associated with higher numerology leads to higher power consumption. This is because more computational resources are required to handle the smaller subcarrier spacing, impacting both network infrastructure and user devices. Therefore, understanding these trade-offs and analyzing the actual impact of employing high numerology-3 is crucial for optimizing 5G network deployments to meet stringent latency demands effectively.

Table 3.1: Supported Numerology in NR V2X Sidelink

μ	**SCS**	**Frequency Range**	**Slots per Subframe**	**Slot Duration**
0	15kHz	FR1	1	1ms
1	30kHz	FR1	2	0.5ms
2	60kHz	FR1,FR2	4	0.25ms
3	120kHz	FR2	8	0.125ms

Another key impact parameter is the **Modulation and Coding Scheme (MCS)**. 3GPP enables flexible 5G-NR Sidelink data rates through a numerous MCS values, which are defined on Table 5.1.3.1-1 of TS 138 214 [74] and reproduced on Table 3.2. Impact of various MCS values on a same packet size is illustrated in the bottom right side of Fig. 2.6. A higher MCS value can effectively compress the packet into fewer sub-channels and consequently improve potential sub-frame packet multiplexing using 5G-NR V2X Sidelink schedulers.
However, the adaptation of packet size multiplexing to fit into the sub-channel is not dynamic. The 5G-NR V2X Sidelink scheduler does not adjust to PDCP-level packets, which means it cannot differentiate between fully or partially occupied sub-channels during resource allocation. Consequently, if a specific MCS and packet size optimally utilize all resources within one or more sub-channels, other combinations of MCS values and packet sizes may lead to partial sub-channel occupation and resource wastage, as illustrated on the right side of Fig. 2.6.
Accordingly, increasing the MCS may reduce the required sub-channels per packet, in turn enabling more channel resources to be distributed to other transmitters, this benefit may be lost if sub-channels end up being partially occupied. As shown on the top right side of Fig. 2.6, the sub-frame has enough *absolute* resources to multiplex TX_1 and TX_3 together in one sub-frame, but the scheduler does not succeed as both TX_1 and TX_3 waste one sub-channel each due to partial sub-channel usage. If the impact of the data rate (i.e MCS) on the performance of 5G V2X broadcast communication is traditionally understood to be sensitive to channel conditions, we can see that for 5G-NR V2X SL, it also depends on how efficiently sub-channels are occupied and packets multiplexed.

Table 3.2: Modulation and Coding Scheme Index

MCS Index	Modulation Order	Target Code Rate	Spectral Efficiency	MCS Index	Modulation Order	Target Code Rate	Spectral Efficiency
0	2(QPSK)	120	0.2344	14	4	553	2.1602
1	2	157	0.3066	15	4	616	2.4063
2	2	193	0.3770	16	4	658	2.5703
3	2	251	0.4902	17	6(64 QAM)	438	2.5664
4	2	308	0.6016	18	6	466	2.7305
5	2	379	0.7402	19	6	517	3.0293
6	2	449	0.8770	20	6	567	3.3223
7	2	526	1.0273	21	6	616	3.6094
8	2	602	1.1758	22	6	666	3.9023
9	2	679	1.3262	23	6	719	4.2129
10	4(16 QAM)	340	1.3281	24	6	772	4.5234
11	4	378	1.4766	25	6	822	4.8164
12	4	434	1.6953	26	6	873	5.1152
13	4	490	1.9141	27	6	910	5.3320
				28	6	948	5.5547

Most V2X services are based on broadcast communication and on ad-hoc (infrastructure-less) resource allocation ([41]). Accordingly, vehicles need to select a default V2X MCS. Although V2X MCS has been studied for other radio access technologies over the years, comparatively limited analysis on broadcast MCS 5G-NR Sidelink can be found in recent research. Jiang et al. [75] suggested a QPSK 1/2 MCS value as optimal for ITS-G5/DSRC technology. Although widely adopted by subsequent studies, standards, and even for the LTE-V2X technology, recent works ([76], [77]) shed light on the potential benefit to increase it. Burbano-Abril et al. [78] propose a dynamic adaptive MCS methodology based on diverse traffic scenarios in order to optimize overall performance for the LTE-V2X technology. Recently, Ali et al. [66] utilise various MCS values for 5G-NR V2X Sidelink under a single packet, fixed packet size, and periodic traffic, corresponding to a day-1 Cooperative Awareness (CA) service. Under these conditions, 5G-NR MCS 14 appeared to be optimal. However, day-2 V2X scenarios include multiple V2X services involving packets of various sizes and more stringent topology conditions, which requires a generalized investigation.
Combining two key physical layer parameters—numerology and MCS—requires careful analysis. Numerology-0, widely used across general V2X scenarios, offers a baseline for optimizing MCS to enhance C-ITS communication, identifying the optimal MCS for higher numerology, such as numerology-3, is crucial for constructing a dependable network capable of providing URLLC services via Sidelink communication in 5G-NR.

3.1.2 Topology and Evaluation Design

To determine the optimal MCS setting under a general traffic scenario, we consider a simplified two-lane traffic topology. In this model, all transmitting vehicles are located at a configurable uniform inter-distance on the first lane, the receiving vehicle is located at the center of the topology on the second lane, an average communication performance is to be examined on receiving vehicle from all transmitters. Mobility is not considered in this study, assuming either an static or a mutually static topology. We evaluate MCS values considering three varying representative parameters: *message transmit rate*, the *number of transmitters*, and *the packet size*.
As we want to avoid the impact of other parameters than the previous three on the evaluation of the MCS, we rely on a harmonizing metric called *Communication Density*

and defined as follows:

$$Dens^{comm} = \frac{Msg^{Rate} \times Tx^{range}}{Dist^{v2v}} \tag{3.1}$$

This function helps us to generate wide range scenarios with low complexity, in the meantime maintaining channel load so as to exclude impact brought by resource scheduler itself, we inherit and adapt the concept of communication density in our study as the benchmark for traffic conditions. Authors by [75] proved that under broadcast transmission with the same power, in scenarios characterized by the same composite communication density, produce equivalent traffic environment impact.

Figure 3.3: Topology varying the message transmit rate.

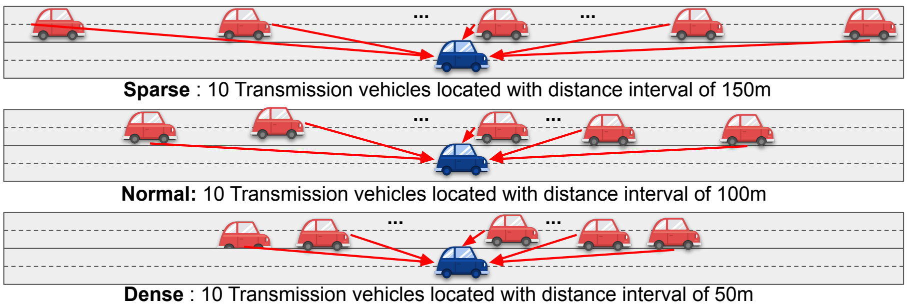

Index	$Dist^{v2v}$ (m)	Tx^{rg} (m)	Msg^{Rt} (Mbps)	$Dist^{v2v}$ (m)	Tx^{rg} (m)	Msg^{Rt} (Mbps)
	Level Reference			**Level A**		
Dense	20	100	0.024	20	100	0.1
Normal	50	250	0.024	50	250	0.1
Sparse	100	500	0.024	100	500	0.1
	Level B			**Level C**		
Dense	20	100	0.5	20	100	1
Normal	50	250	0.5	50	250	1
Sparse	100	500	0.5	100	500	1

Table 3.3: Settings for varying the message transmit rate

We therefore investigate in three levels of communication densities (Level A, B, C) and for each level, we consider three topology scenarios (sparse, normal and dense). As the communication density is constant in all three topology scenarios, only the metric under study will impact the MCS performance. In order to validate our methodology, we also add a reference group (Level Reference) configured similarly to [66] and designed to verify that we reach the same conclusions under the same conditions.

Message Transmit Rate

In the first approach outlined in this section, the focus is on assessing the impact of message transmit rate on communication efficiency within a controlled setting. To achieve this, we maintain a constant number of transmitters but vary their inter-vehicle distance ($Dist^{v2v}$) to modulate the communication density directly through changes in transmit rates. This experimental setup is illustrated in Fig. 3.3, where vehicles depicted in light red act as transmitters, and the dark blue vehicle serves as the sole receiver.

For a structured analysis, we have configured four distinct levels of communication density across three scenarios, as detailed in Table 4.3. Each scenario is designed to maintain a globally comparable level of communication density, as determined by the relationship outlined in Eq. 3.1. This methodical adjustment allows us to isolate and analyze the effects of transmit rate variations on the network's performance, providing valuable insights into how different communication densities influence the overall effectiveness of the network under varying vehicular proximities and activity levels.

Number of Transmitters

The number of transmitters helpes us to explore the influence of transmitter density on the performance of the 5G-NR V2X Sidelink mode 2(a) scheduler. Here, the communication density is solely determined by the density of transmitters, which we modulate by adjusting the message transmit rate as prescribed by Eq.3.1. To systematically analyze this relationship, we have structured the experiment into four levels, encompassing three distinct scenarios. These scenarios, outlined in Table 3.4, vary primarily in vehicle density to provide a comprehensive overview of how transmitter concentration affects network functionality.
This methodological setup allows us to assess the impact that varying numbers of transmitters have on network performance within controlled communication density environments. The scenarios depicted in Fig. 3.4 enable an examination of the network's behavior under different transmitter densities, providing insights into the optimal configurations that balance communication efficiency with resource allocation. This approach helps to isolate the effects of transmitter density, giving a clearer understanding of its influence on 5G-NR Sidelink dynamics.

Packet size

Figure 3.4: Topology varying the number of transmitters.

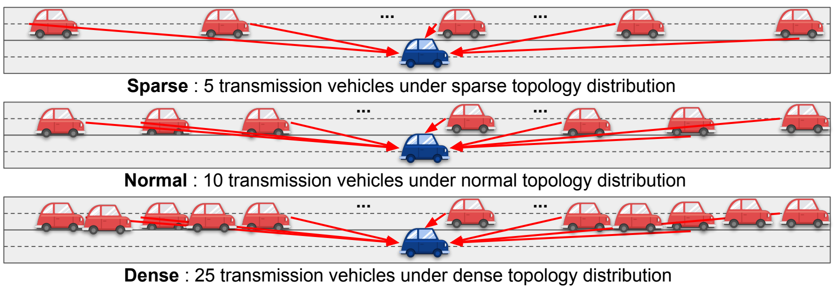

To enhance the efficiency of resource allocation within the 5G-NR V2X Sidelink (SL) subchannel structure, it's vital to consider the variance in packet sizes, which necessitates different resource requirements. Fig 2.6 in Section 2.1.1 has illustrated the different size of packets may requires different number of resource blocks, whereas adjusting the Modulation and Coding Scheme (MCS) value can lead to changes in the required resources per packet, potentially resulting in resource wastage. To address this, we introduce a methodology to assess how well packet sizes fit within the predefined resource structure as a function of MCS.

Index	Dist^{v2v} (m)	Tx^{rg} (m)	Msg^{Rt} (Mbps)	Dist^{v2v} (m)	Tx^{rg} (m)	Msg^{Rt} (Mbps)
	Level Reference			**Level A**		
Dense	20	500	0.0096	20	500	0.04
Normal	50	500	0.024	50	500	0.1
Sparse	100	500	0.048	100	500	0.2
	Level B			**Level C**		
Dense	20	500	0.2	20	500	0.4
Normal	50	500	0.5	50	500	1
Sparse	100	500	1	100	500	2

Table 3.4: Settings for varying the number of transmitters.

The effectiveness of resource utilization is quantified by the effective utilization ratio, ρ, defined by Eq. 3.2. This ratio measures the actual data payload (bytes) accommodated within the allocated resources:

$$\rho = \frac{S}{\gamma \times M} \tag{3.2}$$

S represents the packet size in bytes, γ denotes the number of required sub-channels per packet, as the larger the packet the more sub-channels are required. M represents the capacity of each resource block within a sub-channel, and is specified by the 5G-NR numerology and the MCS.

ρ, however, should not be considered alone, as within a 5G-NR sub-frame, multiple packets can be multiplexed, especially at higher MCS values and under heavy traffic conditions. Thus, we introduce a multiplexing level parameter, δ, defined in Eq. 3.3 as the quotient of the total bandwidth in sub-channels N and the number of sub-channels required per packet γ:

$$\delta = \left\lfloor \frac{N}{\gamma} \right\rfloor \tag{3.3}$$

By integrating Eq.3.2 and Eq.3.3, this methodology enables a detailed assessment of how varying packet sizes influence the selection of the optimal MCS value, ensuring efficient resource utilization tailored to the diverse needs of V2X services. This analysis facilitates better planning and optimization of 5G-NR Sidelink configurations, particularly important for applications requiring stringent QoS metrics like those in V2X scenarios.

3.1.3 Simulation Environment

We perform a system-level analysis relying on the NS3 simulator, enhanced with a 5G-NR V2X Sidelink stack [79]. Without loss of generalities, the wireless channel is modelled according to a standard 3GPP Model [80] for V2X highway communications, we leave a detailed investigation of the impact of more stringent channel conditions to future studies. The major determining parameters are listed in Table A.1. We are calculating the average packet reception rate (PRR) among all transmitters as a key performance indicator(KPI) to determine the impact of MCS values. Each result is obtained over an average of 200 simulation runs with random seeds.

Table 3.5: Simulation Baseline Parameters

Parameter	Value
Randomness	Seeds: 30; Run: 200
Performed Frequency	5.89GHz
Bandwidth	10MHz
Numerology	0, 1, 2, 3
subchannel size	10 PRBs
Available Sidelink symbol per slot	8/14
Sensing Window	100
Selection Window	30
Reservation Period	20
MAC Scheduler	Mode 2(a)
Re-transmission	Disabled
Propagation Model	3GPP LoS Channel Model [80]
Tx Power	23dBm
Transmission mode	Broadcast
Antenna Setting	Array of 1x2 antenna elements

3.1.4 Evaluation of MCS performance under Numerology-0

In this section, we first analyze the impact of MCS values on performance under numerology-0, which is commonly used in the general band for 5G-NR V2X. This analysis serves to provide a foundational performance evaluation for various V2X scenarios.

Message Rate Impact

This section analyses the impact of the message transmit rate on the packet reception rate (PRR) considering four message rate levels described on Table 4.3. This PRR is evaluated from each vehicle's perspective, given that all vehicles operate in broadcast transmission mode. The PRR is calculated as the ratio of successfully received packets to the total number of packets transmitted by all vehicles on the road. Fig. 3.5(a) shows the reference group considering the exact same parameter setting as in [66], which is under a comparatively low communication density. We can confirm that MCS 14 is the ideal modulation scheme value as shown in [66] under all scenarios, with the highest PRR around 0.83 as shown in [66]. As the PRR drops after MCS 14 for the sparse scenario, it remains stable for the normal and dense scenarios. This can be explained by a comparatively reduced transmission range in higher traffic densities according to Eq. 3.1, and an increased traffic capacity offered by higher MCS values mitigating resource exhaustion and packet collisions.
The next three figures of Fig. 3.5 consider different communication conditions than [66]. On Fig. 3.5(b), the message transmit rate is slightly increased, moving the optimal MCS value to MCS 20. Although a higher transmission rate generates a higher chance of collision, the MCS 24 does not provide a significantly reduced performance compared to MCS 20, in particular with normal or sparse scenarios. When increasing the message transmission rate, we can observe that a consistent optimal PRR is reached by MCS 24, as illustrated in Fig. 3.5(c) and Fig. 3.5(d). The improved performance is particularly visible for normal to sparse scenarios, which corresponds to a representative traffic context with V2X services generating a large amount of data, such as joint Cooperative Awareness

(CA) or Collaborative Perception (CP) services[1].
All in all, we can observe that only under a low message rate and communication density MCS 14 outperforms other MCS values as shown in Fig.3.5(a), confirming results from [66]. Under any other scenario, MCS 24 provides consistently better performances than any other MCS value.

Transmitter Density Impact

This section analyses the impact of the density of transmitters on the packet reception rate (PRR) considering four communication density levels described in Table 3.4.
As before, Fig. 3.6(a) shows the reference group, considering the exact same parameter setting as in [66] and again proves that MCS 14 is the optimal choice under all scenarios. With regards to MCS 14, the PRR achieves an optimum at 0.98 in sparse scenarios, while it reaches only 0.65 for dense scenarios. Higher MCS values degrade the PRR, but this is not significant, as MCS 24 only experiences a PRR reduction between 1% to 3%. The next three figures of Fig. 3.6 consider an increased and more realistic communication density compared to the comparatively low value modelled by the reference group in [66].
Fig. 3.6(b) shows that with an already mild increase in communication density, a PRR optimum is no longer reached by MCS 14 but rather by MCS 20. Quite interestingly, this outperforms the negative impact of a reduced Signal-to-Noise Ratio (SNR) on higher MCS values due to the increased communication density. This can be explained by a stronger benefit of an improved channel availability for the 5G-NR V2X scheduler due to reduced resource requirements by higher MCS values.

As represented in Fig.3.6(c) and Fig.3.6(d), higher global communication densities applied, results shows a positive proportional relationship between data rate and overall PRR, suggesting a higher data rate would outperform a lower data rate in most cases.
Moreover, normal and dense scenarios outperform sparse scenarios, this is due to the fact that more transmitters are within the reachable range with higher transmission densities, resulting in a better reception rate. Within each figure, sparse scenarios with fewer transmitters have a more stable performance in reception rate when compared to dense scenarios. This is because more transmitters create more chances of packet collisions and resource exhaustion. When combining the previous analyses, while in certain conditions other MCS values outperform MCS 24, we observe that MCS 24 remains consistently optimum or only experiencing minor loss compared to other MCS values, and it remains definitively better than MCS 14.

Packet Size Impact

This section investigates the impact of packet size on optimum MCS values. We considered realistic packet size ranges between 200 bytes and 1500 bytes according to actual V2X packets sizes measured and reported in [59][81]. We applied five MCS indices from Table. 3.2, namely 8, 12, 14 (as reference value), 16, and 24.
Referring to Eq. 3.2 and considering the basic NR numerology 0, M fully depends on MCS, which means that a higher modulation scheme allows more bytes to be packed into a single

[1] At high vehicular density, the vehicular speed would be proportionally reduced, which would in turn also reduce the message generation rate.

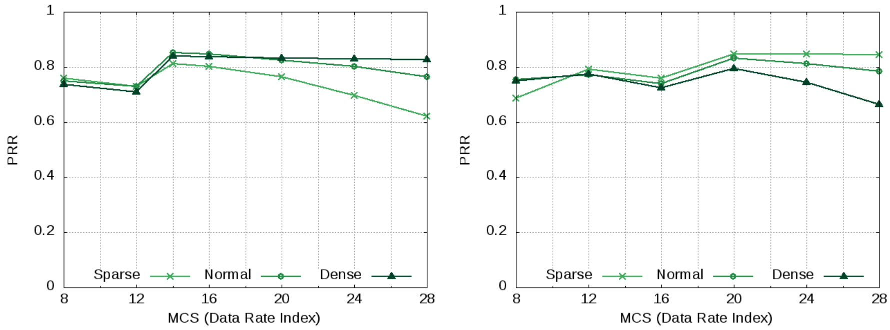

(a) Reference Level [66]   (b) Level A

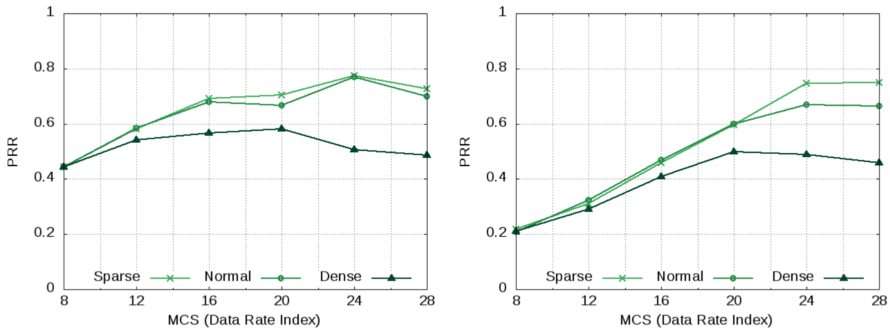

(c) Level B   (d) Level C

Figure 3.5: Message Rate Impact Result

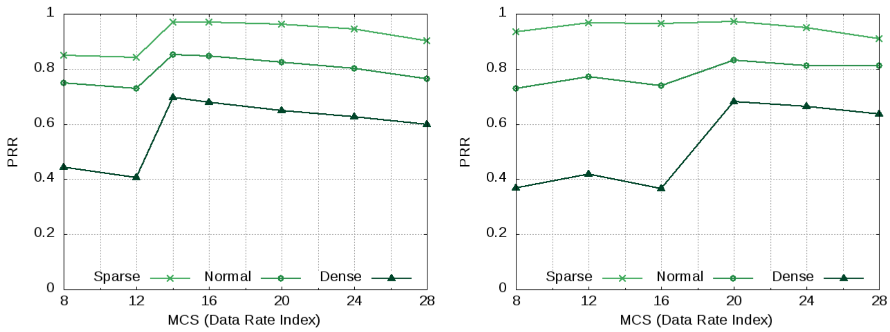

(a) Reference Level [66]   (b) Level A

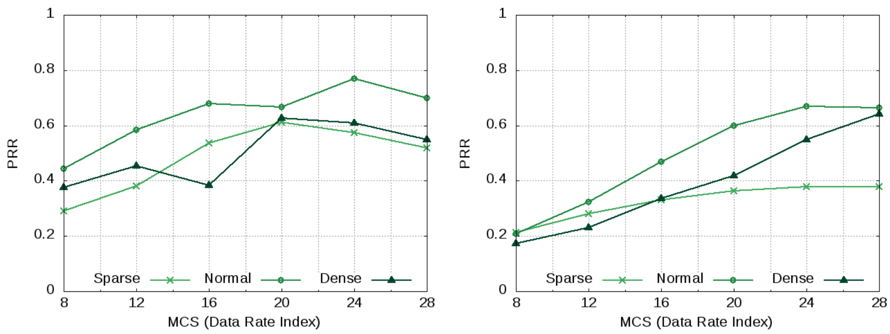

(c) Level B   (d) Level C

Figure 3.6: Number of Transmitter Impact Result

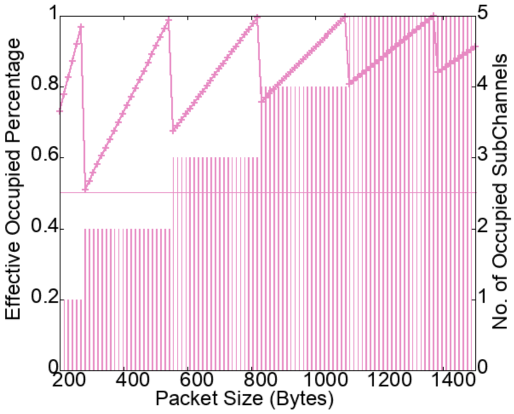

(a) MCS-12

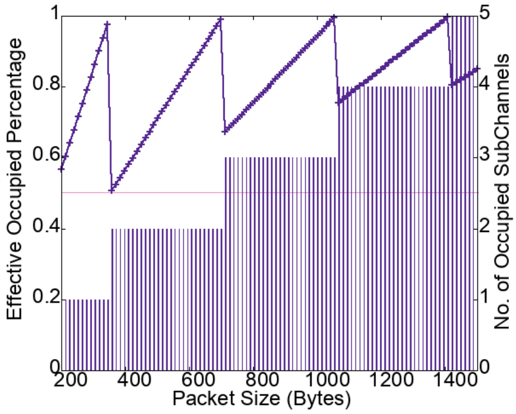

(b) MCS-14

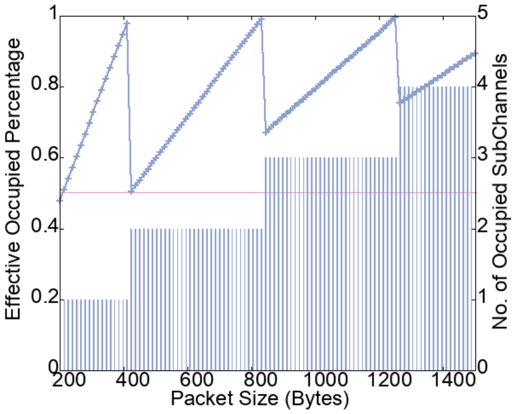

(c) MCS-16

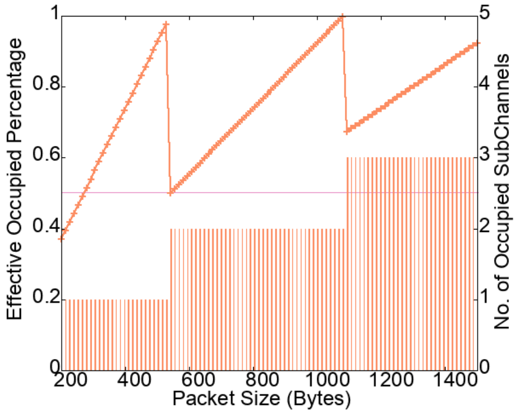

(d) MCS-20

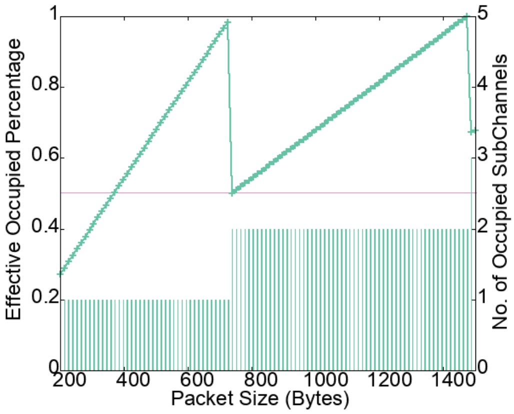

(e) MCS-24

Figure 3.7: Sub-channel Occupation over different Packet size

resource block. Fig. 3.7 depicts the impact of the MCS on 5G-NR V2X Sidelink resource usage efficiency according to ρ (Eq. 3.2) and γ (Eq. 3.3). The zigzagging lines with left side of the y-axis indicators represent ρ, showing periodical changes in the percentage of resource utilization. From these lines we can observe that certain packet sizes and MCS values result in a perfect utilisation of the 5G-NR V2X Sidelink subchannels. However, we can also observe from the periodical gradual increase that, for most of other packet size values, resources are wasted by not fully using all resources granted by each 5G-NR V2X Sidelink subchannel. Besides the available channel resources not actually being used, this also impacts the performance of the 5G-NR V2X Sidelink scheduler, as partially available subchannel resources can not be individually allocated to other transmitters. Still on Fig. 3.7, the block values representing γ shows the number of occupied 5G-NR V2X Sidelink subchannels, as can be read on the right side of the y-axis. A subchannel is considered occupied when at least one of its internal resource is used by at least one packet. The grey part indicates the limited resources available per subchannel does not allow packet sizes larger than 1350 bytes to be transmitted using MCS 14. We can also see that a higher MCS value requires less subchannel occupation for larger packets. If a packet size of 1200 bytes requires all 5 available subchannels with a MCS 14, only 2 subchannels are required for MCS 20 and MCS 24, thus enabling an increased packet multiplexing per 5G-NR V2X Sidelink subframe.

Multiplexity Capacity within One Sub-Frame							
MCS \ Size	**200**	**400**	**600**	**800**	**1000**	**1200**	**1400**
12	5	2	1	1	1	1	—
14	5	2	2	1	1	1	1
16	5	5	2	2	1	1	1
20	5	5	2	2	2	1	1
24	5	5	5	2	2	2	2

Table 3.6: MCS impact on 5G-NR V2X Multiplexing

To better illustrate this point, a theoretical calculation of packet multiplexing numbers is shown in Table 3.6, this table illustrates the impact of MCS on multiplexing capacity within a single sub-frame distinctly.

Specifically for MCS-24, in comparison to MCS-14 as reference, MCS 14 allows for multiplexing of five 200-byte packets per sub-frame, while MCS 24 extends this capability to multiplexing five packets up to 600 bytes each, which represents a significant improvement in the volume of transmitted data but also enhances the system's efficiency. Specifically, MCS 24 supports up to three times the data payload size per packet compared to MCS 14 for the same number of multiplexed packets, which is indicative of a 200% improvement in capacity. This enhancement is critical in scenarios where high data throughput and efficient spectrum use are paramount.

Moreover, the capability of MCS 24 to handle larger packets without a decrease in the number of multiplexed packets per sub-frame implies a reduction in the overhead associated with packet transmission. Fewer sub-frames are needed to transmit the same amount of data, leading to improved latency. This is particularly beneficial for applications requiring real-time or near-real-time data transmission, such as those found in V2X communications where timely and reliable data exchange is crucial for safety and operational efficiency.

3.1.5 Evaluation of MCS analysis under different Numerology

Similar to the previous section analyzing MCS under numerology-0, we now extend our examination to higher numerologies—1, 2, and 3—to gain a comprehensive understanding of MCS performance across a broader range of physical resource settings. As highlighted earlier in this study, adopting higher numerologies is essential for facilitating URLLC services. This strategic adjustment can substantially improve system performance by meeting the stringent demands of URLLC applications.
The mechanism was implemented in NS3, employing the same topology as used in previous configurations. The outcomes are depicted in Figure.3.8 and Figure.3.9. Building upon earlier findings, this analysis includes two higher numerologies in addition to numerology-0, comparing their performances across various MCS and traffic density settings.
The first part of analyses the impact of the message transmit rate on the PRR considering four message rate levels described on Table 4.3.
Figure.3.8(a) illustrates the reference group under the same parameter settings previously detailed in[66]. From the figure, it is evident that numerology-1 offers performance comparable to numerology-0, affirming that MCS-14 remains the optimal modulation scheme, as established in [66]. However, under numerology-3, employing a higher MCS results in poorer performance due to the increased sensitivity to path-loss associated with higher numerologies. This highlights the trade-offs involved in selecting numerologies and MCS levels for different network conditions.
The subsequent figures in Fig. 3.8 examine a broader spectrum of communication conditions across three distinct levels. Level A results align closely with the trends observed in the reference level. However, Levels B and C, which incrementally increase the message transmission rate, display a consistent pattern where increasing the MCS under various numerologies yields similar trends. Notably, in Levels B and C, utilizing higher numerology leads to poorer performance at lower MCS ranges. This performance decrease occurs because lower MCS values restrict resource capacity, and higher numerology introduces more time-domain segmentation similar to full-time division multiple access (TDMA). This is particularly problematic under higher message rates, where the increased frequency of collisions exacerbates the issue, as limited resources must be distributed among competing transmissions. In all, despite variations in performance across different levels and conditions, the data suggests that MCS-24 consistently emerges as the optimal choice for all numerology levels in both Level B and Level C scenarios.

The second part of the analysis focuses on the performance across different numerologies while adjusting the number of transmitters to maintain consistent traffic density.
Same as first part, the Fig.3.9(a) shows the reference group considering the exact same traffic density as in [66]. Fig.3.9(b) shows that with an already mild increase in communication density, while in Fig.3.9(c) and Fig.3.9(d), higher global communication densities applied.
In Figures 3.9(a) and 3.9(b), a distinct advantage is observed under higher numerology settings due to the increased number of slots available within the same time duration, allowing for enhanced support of multiple users. However, as depicted in Figures 3.9(c) and 3.9(d), this advantage diminishes with escalating message rates. At higher rates, lower numerologies yield better Packet Reception Ratios (PRR) because they offer more available slots per transmitter, crucial for managing increased transmissions. Conversely,

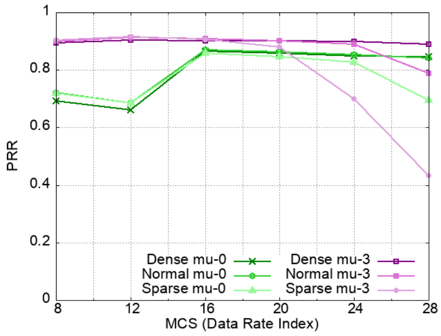

(a) Reference Level [66]

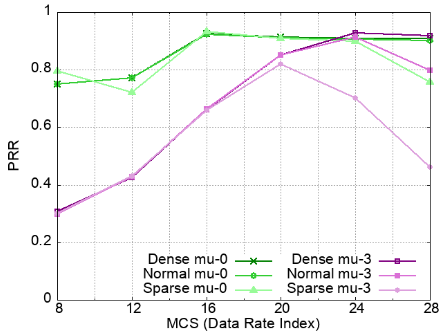

(b) Level A

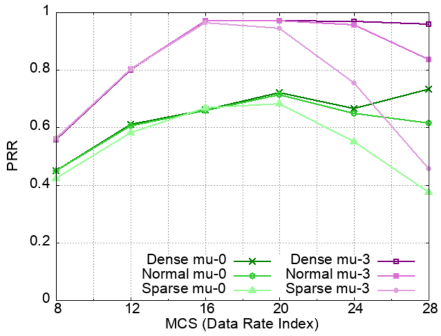

(c) Level B

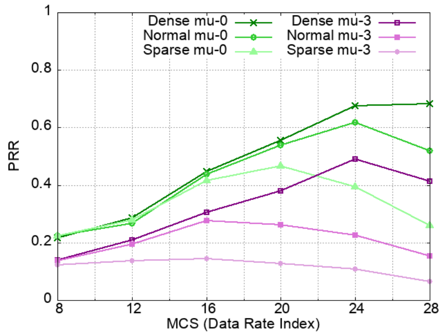

(d) Level C

Figure 3.8: Message Rate Impact Result

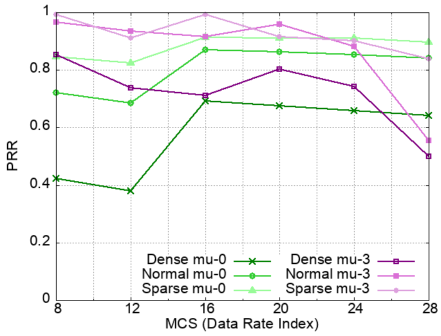

(a) Reference Level [66]

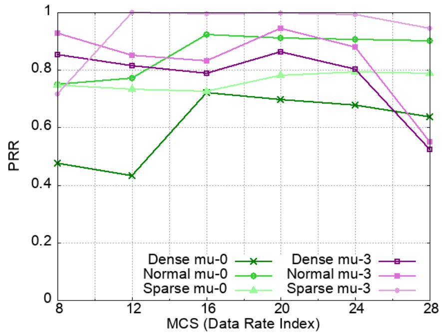

(b) Level A

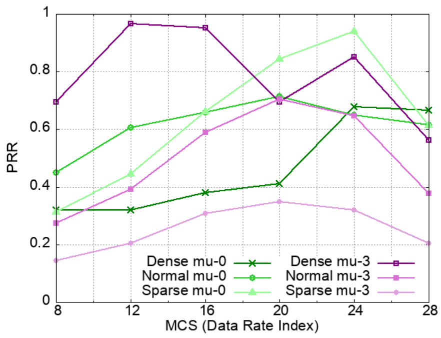

(c) Level B

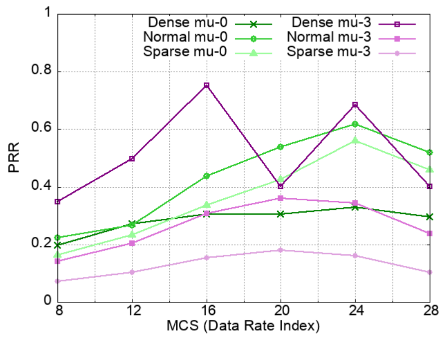

(d) Level C

Figure 3.9: Number of Transmitter Impact Result

higher numerologies, which condense the slot duration for each transmission, lead to a scarcity of available capacity, exacerbating collisions and degrading performance. Notably, numerology-3 fluctuates significantly in dense scenarios, where a lower MCS improves overall PRR compare with MCS-20. This may be because, with higher numerology, lower MCS can support multiple transmissions. However, from an overall perspective, MCS-24 still outperforms across all scenarios under numerology-3.
Regarding the optimal Modulation and Coding Scheme (MCS), MCS-24 consistently emerges as the most suitable choice across various transmitter densities, regardless of the numerology applied. While lower MCS levels perform better under baseline conditions by providing a stable performance, their advantage diminishes as communication density increases. This shift underscores the superiority of MCS-24, particularly evident in scenarios with heightened transmission demands, where its ability to efficiently handle higher data rates proves advantageous.
In conclusion, our findings establish 64QAM (MCS-24) as the optimal modulation and coding rate for 5G-NR V2X Sidelink broadcast communications across various numerology settings, marking a significant shift from previously recognized standards. By accounting for heterogeneous transmission characteristics and densities—reflective of the diverse and dynamic communication patterns anticipated in 5G V2X services—MCS-24 consistently outperforms other configurations. This robust adaptation to varying vehicular scenarios underscores its potential to enhance the systematic performance of 5G-NR Sidelink communication. These insights pave the way for further research aimed at optimizing 5G communication frameworks for advanced vehicular applications.

3.2 Ensuring High Reliability in 5G-NR Sidelink Communication

For URLLC services in V2X applications, a reception reliability of 10^{-5} is required. Despite the previously analyzed physical resource arrangements, the effectiveness of this reliability level also significantly depends on the scheduler selection at the MAC layer. Moreover, due to the stringent quality of service demands, this service is specifically designed for a limited subset of Vehicular UEs (VUEs). The subsequent sections will offer an in-depth analysis of these elements, providing insight into how high reliability is achieved within this specialized framework.

3.2.1 Methodology

Sidelink Scheduler

As outlined in Section 2.1.1, in the context of 5G-NR Sidelink communication, Mode 2 operates independently of network infrastructure, enabling vehicles to manage their own resource allocations in ad-hoc environments. In regards of the four enhanced sub-modes: in 2(a), each vehicle can select its resources autonomously based on semi-persistence sensing-based scheduling; 2(b) is a cooperative distributed scheduling approach, where UEs can assist each other in resource selection, for instance by sharing their selection window with neighboring VUEs and mitigating near-far effects; in 2(c), a VUE assigns resources for

others based on (pre-)configured transmission patterns; in 2(d), a VUE schedules the Sidelink transmissions for its neighbouring VUEs.
In the pursuit of refining the 5G-NR Sidelink scheduling for URLLC applications, we develop into modes 2(c) and 2(d). As previously pointed out, these modes are foundational for achieving the high reliability and low latency essential for URLLC services, making them suitable for critical vehicular communication scenarios.
In our research, we introduce a scheduling approach based on Optical Orthogonal Codes (OOC) for a deterministic mode-2(c) scheduler, which ensures channel access within defined delay bounds. OOCs have been widely adapted across various channel access technologies, with notable applications in Cellular Vehicle-to-Everything (C-V2X) communications, as demonstrated by Gallo et al. [82]. The core advantage of OOCs lies in their capability to minimize cross-correlation between any pairs of codewords v, u, significantly reducing the likelihood of transmission interference as formalized in Eq.3.4:

$$\sum_{j=1}^{L} v_j \cdot u_j \leq \lambda \qquad \forall u \neq v \tag{3.4}$$

In detailed, OOC generated codewords ensuring that the overlap in code elements between any two distinct codewords v and u across all slots does not exceed a small, predefined threshold λ. This characteristic, known as the cross-correlation property, essentially limits the likelihood of collisions or conflicts when multiple users attempt to access the same communication channel simultaneously.

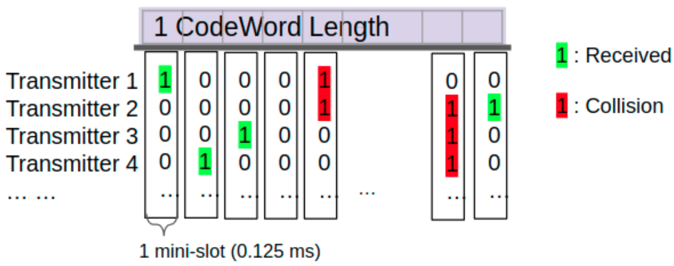

Figure 3.10: Example of OOC Access

By applying the OOC codewords, and with illustration in Fig. 3.10, our deterministic scheduling process is structured as follows:

- Each L-bit long OOC codeword configures a transmission pattern that adheres to the cross-correlation constraint. Each bit of the codeword corresponds to one *mini-slot*, with a duration of 0.125 ms, providing a granular time scale for transmission scheduling.
- VUE are permitted to transmit a packet during a *mini-slot* if the corresponding bit in the OOC codeword is a 1-bit. Conversely, VUEs are set to receiving mode when the OOC indicator is a 0-bit.
- The efficacy of this structured transmission protocol is illustrated in Fig. 3.10. Here, the codeword structure is visualized, with transmission slots indicated by red 1-bits signifying potential collision risks, and green 1-bits highlighting successful, conflict-free transmission windows.

- The re-transmission frequency, indicated by parameter w, is calibrated by the count of 1-bits within the codeword. This parameter dynamically influences how often a VUE can attempt transmissions within a designated cycle, effectively balancing between communication reliability and network resource utilization.

With the OOC cross-correlation restriction, this deterministic MAC layer scheduling structure reduces collisions and guarantees maximum successful transmission and reception. This represents an advancement over the Mode 2(c) MAC layer Sidelink scheduler, significantly enhancing reliability for URLLC services.

Physical Resource Arrangement

Since a higher numerology can effectively reduce the duration of a *mini-slot*, which is compensated for by its expansion of the frequency domain, we therefore apply numerology-3, which enables a unit duration as small as 0.125 ms. Considering the limited V2X bandwidth in 5.9 GHz frequency, in order to meet the 300 bytes packet size specified for URLLC Sidelink from [73], and to avoid the half-duplexing problem, we consider a pure time-domain multiplexing. As depicted in the right-hand image in Fig 2.6, considering a 10 MHz assigned V2X bandwidth under numerology-3, all 6 available PRBs are uniformly assigned to one user[2]. Under this method we can analyse the maximum capacity for transmission under this potential exhaustion.

Two Modulation and Coding Scheme (MCS) values, specifically MCS-8 (1/2 QPSK) and MCS-24 (64 QAM), are examined for their effectiveness in V2X communication. MCS-8, which is the default modulation for V2X, facilitates a data rate of 6 Mbps. This is a benchmark setting for ensuring broad compatibility across various vehicular communication scenarios. On the other hand, MCS-24, utilizing 64 QAM, offers enhanced overall performance. As detailed in the results section of the previous Chapter 3.1, MCS-24 demonstrates superior efficacy under a range of numerology values, highlighting its potential for higher data throughput and improved reliability in more demanding communication environments.

The maximum capacity S^M supported per allocation unit—specifically, one *mini-slot* can be approximated using Equation 3.5 as following :

$$S^M = 1/8 \times CR \times Q^m \times N^{Sym} \times N^{PRB} \times N^{sub} - S^h \tag{3.5}$$

In this function, we addressed two MCS impact factors : effective code rate value (CR) and modulation order (Q_m), which are described in Tables 5.1.3.1-2 in 3GPP standard [83]. N^{sym} represents the available symbols per slot for V2X traffic load (we consider 8 out of 14 symbols), N^{PRB} indicates the total available number of PRB in the frequency domain, N^{sub} indicates the number of subcarriers per slot, which is fixed to 12, and finally S^h is a 3-byte reservation for CRC_Length. This calculation is essential for understanding the potential bandwidth and service quality that can be achieved with these MCS settings under typical network conditions.

The maximum capacity for different numerology values, as calculated based on Eq. 3.5, is detailed in Table. 3.7. This table highlights the capacities associated with different

[2]Although 20 MHz is also baseline of bandwidth assigned for 5G-NR V2X communication, this is left for future study.

modulation schemes and mini-slot duration, specifically for numerologies ranging from 0 to 3.
Focusing on numerology-3 with a mini-slot duration of 0.125 ms, MCS-24 shows a capacity of 322.5 bytes per mini-slot. This capacity is well-suited for supporting V2X standard 300-byte packets, suggesting that MCS-24 can efficiently handle typical V2X data payloads with room to spare. This reflects MCS-24's capability to deliver higher throughput and potentially support more complex or data-intensive applications within the V2X domain
In contrast, MCS-8 at the same mini-slot duration can handle up to 83.3 bytes. Although significantly lower than MCS-24, this capacity is still adequate for basic control packets which are often smaller, around 32 bytes. This suggests that even with lower modulation, MCS-8 can effectively support essential V2X communication, particularly for sending control signals which generally require less data capacity.
It's important to note that although numerology-3 is not defined for Frequency Range 1 (FR1) at 5.9 GHz by 3GPP, its implementation could significantly enhance system performance in terms of latency and traffic capacity. This is particularly true even with the limited 10 MHz bandwidth allocated for V2X communication, as both MCS-8 and MCS-24 demonstrate reasonable capacities across the presented numerologies, confirming that advanced scheduling and modulation techniques can maximize throughput and reliability in constrained bandwidth scenarios.

μ	**mini-slot**	**MCS-8**		**MCS-24**	
	Size(ms)	$\mathbf{N^{PRB}}$	$\mathbf{S^{M}}$(bytes)	$\mathbf{N^{PRB}}$	$\mathbf{S^{M}}$(bytes)
0	1	53	736.2	53	2848.7
1	0.5	26	361.1	26	1397.5
2	0.25	13	180.6	13	698.8
3	0.125	6	83.3	6	322.5

Table 3.7: Max Capacity of one $mini - slot$

Admission Control

URLLC services have specific traffic patterns and in exchange, V2X URLLC services need to meet extreme reliability and delay requirements. In the current rel. 16 specification, 5G-NR V2X Sidelink mode 2 is designed to admit any VUE [35], however works from Garcia et al. [41]proved that its performance quickly degrades as a function of the number of VUEs. Therefore URLLC QoS cannot be met under unrestricted access policy, and a robust admission control strategy is required to accept the optimal number of VUEs for which stringent requirements can be met.
Admission control defines maximum users that can be admitted simultaneously to the system while efficiently using the available resources and satisfying QoS requirements. Admission control is therefore central to any 5G systems and more specifically to optimizing 5G-NR services (enhanced Massive Broadband (eMBB), massive Machine-Type Communication (mMTC) or URLLC).
Shashika et al. [49] proposed an optimization algorithm to tackle admission control optimization in a Multiple-Input Single-Output system. In [50], Ginige et al. proposed a coexistence support for both eMBB and URLLC users in 5G-NR, and pointed out the necessity of controlling the admissions of eMBB users to facilitate scheduling for all URLLC

users.
3GPP so far does not describe admission control strategies for 5G-NR V2X Sidelink mode multiple services support. Therefore in this work, we need to evaluate the optimal number of users that can be admitted into a 5G-NR V2X Sidelink URLLC services, consisting of a NR numerology-3 and a dedicated mode 2(c) scheduler, and guaranteeing URLLC QoS requirements.
URLLC services require to restrict access to a limited number of users. To analyse such limit, the maximum capacity for the accessible VUE needs to be analyzed. We formulate the admission control problem into an optimization equation in Eq. (3.6). The binary array $K(i)$ indicates whether Sidelink link i meets both reliability and latency demands, as expressed in Eq. (A.1), therefore the optimal target is to maximize Sidelink access link connections, indicating maximum system capacity.

$$\begin{aligned} \max_{w,L,N} \quad & \textstyle\sum_{i=1}^{N} k(i) \\ \text{s.t.} \quad & w \leq 3, \lambda = 1 \\ & L \in (0, 150], \forall L, w \in \mathbb{Z}^{+} \end{aligned} \tag{3.6}$$

$$k(i) = \begin{cases} 1 & \text{if } P_e \leq 10^{-5}, \text{ and } P_{T_d} \leq P_t^{min} \\ 0 & \text{otherwise.} \end{cases} \tag{3.7}$$

Constraints for the optimization problem relate to both reliability and latency URLLC service requirements. We focus on a reception reliability P_e of 10^{-5}, and a T_d ms delay with reliability of P_t^{min}. P_e is expressed in Eq. (3.8), as a function of the probability of success reception P_{sw} of one transmit packet over w transmission attempts.
In this study, λ is set to 1 so that every pair of codewords can have at most one overlapping '1'. μ represents transmission probability which is set to '1'. A uniform random access selection is considered, therefore Eq. (3.8) can be simplified as $P^{*}_{s_w}$. Moreover P_{T_d} is defined in Eq. (3.10).

$$P_e = (1 - P_{s_w})^{w} P_{s_w} = \mu \frac{\binom{L-w}{w-j}}{\sum_{l=0}^{\lambda} \binom{w}{l} \binom{L-w}{w-l}} \tag{3.8}$$

$$P^{*}_{s_w} = (1 - \frac{w}{L})^{N-1} \tag{3.9}$$

$$P_{T_d} = P^{*}_{s_w} + \sum_{i=0}^{\lceil \frac{T_d \times 8 \times W}{L} \rceil} w/L \times P^{*}_{s_w} \times (1 - P^{*}_{s_w})^{i} \tag{3.10}$$

We can see that L and w have cost-benefit trade-offs on both P_e and P_{T_d} performance: longer OOC codes L are capable of guaranteeing more admitted Sidelink links, but are inclined to allocate re-transmission slots separately, which significantly increases delay. Moreover, longer OOC codes reduce the system efficiency, particularly for periodical connections, which is relevant to URLLC service. Higher values for w promise a higher probability of successful reception, however resource exhaustion is reached more quickly.
The process of solving this admission control optimization is described in Algorithm 1, which provides the maximum number of Sidelink users that can be admitted under each L.

Algorithm 1 Admission Control Algorithm

while $w < 4$ **do**
    while $N < N^{max}$ **do**
        $i \leftarrow N$
        if $P_e \leq 10^{-5}$ and $P_{T_d} \leq P_t^{min}$ **then**
            $k(i) \leftarrow 1$
        else
            $k(i) \leftarrow 0$
        end if
        $N \leftarrow N + 1$
    end while
    return $K_w^*(N) = \sum_{i=1}^{N} k(i)$
    $w \leftarrow w + 1$
end while

3.2.2 Simulation and Result Analysis

Simulation Environment and KPI

We evaluate the proposed mechanism by Matlab simulations according to parameter settings described in Table A.1. All vehicles are allocated on a one-lane road scenario sending messages in broadcast to one reception vehicle[3]. A configurable number of transmitters are randomly generated according to the target 1km-wide communication density. Analysis of the impact created by channel fading, phase shifting and other physical layer criteria is left for future studies. Data traffic is generated at 10 Hz (100 ms) over the total simulation time to allow an ergodic analysis.

Table 3.8: Simulation Parameters Setting

Parameter	Value
Bandwidth	10 MHz
Applied Numerology	3
Hamming Weight w	1,2,3,4
Transmission Range	1000 m
Packet Rate	100 ms
Simulation time	30 s
Runs	300

Three key performance indicators (KPI) are selected in this paper:

- *Packet Reception Rate (PRR)* : This parameter is expressed in a Complementary Cumulative Distribution Function (CCDF) in relation to the number of transmitters.
- *Delay* : Delay is considered from two dimensions as depicted in Fig 3.11: the *absolute delay* measures the time interval from the generated data packet; the *relative delay* only considers the exact air time including channel access delay. Without

[3]The broadcast transmissions are received by all vehicles, we target for only 1 receiving vehicle for analysis purpose.

re-transmission, this value is set to one mini-slot (0.125 ms), whereas with re-transmissions this value is calculated as the time between the first successful reception and the relative starting time.

- *Number of controlled admissions* : This indicates the maximum number of admitted V2V (SL) links when both the packet reception rate and the delay conditions are satisfied.

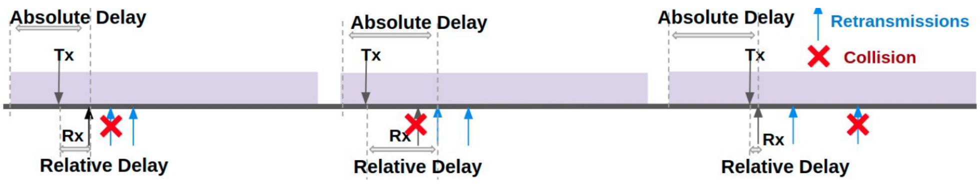

Figure 3.11: Delay Illustration

Performance Analysis under a fixed L

In this section, we analyze the PRR and delay performance using a fixed code-length of $L = 90 \times 8$, specifically focusing on stringent sub-millisecond (<1ms) latency requirements, illustrated in Figure 3.12. The figure compares analytical results (dashed points) with simulation outcomes (bold lines), highlighting discrepancies between the two.
Generally, both PRR and delay reliability deteriorate with an increase in user density. The analytical model tends to overestimate the optimal number of users due to its inability to account for near-far issues—a phenomenon where collisions from out-of-coverage users reduce the effective number of manageable users in simulations. This discrepancy is particularly pronounced in high-density scenarios, where near-far effects are more significant, thus widening the gap between analytical predictions and simulated realities. Consequently, the analytical model should be viewed as an idealized benchmark.

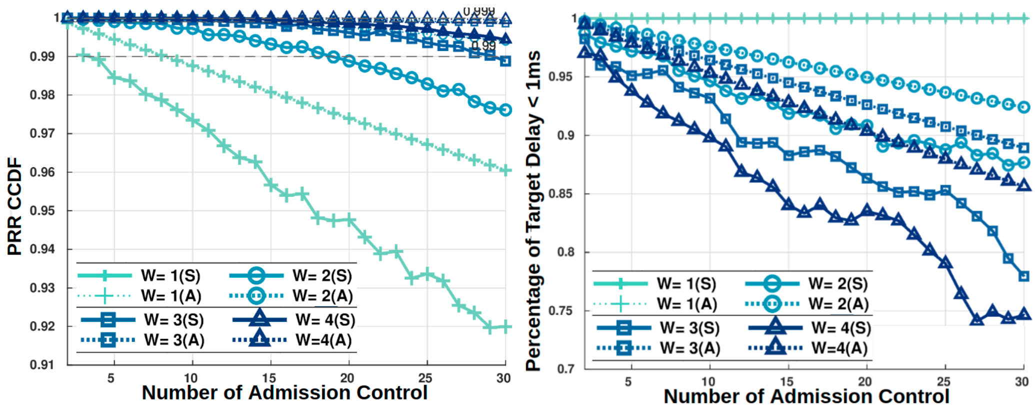

(a) PRR ccdf distribution (b) Probability (Delay $\leq$ 1ms)

Figure 3.12: PRR and Delay Distribution Graph of $L = 90 \times 8$

Nevertheless, we may observe correlated relationships between the analytical model and simulations under different re-transmission time w values: firstly a higher w can effectively improve the overall reliability suggested in Fig. 3.12(a), we can also verify that with lower $w = 1, 2$, it is extremely difficult to achieve the target reliability demand; secondly in terms of latency depicted in Fig. 3.12(b), as additional re-transmissions produce higher delays, the probability of fulfilling the sub-ms latency requirement is considerably reduced when more re-transmissions are generated. We can therefore identify that $w = 3$ achieved the optimal number of users admitted under the target URLLC requirement.

In this analysis, we also compare the impact of different traffic densities on communication performance, using scenarios with 5 and 20 transmitters as depicted in Figures 3.13(a) and 3.13(b), respectively. With fewer transmitters, delay metrics tend to cluster tightly around lower values, indicating a smoother transmission process. Conversely, as the number of transmitters increases, collisions become more frequent, particularly during the initial transmission attempts w. This leads to a broader spread of successful reception times, escalating the overall delay.

Additionally, higher w values, denoting a higher retransmission times, generally yield better performance in environments with fewer transmitters. However, as the transmitter count rises, the likelihood of initial collisions increases, offsetting the benefits of higher w values.

Examining the absolute delay in more depth via simulations, Fig. 3.13 depicts the distribution of the absolute delay, as we are interested in estimating the probability of a user being admitted under a given delay threshold. Accordingly, we rely on a kernel density estimate providing an overall evaluation of various distribution tendencies. It can be observed that the number of peaks for certain delay values is correlated with w, each peak representing the average delay of a transmission event.

This variance in performance underscores the necessity for a dynamically adaptable scheduling approach, like the proposed OOC mode 2(c) scheduler, which demonstrates efficient URLLC capabilities under certain conditions. To optimize performance across a wider range of scenarios, future research should focus on developing codewords with dynamic correlation properties, enhancing their adaptability to fluctuating traffic densities and transmission dynamics.

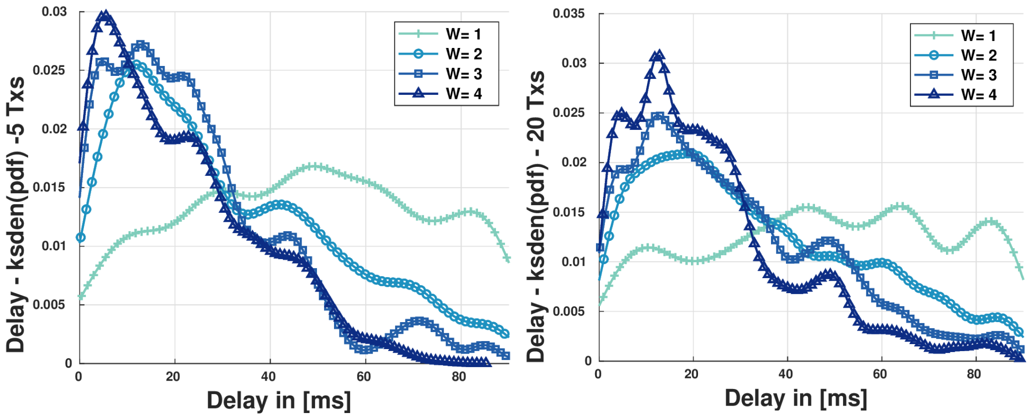

(a) 5 Transmitters (b) 20 Transmitters

Figure 3.13: Absolute Delay of $L = 90 \times 8$

General Result Analysis

In this section, we extend our analysis to include a broader range of codeword lengths, with the summarized results depicted in Table 3.9. Note that lower w values can only support an extremely limited number of Sidelink links under URLLC requirements. We therefore only focus on $w = 3$ and $w = 4$.
Without loss of generality, we conduct simulations with a codeword length of $[8 \times 60, 8 \times 120]$ (60, 120 indicating length in ms) to evaluate if an optimal codeword length can be identified. Considering L, the lower bound is the minimal requirement to support at least 2 transmitters to meet the target reliability constraint, whilst the upper bound is designed to limit one transmission per link within one frame. The $A - Result$ values derived from the analytical model generally overestimate the outcomes compared to the $S - Result$ values from practical simulations from scenarios described in Section 3.2.2, reflective of random variability and the near-far problem encountered in simulations. The discrepancies between analytical and simulated results underscore the complexities of real-world communication environments.
N^* represents the maximum supported Sidelink links to meet the target reliability P_e of 10^{-5}, while $P_{Td} \leq 1ms$ gives the corresponding probability for a successful reception within 1 ms latency. Again, the analytical results generally overestimate the simulation results, due to simulation randomness and the aforementioned near-far problem.
With higher w both analytical and simulation results show correlated benefits maximizing the supported admission Sidelink links. However, the relative delay increases, and the benefit is accordingly not significant enough to justify an increase from $w = 3$ to $w = 4$, or higher. Overall with $w = 3$ and an optimal code-word length ranging from $[8 \times 90, 8 \times 95]$, the investigated 5G-NR V2X Sidelink URLLC service cluster may support approximately 6 users.
It must be noted that this study is based on a worst-case scenario, only considering absolute collisions, and ignoring mobility, which has a favorable impact on fading and channel coding that could mitigate the number of packet losses due to collisions. It is therefore possible to expect a better performance under more realistic conditions, which we plan for future work.
The reliability of a given delay to be met is also listed in Table. 3.9, with relative delay threshold P_t^{min} of 99%, 99.9% and 99.99% (i.e. 10^{-1}, 10^{-2} and 10^{-3} failure for exceeding the target delay). Although some of the delay times are excessively long, this can still be considered a positive result, as it shows that 5G-NR V2X Sidelink at 5.9Ghz with 10Mhz bandwidth may provide a 10^{-4} reception reliability and a 10^{-1} delay reliability lower than 1 ms. Such reliability is better than what can be provided by the current 5G-NR V2X Sidelink communication systems.
In conclusion, the proposed architecture evaluated a solution for 5G-NR V2X Sidelink to support URLLC at 5.9GHz. Our proposed concept consists of applying a 5G-NR numerology-3, a 5G-NR V2X mode 2(c) deterministic scheduler and an analytical V2X Sidelink URLLC admission control mechanism. We demonstrated that 5G-NR V2X Sidelink can achieve a reliability of 10^{-4} at a latency lower than 1 ms with reliability of 10^{-1}. Although such URLLC performance is limited to a group of fewer than 10 vehicles in 300-byte packets, it is a reasonable density, and a comparative high packet capacity for a 5G-NR V2X Sidelink URLLC service.

Index		**Code Length L**	$\mathbf{60 \times 8}$	$\mathbf{70 \times 8}$	$\mathbf{80 \times 8}$	$\mathbf{85 \times 8}$	$\mathbf{90 \times 8}$	$\mathbf{95 \times 8}$	$\mathbf{100 \times 8}$	$\mathbf{110 \times 8}$	$\mathbf{120 \times 8}$
$\mathbf{w = 3}$	**A-Result**	$\mathbf{N^*}$	8	9	11	11	12	13	13	14	16
		$\mathbf{P_{Td \leq 1ms}}$	0.9591	0.9596	0.9557	0.9582	0.9565	0.9550	0.9571	0.9577	0.9552
	S-Result	$\mathbf{N^*}$	2	3	4	4	6	6	5	7	8
		$\mathbf{P_{Td \leq 1ms}}$	0.92	0.971	0.964	0.97	0.947	0.962	0.985	0.956	0.959
		$\mathbf{P_t^{min} \leq 0.9}$	$\leq 1ms$	$\leq 1ms$	$\leq 1ms$	$\leq 1ms$	$\leq 1ms$	$\leq 1ms$	$\leq 1ms$	$\leq 1ms$	$\leq 1ms$
		$\mathbf{P_t^{min} \leq 0.99}$	$\leq 30ms$	$\leq 30ms$	$\leq 35ms$	$\leq 35ms$	$\leq 35ms$	$\leq 40ms$	$\leq 10ms$	$\leq 30ms$	$\leq 50ms$
		$\mathbf{P_t^{min} \leq 0.999}$	$\leq 40ms$	$\leq 45ms$	$\leq 70ms$	$\leq 60ms$	$\leq 80ms$	$\leq 70ms$	$\leq 40ms$	$\leq 90ms$	$\leq 95ms$
$\mathbf{w = 4}$	**A-Result**	$\mathbf{N^*}$	13	15	17	18	19	20	22	24	26
		$\mathbf{P_{Td \leq 1ms}}$	0.9102	0.9094	0.9088	0.9086	0.9084	0.9082	0.9036	0.9037	0.9037
	S-Result	$\mathbf{N^*}$	5	7	8	8	7	6	12	13	14
		$\mathbf{P_{Td \leq 1ms}}$	0.932	0.906	0.915	0.909	0.934	0.922	0.886	0.909	0.892
		$\mathbf{P_t^{min} \leq 0.9}$	$\leq 1ms$	$\leq 1ms$	$\leq 1ms$	$\leq 1ms$	$\leq 1ms$	$\leq 1ms$	$\leq 5ms$	$\leq 1ms$	$\leq 5ms$
		$\mathbf{P_t^{min} \leq 0.99}$	$\leq 30ms$	$\leq 40ms$	$\leq 40ms$	$\leq 30ms$	$\leq 40ms$	$\leq 50ms$	$\leq 45ms$	$\leq 50ms$	$\leq 55ms$
		$\mathbf{P_t^{min} \leq 0.999}$	$\leq 40ms$	$\leq 55ms$	$\leq 60ms$	$\leq 45ms$	$\leq 65ms$	$\leq 70ms$	$\leq 75ms$	$\leq 80ms$	$\leq 90ms$

Table 3.9: General Result under different Code-word Length

3.3 Conclusion

In this section, we introduced a novel architecture to realize dependable 5G-NR Sidelink communication through a URLLC service for V2X communication. This design is based on the strategic reorganization of three key 5G-NR concepts influencing latency and reliability: NR numerology, MCS, and resource scheduling. Through extensive optimization of each parameter, we proposed a novel default configuration delivering exceptionally high performance compared to the default one.

Specifically, simulations conducted using an NS3 simulator have demonstrated that 64QAM (MCS 24) offers the optimal modulation and coding rate for 5G-NR V2X Sidelink broadcast communications. This represents a significant departure from traditionally favored settings such as QPSK (MCS 4) [75] and 16QAM (MCS 14) [66], suggesting that a thorough reevaluation of MCS settings is necessary to enhance performance across diverse traffic scenarios. The results underscore the potential of our proposed architectural adjustments in advancing the capabilities of Sidelink communications to meet the demanding requirements of URLLC.

The second phase of this study concentrated on developing a comprehensive architecture to realize URLLC via 5G-NR Sidelink communication. By fine-tuning key parameters such as MCS, numerology, and implementing a deterministic MAC layer scheduler, we jointly achieved low latency and high reliability, althouh it required a stringent admission control mechanism to limit the number of accepted Vehicle User Equipment (VUE). Initial mathematical models confirmed the viability of meeting rigorous V2X URLLC requirements through 5G-NR Sidelink. Integrating realistic channel models, we demonstrated that the proposed triplet (NR numerology, MCS, scheduler) can reach a reliability of 10^{-4} with a sub-ms latency.

It is important to note that while the URLLC standard from 3GPP Release 17 targets a reliability of 10^{-5} [73], our study achieved 10^{-4}. This discrepancy stems from the intentional design choice to reserve only 1 ms for URLLC services to evaluate the system's performance while preserving the majority of resources for general V2X communications (as discussed in Chapter 4). Allocating multiple 1-ms subframes for URLLC would support more VUE and enable retransmissions, which enable to get closer to the 3GPP URLLC limit. Nevertheless, Chapter 6 will demonstrate the true requirements on a realistic platooning use case, and will show that a 10^{-4} reliability is sufficiently rigorous for 5G-NR Sideling dependable V2X communication.

In the next chapter, we will integrate this URLLC triplet as a URLLC network slice on 5G-NR Sidelink and demonstrate its coexistance with other V2X services.

Chapter 4
Slicing the PC5 interface for Dependable 5G-NR Sidelink Communication

The previous chapter demonstrated the feasibility of providing a URLLC service on the 5G-NR SL for V2X communication. However, this service is based on non-standard parameter sets, which conflict with the parameter set specified by ETSI EN 303 798 [84] for 5G-NR V2X communication. A coexistence mechanism between the URLLC and the V2X services is therefore required. Considering the limited channel available for 5G-NR V2X, a multi-channel operation is not suited for operating 5G-NR SL URLL services. In this chapter, we therefore propose a dynamic channel sharing mechanism inspired by IEEE 1609.4 [85] and jointly based on network slicing concepts as well as 3GPP Proximity Services (ProSe) [86]. The mechanisms we present in this chapter first provide a URLLC service announcement mechanism for 5G-NR SL and then build dedicated URLLC slices configured according to the parameter set defined in Chapter 3. This work transposes the slicing concepts for 5G-NR UL/DL to the Uu interface (i.e. URLLC, eMBB, mMTC and V2X) over the 5G-NR SL on the PC5 interface by differentiating between a V2X slice for default ETSI ITS services and a URLLC slice for dependable 5G-NR SL V2X communications.
This chapter starts with an introduction of the ETSI ITS V2X services (awareness, perception, emergency notification, maneuvering, etc.). It then presents our proposed 5G-NR SL slicing mechanism to enable a set of protected slices with their own 5G-NR configuration (numerology, MCS, scheduler). The chapter continues with the definition of the slicing mechanism as a ProSe service, allowing on-demand and flexible slice creation on decentralized 5G-NR SL V2X communication. Finally we demonstrate via simulations the potential coexistence between 5G-NR SL V2X and URLLC slices on the PC5 interface.

4.1 ETSI Stack and Current Application Requirements

4.1.1 ETSI Stack for 5G-NR Applications

The ETSI stack, as detailed in Chapter 2, serves as the architectural foundation for managing V2X services operating on the C-ITS spectrum (i.e. 5.9GHz) in compliance with industry standards. This framework ensures that all V2X services adhere to standardized

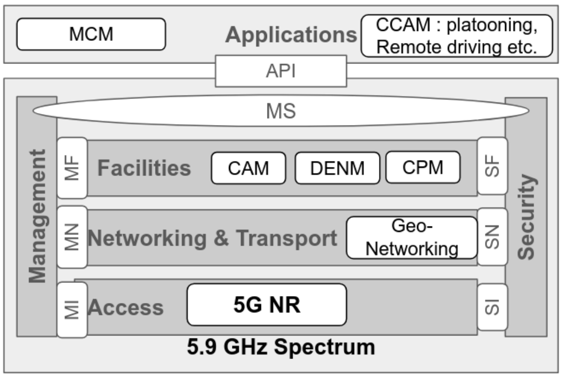

Figure 4.1: ETSI Stack over 5G-NR

protocols, particularly within the access layer, to facilitate seamless communication across vehicular networks as well as fair channel access between all V2X communicating devices. Specifically, within the 5G-NR context, as illustrated in Fig. 4.1, V2X services must be processed through the ETSI C-ITS architecture in order to access the 5.9 GHz C-ITS spectrum.

Each V2X *day-1* and *day-2* messages and also other CCAM messages is critical to support the dynamic usage of V2X applications. Messages such as CAM and DENM are fundamental for ensuring basic safety, while CPM provides cooperative sensor perception notably critical for automated driving functions. Furthermore, these messages exhibit dynamic characteristics; for example, the transmission rates of CAM and CPM, as well as the size of these messages, can fluctuate based on the traffic conditions.

The ETSI ITS stack proposed standardized layer-specific configurations across the 5G-NR spectrum as detailed in ETSI EN 303 798 [84]. These configurations are critical for ensuring performance under common operational parameters, as depicted on the left side of Fig. 4.2. Here, day-1 ETSI V2X messages adhere to ETSI defined QoS requirements, but the limited QoS provided by the 5G-NR V2X mode 2(a) Listen-before-Talk scheduler cannot provide better than a best-effort service without any delay guarantee.

In contrast, Advanced Cooperative, Connected, and Automated Mobility (CCAM) applications, which fall under URLLC services, require significantly more stringent latency and reliability standards compared to typical 5G-NR V2X QoS requirements. While standard 5G-NR V2X QoS aims for reliability between 90% to 99% and latency below 100 ms, CCAM demands escalate to a reliability of 99.99% to 99.999% and latency under 10 ms, as specified by 3GPP [62]. Achieving these elevated requirements with standard 5G-NR V2X parameter settings is challenging, underscoring the need for a robust system with a dedicated PC5 link, depicted on the right side of Figure. 4.2. This distinction emphasizes the necessity for specialized configurations to support the high demands of CCAM applications effectively.

The V2X day-1 and day-2 messages already subject the system to heavy traffic loads, while CCAM additional QoS-critical applications with stringent requirements must compete under the same resources. As outlined in ETSI TR 103 853 [18], the limited spectrum allocation of 10 or 20 MHz for V2X communications necessitates a sophisticated system architecture capable of efficient segmentation and dynamic resource management. This approach is essential not only for effectively sharing the V2X 5.9 GHz spectrum but also for dynamically adjusting layer-specific configurations to meet the diverse needs of various applications effectively.

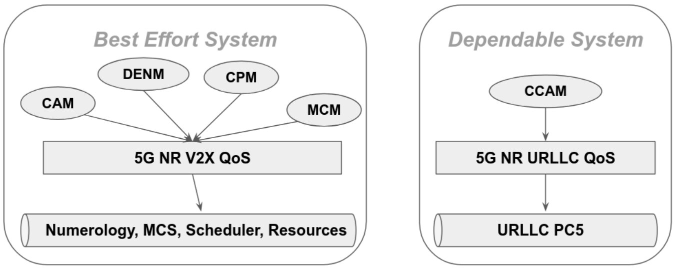

Figure 4.2: 5G-NR System QoS Mapping

4.1.2 Advanced CCAM QoS Requirements

This section highlights the critical communication requirements for Connected and Automated Mobility (CCAM), an advanced vehicular connectivity framework designed to enhance road safety, traffic efficiency, and driving comfort through integrated communication technologies and automation. As vehicular communication systems evolve, the support for QoS-critical CCAM applications that demand high reliability and precise timing becomes imperative. These requirements for applications such as vehicular platooning, remote driving system etc., are detailed in Chapter 2, Table. 2.4, and are aligned with the standards defined by 3GPP [62].

The focus of these applications is on enhancing traffic efficiency and increasing road safety, with stringent demands on latency, which can be lower than 10 ms, and high reliability, promised up to 99.999%. These applications are categorized under the service requirements of Ultra-Reliable and Low-Latency Communication (URLLC) in the 5G-NR framework, hence referred to as URLLC-demanding applications. Addressing the needs of these applications and ensuring the network can meet their requirements is a critical step in the development of 5G-NR V2X communication.

In particular, the current researches in focusing on providing the high QoS for these V2X applications have been studied widely. Ahmad et al. [12] provides a comprehensive review of QoS-critical V2X use cases, detailing the specific demands of each and the developments in enhancing QoS through resource reuse strategies such as subdivision into smaller cells and spectrum exploitation at higher mmWave frequencies. While the study has not yet explored these application realization from a pure Sidelink perspective. This oversight highlights a gap in understanding how to efficiently utilize the limited spectrum available for Sidelink V2X communication. Specifically, methodologies for creating smaller, corresponding clusters within the Sidelink framework remain to be clearly defined, indicating a pressing need for further research in this domain.

On top of this, there is an increasing demand for enhanced QoS in PC5 Sidelink communication from other advanced applications. For instance, decentralized federated learning for V2X, as highlighted by Barbieri et al. [17], relies on robust direct V2V links to facilitate rapid and reliable data exchanges among vehicles. This approach enables vehicles to share and process data locally using AI models, necessitating the capability to handle large data packets—up to 2.61 Gbps—within extremely tight latency constraints, approximately 1 ms. This requirement underscores the need for advanced, high-capacity, low-latency V2X

connectivity, which is a central aim of current 5G-NR and forthcoming 6G network technologies.
Building upon the need for advanced communication architectures, Zhang et al. [87] outline the future trajectory of 6G highlights the need for a highly heterogeneous and ultradense terrestrial network that also integrates innate intelligence and dynamic capabilities. This evolution extends beyond V2X to encompass the Internet of Things (IoT), incorporating a wider array of devices and diverse traffic types. The development of advanced D2D communication technologies that can efficiently handle dynamic, heterogeneous traffic scenarios is essential for the future growth of wireless communication systems, supporting a broader and more complex digital ecosystem.
The demands of high-performance V2X applications highlight the need for a direct communication system capable of managing traffic under varied conditions, where message rate and size differ significantly among applications. Additionally, the system must sustain ubiquitous connections to accommodate the high mobility dynamics typical of vehicular environments.
Advancements in pure PC5-based Sidelink communication over 5G-NR have been achieved through improvements in resource allocation. For instance, Hegde et al.[16] have enhanced group scheduling and mobility management for platoon groups within the Sidelink framework, introducing a simulation model that optimizes resource allocation within these groups. Similarly, M.C. Lucas-Estañ et al.[19] have developed a sensing-based, grant-free scheduling mechanism for vehicles within a group. This approach, assisted by uplink/downlink (UL/DL) channels, effectively delivers reliable URLLC services for the transmission of small data packets. However, most of these studies primarily focus on applying resource scheduling strategies with the assistance of 5G-NR infrastructure gNB, not from a pure Sidelink PC5 point of view.
Furthermore, it is crucial for the system to continually support the basic safety messages required by ETSI V2X, which consume a significant portion of the network resources. Given the varying requirements for delay, reliability, and data capacity across different applications, it becomes essential to allocate distinct resources that are specifically tailored to each application's needs. This not only optimizes the communication services for their intended functions but also guards them against mutual interference, a critical factor in high mobility and safety-sensitive environments.
These diversity and complexity make PC5 slicing an essential, yet largely understudied strategy for 5G-NR Sidelink communication. By creating separate slices, each with exclusive resources, interference is effectively eliminated, enhancing the reliability of critical communications. Furthermore, each slice can be customized with its own physical layer layout and specific resource allocation schedule, allowing the network to meet the dynamic quality of service demands of various applications. This tailored slicing strategy and its impact on V2X communication efficiency will be explored in greater detail in the subsequent section.

4.2 Slicing Methodology on 5G-NR Sidelink

In this section, we first formalize a method for defining network slicing, then examine the feasibility of implementing network slicing directly over 5G-NR Sidelink communication. By analyzing the basic structure of existing network slicing, our goal is to propose an full functional architecture that facilitates comprehensive management and configuration of network slicing solely through 5G-NR Sidelink communication.

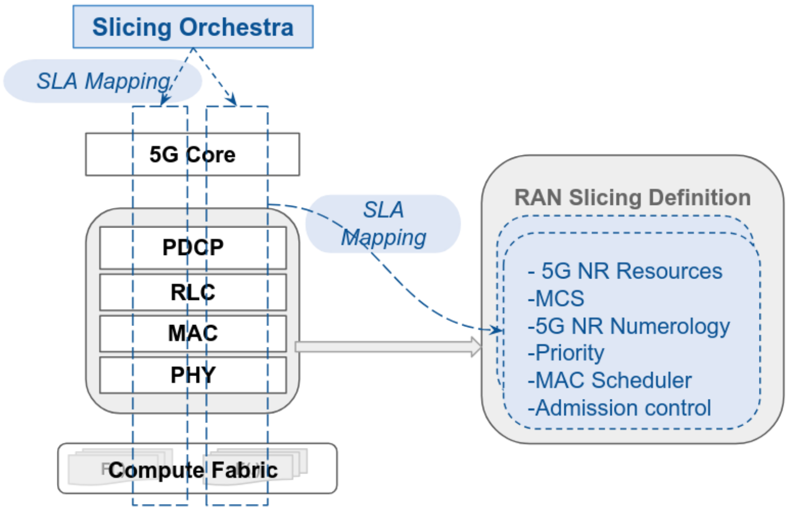

Figure 4.3: Proposed Network Slice Definition

4.2.1 Network Slice Definition

There is extensive ongoing research aimed at refining network slicing methodologies for 5G-NR, beginning with the initial standardization efforts in 3GPP Release 15 [88]. Subsequent definitions and enhancements have been contributed by various industry stakeholders, including notable inputs from Nokia [52] and the NGMN Alliance [89].

The overview of network slicing definition is illustrated in Fig. 4.3, network slicing spans end-to-end, encompassing both the Core Network (CN) and the Radio Access Network (RAN), and potentially even the network compute fabric. This methodology enables the division of a single physical infrastructure into multiple virtual networks. Through management by a slicing orchestrator, each network slice specifies its service requirements through Key Performance Indicators (KPIs) or Quality of Service Class Identifiers (QCIs), detailed in a Service Level Agreement (SLA). This agreement outlines how the network operator should configure the network to meet these specified needs.

In this study, we introduce a newly designed definition for network slicing which focus exclusively on RAN slicing; considerations of the CN, typically involving Software-Defined Networking (SDN) and Network Function Virtualization (NFV), are beyond this work's scope. Moreover, for simplicity, all communications are considered to occur via a single antenna setup without multi-tenancy sharing.

For RAN slicing specifically, the SLA-mapped parameters define the RAN layer settings. The proposed RAN slicing design focuses on several parameters: reserved resources over the physical spectrum, the Modulation and Coding Scheme (MCS) which determines the data rate within the slice, 5G-NR numerology choices, slice priority, the MAC layer scheduler—which dictates resource allocation to users within the slice—and admission control. The latter ensures a controlled number of users within the slice to maintain the desired QoS.

4.2.2 Network Slice Architecture

The 3GPP standards [63] and most of the researches focus primarily on uplink/downlink (UL/DL) Uu link slice management, where a service requirement must pass through a base station before being assigned to the target user.
For example, the study by Campolo et al.[23] presents a methodology for implementing network slicing from the RAN to the core network specifically for V2X communications. This research proposes multiple network slices tailored to distinct categories of V2X services, encompassing a comprehensive slicing framework that extends through the higher layers of the core network infrastructure.
Building on the Sidelink methodology recently outlined by Qualcomm [26], we have tailored the scenarios to better fit our objectives and have refined the Sidelink slicing methodology accordingly. This adjusted approach is detailed in Fig. 4.5, where we present our specific adaptations and enhancements to the original structure.
The figure compares UL/DL with Sidelink slicing methodologies in the context of 5G-NR V2X D2D communication. Fig. 4.4(a) depicts the conventional network slicing approach. In this UL/DL setup, the transmitting UE initially identifies the appropriate slice based on the application requirements—labelled as V2X *App1* and *App2*. This detailed slice information is then communicated to the gNB through Uu-link, which acts as the intermediary between the TX UE and the core network. The core network plays a crucial role in determining the final slice configuration, which is subsequently announced back to both the TX and receiving UE (RX UE) via the gNB. This method ensures that all communication through the slices is managed and orchestrated centrally by the core network and the gNB, providing robust control but at the expense of increased communication latency. However, in V2X scenarios, direct communication among vehicles can support numerous applications, owing to the high mobility and dynamic nature of V2X environments. Therefore, enabling the PC5 direct control for network slicing can significantly enhance V2X system performance, providing substantial benefits for future V2X studies. In contract to UL/DL network slicing, Fig. 4.4(b) presents the Sidelink slicing methodology, which simplifies and optimizes the configuration process. In this model, slice determination and configuration are managed directly between the TX-UE and RX UEs through the PC5 interface, completely bypassing the gNB. For the exchange of network slicing information over Sidelink, our design includes crucial elements as outlined in the accompanying table. This includes the Slice ID for identifying the correct slice, the allocated resource blocks for that slice, the numerology value applied, and the choice of MAC layer scheduler. These parameters ensure that any newly accepted UE can seamlessly integrate with the existing slice configuration, adapting 5G-NR parameters as necessary to fit within the designated slice. The table also indicates the current availability of each slice, showing how many additional UEs it can accommodate, thus allowing for dynamic scaling of network resources. In this preliminary study on D2D slicing, which aligns with V2X standard requirements outlined in Section 2.3, we aim to formalize a network slicing framework over 5G-NR Sidelink. This framework is designed to support the continuous transmission of general V2X messages, such as CAM and DENM, enhances process speed and reduces dependence on core network infrastructure. This is particularly beneficial for advanced decentralized technologies like federated learning. By utilizing Sidelink slicing, users gain a localized view of current statuses and requirements, enabling more efficient resource allocation.

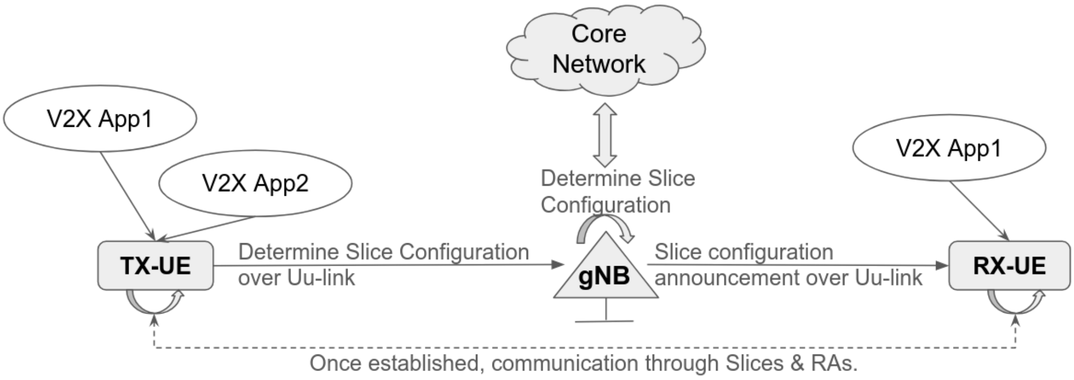

(a) UL/DL Slicing Methodology

Slice ID	Resources	numerology	MAC Scheduler	Slice Availability
Slice1	RA1	mu-x	Mode2 - (x)	n_x
Slice2	RA2	mu-y	Mode 2 - (y)	n_y

(b) Sidelink Slicing Methodology

Figure 4.4: Slicing Comparison between tradition and Sidelink network

4.2.3 5G-NR Sidelink Slicing Methodology

Based on the foundational concepts for 5G-NR Sidelink Slicing introduced in the previous section, the architectural challenges remain to be addressed before a fully functional architecture can be realized. These challenges include unclear mechanisms for translating network slicing requests into service announcements over the PC5 link; the need for further design in group management within slicing; and the essential provision of robust security measures for managing and configuring different slices. These issues form critical barriers that must be overcome to enable effective and secure network slicing on the 5G-NR Sidelink.

To have a benchmark for this novel structure design, we based on the work from Ciprian et al. [27], who proposed a framework that addresses resource allocation for slice coexistence in V2X communications alongside multiple other service types. This framework, as depicted in Figure4.5(a), begins when a vehicle requests a service from the base station. The base station then checks its current list of available slices. If the appropriate slice is available, the base station allocates it to the vehicle for the targeted slice. This work also accounts for the dynamic movement of vehicles by defining lock, leave, release, and move states. This framework ensures that if a vehicle moves beyond the range of the current base station, it can be seamlessly handed over to the nearest base station and assigned a new slice.

Based on their proposal, we design our Sidelink slicing procedure as illustrated in Fig. 4.5(b), the slice leader continuously broadcasts its current in-service slice information.

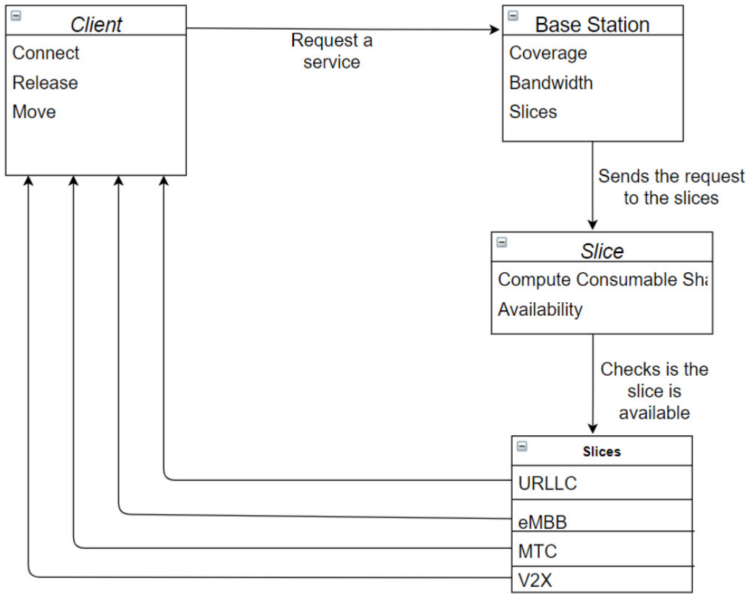

(a) Reference Network Slicing Framework for V2X [27]

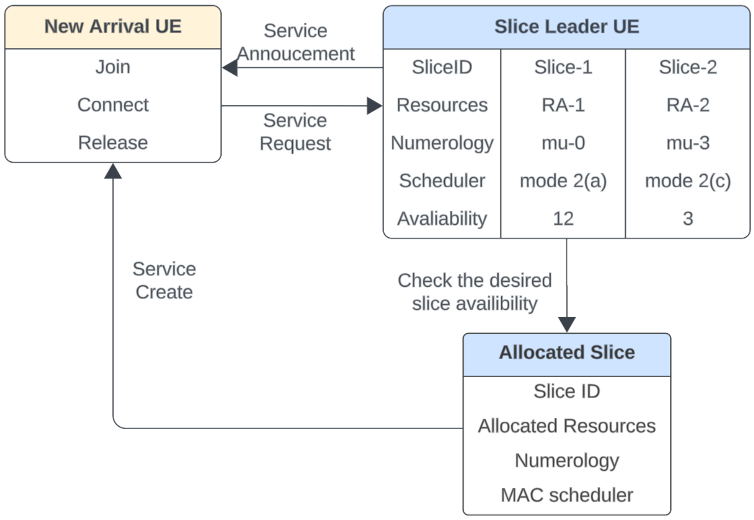

(b) Proposed PC5 Sidelink Slicing Framework

Figure 4.5: Network Slicing Framework

Similar to the slice table design we've proposed in Figure. 4.4(b), further slicing definition information are stored at the leader UE, such as resources allocation, numerology, MAC-layer scheduler. The detailed settings for various parameters will be discussed in the following section.

When a new UE desires to join a particular service, it submits a direct request to the slice leader. The leader then checks its local slice list to locate the requested service and evaluates admission control parameters to determine the slice's capacity to accommodate new members. If feasible, the slice leader UE sends the slice configuration to the new arrival, and resources are allocated to integrate this vehicle into the slice. Additionally, each UE member within the slice has the option to exit the slice under a release state, and the allocated resources are consequently freed.

4.3 ProSe-based Slicing for V2X 5G-NR Sidelink

The URLLC service presented in Chapter 3 as well as the slicing mechanism described in Section 4.2 are both based on the concept of groups/clusters, assuming the existence of a cluster/group leader coordinating the actions of the cluster/group members. In this section, we specifically address the challenge of creating and managing such groups for 5G-NR Sidelink.

3GPP 5G-NR V2X rel.16 does not *per se* handle group management and delegates such management to upper protocol layers. In practice, 5G-NR V2X rel.16 group management is handled in Europe by the ETSI ITS Geonet stack. Defining 5G-NR Sidelink URLLC services, we would like to avoid depending on non-3GPP services to reach that objective. 3GPP however introduced the concept of Proximity Services (ProSe) since rel.12 for LTE and more recently in rel.17 for 5G-NR. In this section, we therefore use and extend the 3GPP ProSe to enable group management for the previously described URLLC and URLLC Slice services.

We first introduce the 3GPP ProSe standard, then describe the required extensions to ProSe messages to enable 5G-NR Sidelink URLLC slicing and finally evaluate the performance of 5G-NR Sidelink communication with ProSe enabled V2X and URLCC slices.

4.3.1 5G ProSe Standard

The 5G Proximity Services (ProSe) standard is a significant advancement within the 3GPP framework, first introduced in 3GPP TS 33.303 rel.12 [90] and further refined in ETSI TS 124 554 rel.17 [86] for 5G-NR. It extends the 3GPP NR V2X mechanisms to any other type of proximity service requiring D2D communication by facilitating effective group management through service announcements. This standard plays a key role in both public safety and commercial applications by enabling devices to discover the existence of D2D services and enable to securely communicate over the PC5 Sidelink interface. Similarly to 5G-NR V2X, ProSe operates without the need for higher network infrastructure as gNB, which is particularly beneficial in scenarios where network coverage is unreliable or unavailable.

The ProSe standard in 3GPP TS 124.554 rel.17 [86] specifies the procedures for setting up and managing direct communications in 5G networks. We listed these messages in Table. 4.1, with key parameters and the main purpose of each message. This includes the *ProSe direct discovery process*, where an authorized UE (the announcing UE) broadcasts a ProSe PC5 Discovery message. This message is picked up by monitoring UEs that wish to join the ProSe service. There are two models for this discovery process: Model A, which solely involves announcements, and Model B, which requires solicitations and responses, necessitating feedback from monitoring UEs. For simplicity and broader applicability, our study employs Model A, thus eliminating the need for response messages.

The *ProSe direct link establishment procedure* is another critical component, enabling the formation of a direct communication link between two UEs—the initiating UE and the target UE. This process involves exchanging request and acceptance messages that also communicate the PC5 QoS parameters for the intended QoS flows. Additionally, the ProSe standard outlines conditions under which a direct link establishment can be rejected. A primary condition is the availability of an admission control mechanism, this enables leader UE to reject a joining request on varies conditions, such as due to insufficient resources to support a new 5G ProSe direct link. Furthermore, ProSe allows for the termination of a direct link through a structured release procedure. This process is initiated by the UE desiring to end the link and involves the exchange of direct link release request and acceptance messages.

Table 4.1: ProSe Message List

Message Name	Parameters	Purpose
ProSe PC5 Discovery Announcement Message	Slice ID, QoS, Availability	Broadcast the available slice(s).
ProSe Direct Link Establishment Request	UE ID, Slice ID	Request to target slice.
ProSe Direct Link Establishment Accept	Slice ID, assigned PRB, numerology MCS etc.	Join accept with slice parameters set.
ProSe Direct Link Establishment Reject	UE ID, Slice ID	Join reject under conditions.
ProSe Direct Link Release Request	UE ID, PRB reservation, Slice ID	Inform the slice leader of leaving request.
ProSe Direct Link Release Accept	-	Once accepted, the reserved PRB resources are released.

On top of the configuration procedure, ProSe can further support direct applications of lower-layer resource allocation and parameter settings through direct 5G-NR Sidelink network slicing. Its service announcement architecture not only provides fundamental security assurances by restricting access to predefined groups and managing encryption but also supports robust group management functionalities. These features are crucial for V2X communications, facilitating the formation of local clusters where devices within proximity efficiently self-organize and manage communications to enhance operational efficiency and response times.

We thereby proposed the novel framework leverages ProSe-defined communication messages for seamless service management, where service requests and acceptances are conducted through ProSe link requests and establishment procedures, respectively. This integration is depicted in Figure. 4.6, illustrating how ProSe effectively merges into the lower layers such as RRC and PDCP. By functioning as a service announcement layer, ProSe enhances safety at the application layer, ensuring a robust connection that optimizes network performance by leveraging direct communication pathways. This methodology not only enhances the efficacy of the design but also ensures the flexibility and security necessary for managing slice memberships within the network slicing architecture. This integration ensures a robust connection, enhancing reliability and optimizing network performance by leveraging direct communication pathways.

4.3.2 ProSe-based Cluster Management

This section elaborates on the specifics of ProSe-based cluster management and configuration, outlining the message exchanges and procedures for cluster join and leave management, as well as slice assignment. Figure 4.7 visually represents these processes across four main phases:

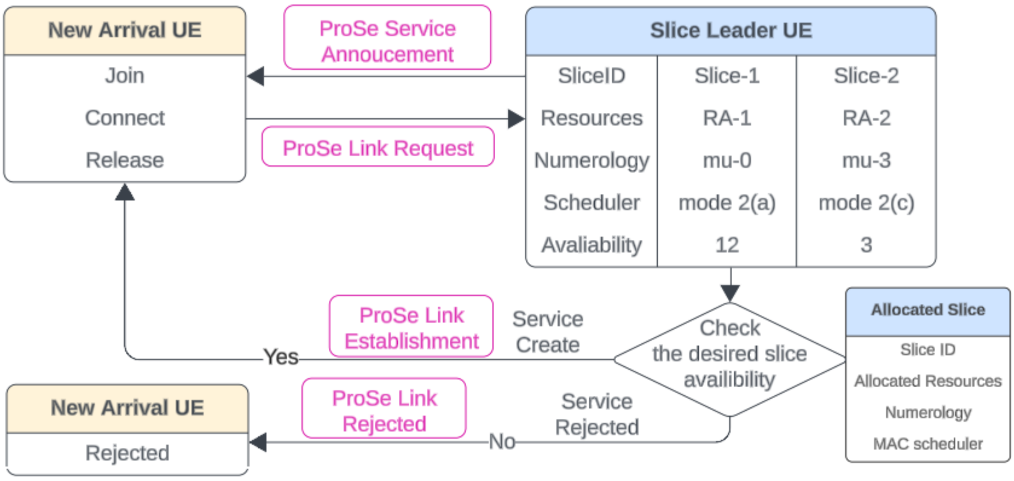

Figure 4.6: Proposed ProSe-based Sidelink Slicing Framework

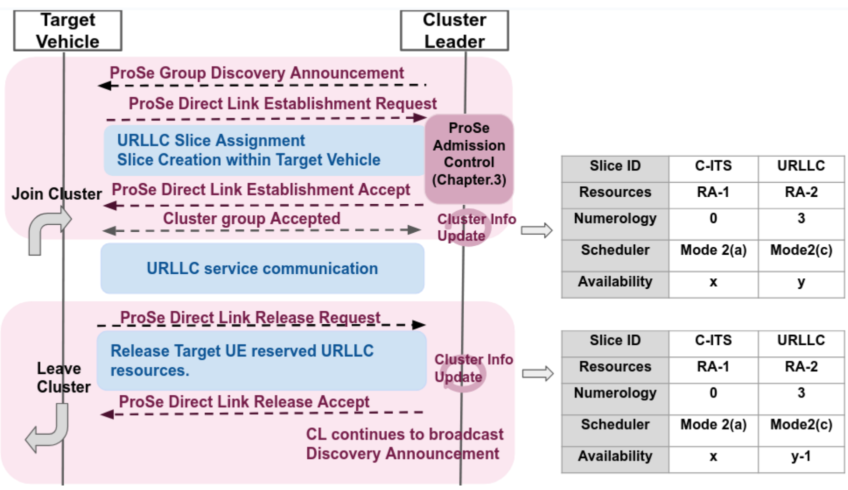

Figure 4.7: Proposed Group Configuration Architecture

- *Group Management Initial Announcement:* Initially, the cluster leader(CL) is authorised to act as the announcing UE, allowing it to transmit group service announcements to its neighbours via the ProSe PC5 Discovery Message. Nearby target vehicles who want to join the current group act as monitoring UEs, constantly listening to their neighbours' ProSe discovery messages from current adjacent cluster before they are accepted by any cluster. To simplify the system, we applied the ProSe Model-A discovery procedure, where no response is required from neighbouring vehicles.

- *Joining Cluster Group:* When a new vehicle wants to join a cluster, it will piggyback its joining request through a ProSe Direct-Link-Request message to the CL. The CL is obliged to check its local cluster list first. We apply an admission control scheme, that has been proposed from Chapter 3. Meanwhile in correlation with the standard, this admission control scheme is through adjustment of the ProSe Standard Section 7.2.3.5 in [86], under condition #5: "when leader rejects a joining request because of lack of resources for 5G ProSe direct link." The CL is obliged to consult its local table to determine the current availability within the cluster. If there is a vacancy, the new arrival can be accepted into the cluster. However, if no slots are available, the CL will issue a rejection to the new arrival.

- *URLLC for Intra-Cluster Communication:* Upon acceptance, the new cluster member triggered by the ProSe establish messages, starts to allocate its local resources for URLLC slices according to the cluster slice design. Additionally, the design of the protected URLLC slice parameters are listed inside the table, as illustrated on the right side in Figure. 4.7, and will be transferred to the target vehicle. In details, the CL assigns a slot to this new member based on a predetermined pattern from the deterministic Mode 2(c) scheduler scheme. The new member is allocated a specific URLLC resource slot according to the CL's scheduling pattern, this scheduling pattern design is to be investigated in the following. Note that security configurations are not considered in this study. Subsequently, each cluster member is restricted to transmitting intra-cluster messages solely on its reserved slots and continues listening during other slots within the URLLC Slice. Therefore, high reliability and low latency can be guaranteed for cluster critical URLL communication.

- *Leaving Cluster Group:* When a member vehicle wants to leave the current cluster, it generates a ProSe Direct-Link-Release message to inform the CL of its request to leave. The CL first releases the reservation within the URLLC slice for this target vehicle and then replies with a ProSe Direct-Link-Release Accept message to complete the departure procedure. This target vehicle will then release its local cluster slice reservation and return to its initial state; meanwhile, the CL must update the local information of the cluster.

Under this construction, cluster management and intercommunication can be fully realised using ProSe-based Sidelink communication. It should be noted that the URLLC slice assignment and release require authentication and authorization from the upper-layer infrastructures, which are beyond the scope of this study and are assumed to be fully functional.

4.3.3 Cluster URLLC Slice Design

The default pure C-ITS communication frequency band, as illustrated in Fig.4.8(a), is to support general ITS messages for basic road safety, such as CAM, DENM, and CPM as mentioned before. In this research, we propose a novel combined-slice design, outlined in Fig.4.8(b), where a periodic reservation in the time domain is allocated for cluster group communication. The cluster slice (depicted in light blue) is designed for communication needs of high stringency with minimal resource demands. Consequently, the reservation period for the cluster slice is significantly shorter than that of the C-ITS slice. Additionally, adhering to the standard inter-packet gap of 10 ms in V2X technologies, as recommended by 5GAA [91], only 1 ms is designated for the cluster slice within each 10 ms C-ITS slice.

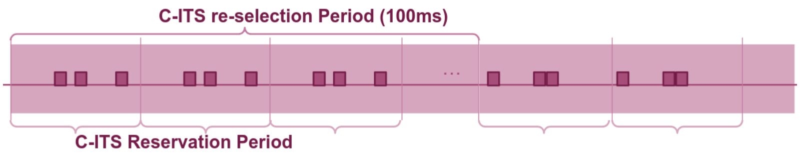

(a) Pure C-ITS Slice

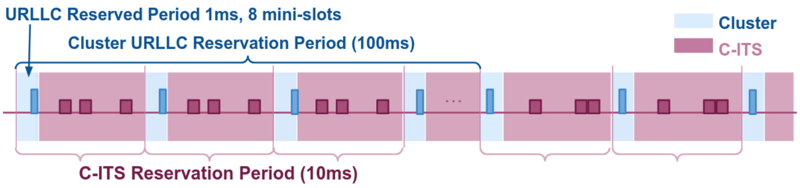

(b) Combined Slice : C-ITS and Cluster

Figure 4.8: Slices Physical Layer Illustration

In order to meet the stringent demands of URLLC in terms of low latency and high reliability, certain key parameters within the communication framework are strategically reconfigured. This approach is distinctly outlined in a comparative analysis between general C-ITS and more specialized cluster slices, as depicted in Table. 4.2. For the cluster slice, several modifications are detailed:

- The numerology applied is increased to $\mu - 3$, which notably reduces the duration of each mini-slot to just 0.125 milliseconds. This alteration is crucial as it facilitates up to eight distinct transmissions within a singular 1-millisecond frame, effectively complying with the 1-millisecond latency requirement. These subdivisions are visually represented by blue partitions in Fig.4.8(b), this adjustment ensures the 1 ms latency bound is met.

- A higher Modulation and Coding Scheme (MCS) is applied. With the allocated bandwidth for V2X communication capped at 20 MHz, the implementation of a higher MCS, specifically MCS-24, is pivotal. This selection is aimed at maximizing the data throughput within the limited spectrum, thereby enhancing the overall capacity of the URLLC Slice. The choice of MCS-24 has been rigorously analyzed and proven to be optimal in heterogeneous V2X Sidelink scenarios in previous Section. 3, ensuring robust and efficient data transmission.

- Resource allocation for communication is meticulously organized into 10-millisecond segments. Within this framework, the initial 1 millisecond of each segment is exclusively reserved for URLLC communications, ensuring that the critical latency requirements are met without disruption. The subsequent 9 milliseconds are then allocated for general V2X communications. This pattern of periodic reservation recurs every 100 milliseconds, creating a structured yet dynamic allocation system that supports varied communication needs efficiently.

- Unlike the conventional sensing-based Scheduling mode 2(a) utilized in the C-ITS slice, the URLLC slice adopts a deterministic Time-Division Multiple Access (TDMA) scheduling approach, specifically mode 2(c). This method involves the creation of a pre-defined transmission pattern by the cluster leader, which is then disseminated among the cluster members. In practical terms, this scheduling ensures that each member within a cluster is allotted one mini-slot per millisecond, as depicted in Fig. 4.8(b). Such an arrangement permits a total of eight precise assignments within each millisecond frame. In cases where the cluster size exceeds eight, a random slot selection mechanism is employed within the current slice reservation to evaluate the maximum admission control limit, thereby ensuring that all members achieve direct transmission with the required low latency.

Under this methodology, the system ensures dynamic management and efficient utilization of network resources in a decentralized manner. By allowing direct, local management of slices, the system can adapt more quickly to the needs of individual users and specific applications, effectively minimizing latency and maximizing the reliability of communications. This approach is particularly advantageous in V2X scenarios where rapid adaptability and high reliability are critical.

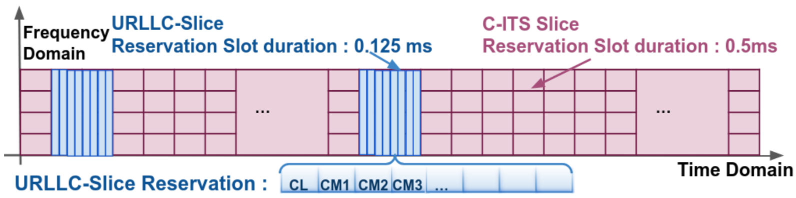

Figure 4.9: Combined Slice Design and Reservation Indication

Table 4.2: Slices Configuration Parameters

Parameters	C-ITS Slice	Cluster Slice
Numerology	1	3
Reserved Period	9ms/10ms	1ms/10ms
Re-selection Period	100 ms	-
Operation Frequency	5.9 GHz	5.9 GHz
Applied Bandwidth	20 MHz	20 MHz
MAC Resource Allocation	mode 2(a)	mode 2(c)

4.3.4 Simulation Result Analysis

Simulation Environment Campaigns

We implement the combined slice design described in the methodology onto 5G-LENA Network Simulator (NS3), on version *nr-v2x-dev* which enables 5G-NR direct Sidelink communication simulation [65]. For performance evaluation we focus on the general communication traffic performance between different slice designs, therefore the previous proposed ProSe-based cluster configurations are taking operational assumptions as completed.

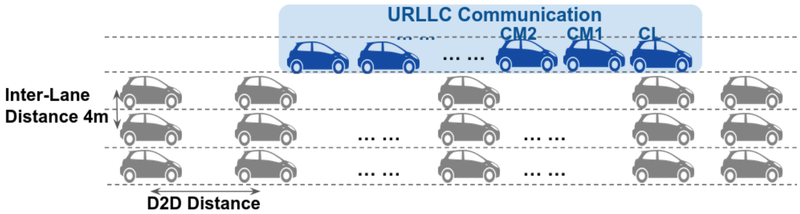

Figure 4.10: Scenario Topology

A four-lane highway V2X scenario is constructed for our simulation topology, as shown in Fig. 4.10. One lane is reserved for cluster vehicles, the rest lanes are occupied by outside vehicles. V2V distance varies according to target communication densities. For C-ITS communication, transmitters broadcast typical CAM messages of 300 bytes at a rate of 1Hz, all directed to a single reception vehicle.[1]. For inter-cluster communication, transmissions are generated by all other cluster members to one cluster receiver. To evaluate the maximum capacity of this cluster slice, the sent packet size is set to 300 bytes, at a high transmission rate of 10 Hz.

3GPP Channel Model[92] is applied in the simulation, which takes into consideration for both fading and shadowing to produce a realistic physical channel environment. For each scenario, 40 random channel realisations are performed in order to acquire statistical performance results. All results are illustrated within a confidence interval (CI) of 90%.

When analysing impact on the overall performance, in order to not to lose generality, we rely on a harmonizing metric which is called *Communication Density*, defined as follows:

$$Dens^{Comm} = \frac{Msg^{Rate} \times Tx^{Range}}{Dist^{V2V}} \tag{4.1}$$

Varying the parameters of transmit range, traffic density, and message rate, while maintaining a overall constant communication density, will lead to similar broadcast communication performances as discussed in [75].

Impact of URLLC Slice Cluster on V2X Communication

This section explores the impact of cluster slices on general V2X communication, focusing on general C-ITS message exchanges; the intra-cluster performance will be discussed in the following section. In practice, all vehicles, including those in clusters, are required to communicate general C-ITS messages. To simplify the scenario and maintain equivalent topology across both slice designs, for cluster topology, we assign 8 vehicles at a distance interval of 10 meters, this distance interval will be investigated in the following section. These vehicles are configured solely to transmit cluster messages and to function as receivers for C-ITS messages.

For the outside vehicles, three groups of simulations regarding to different aspect of communication densities are generated for both slicing designs, detailed topology settings are

[1]The broadcast transmission is intended to all vehicles, but we only consider 1 receiving vehicle for analysis purpose.

Table 4.3: Different Groups Scenario Setting

	Group A					Group B				
Dist$^{\mathbf{v2v}}$ (m)	50	40	20	10	8	10	20	40	50	60
Tx$^{\mathbf{rg}}$ (m)	200	200	200	200	200	50	100	200	250	300
Msg$^{\mathbf{rt}}$ (Hz)	12.5	10	5	2.5	2	10	10	10	10	10
	Group C									
Dist$^{\mathbf{v2v}}$ (m)	40	40	40	40	40					
Tx$^{\mathbf{rg}}$ (m)	80	120	200	320	400					
Msg$^{\mathbf{rt}}$ (Hz)	25	16.7	10	6.25	5					

provided in Table 4.3. Each group controls a specific density parameter: Group A focuses on a fixed transmission range; Group B keeps a constant overall message rate per vehicle; and Group C maintains a consistent V2V distance. Results regarding to the V2X C-ITS messages communication are depicted in Fig. 4.11. These results are evaluated primarily on Packet Reception Rate (PRR), and averaged with confidence interval of 90% over 40 runs. Results from the pure C-ITS slice design are illustrated in red, whereas those from the combined slice design are plotted in blue.

From the overall distribution, under the same communication densities, Groups A and C, which maintain transmission range and V2V distance respectively, show that varying communication density significantly affects performance, while Group B maintains stable performance at a consistent message rate. Additionally, for all groups, deploying a URLLC slice appears to have only a minor impact on overall C-ITS communication, as packet reception rates are similar for both slice designs.

Further observations reveal that the URLLC slice has a slightly greater impact under conditions of lower transmission rates or lager transmission ranges. This is due to resource exemptions by URLLC reservation leading to some packet reception loss. This effect is particularly noticeable when the actual reception rate is low; however, this impact becomes negligible when the reception rates are higher, implying that the URLLC slice integration does not significantly disrupt the overall C-ITS communications under typical operational conditions.

The conclusion from this part of results show that integrating a URLLC slice within the general 5G Sidelink V2X communication framework minimally affects the robustness of C-ITS services across a range of communication densities. The observed differences between the pure and combined slicing approaches are minor and cause limited impact on the overall network performance, even under varied communication topology settings. This analysis confirms the feasibility of employing Sidelink network slicing to manage diverse traffic demands while maintaining high communication integrity within V2X scenarios.

Performance Analysis of Intra-Cluster on V2X Communication

In this section we investigates into the performance characteristics within the cluster slice, aiming to satisfy the stringent requirements for URLLC's high reliability and low latency. In the intra-cluster scenario, one vehicle serves as a receiver and the rest of cluster vehicles act as transmitters. By adjusting the number of transmitters, we assess the maximum capacity of the configured cluster slice.

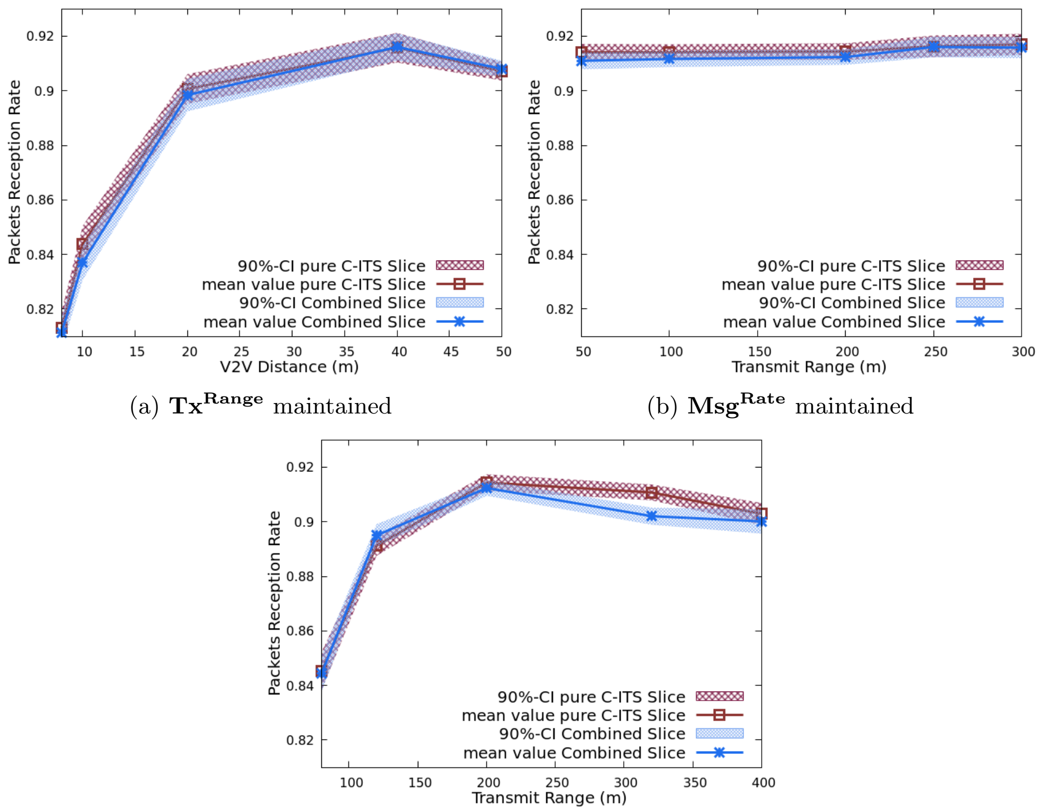

(a) $\mathbf{Tx}^{\mathbf{Range}}$ maintained

(b) $\mathbf{Msg}^{\mathbf{Rate}}$ maintained

(c) $\mathbf{Dist}^{\mathbf{V2V}}$ maintained

Figure 4.11: Comparison of PRR between Pure C-ITS Slice and Combined Slice

We investigate two cluster topology layouts with V2V distances of 5 and 10 meters[2]. The differences in results between these two layouts can be attributed to the degradation of communication quality solely due to physical channel propagation. Packet reception rate results are shown in Fig. 4.12(a), where both layouts exhibit stable communication until the number of transmitters exceeds 7. This behavior aligns with our designed resource allocation scheme. In this scheme, the MAC layer scheduler self-adjusts based on the actual cluster size. When the size is fewer than 8, *mini-slots* are deterministically allocated based on member indices using a TDMA scheduling scheme—specifically, one *mini-slot* per user over 1 ms. When the cluster size surpasses this limit, a random selection mechanism is triggered, leading to increased packet collision and loss.
The red lines represent the targeted URLLC service requirements of 99.999% and 99.99% reliability. While the 3GPP standard requires a 99.999% reliability level for URLLC services, this threshold is widely recognized as exceedingly challenging to meet in practice. Our results demonstrate this argument, indicating that such high reliability can only be achieved within a given confidence interval. Importantly, this decrease in reliability arises from realistic channel model limitations, not from any methodological issues in our system, and thus lies beyond the scope of this study. However, the 99.99% reliability level is readily achievable and is considered a practical requirement for current URLLC services.

[2]This distance is distinct from the physical vehicle interval; it represents the point-to-point distance from which the actual vehicle length must be subtracted

These findings show that to reach 99.999% reliability, only 6 and 5 transmitters can meet this criterion when the cluster vehicles are spaced 5 and 10 meters apart, respectively. This is achieved within a 90% confidence interval. If the reliability requirement is relaxed to 99.99%, then the system comfortably meets the criteria with 7 and 6 transmitters for cluster vehicles spaced 5 and 10 meters apart, respectively.
In regard to latency, Fig. 4.12(b) illustrates the average Packet Inter-Reception Time (PIR) as a function of time, serving as an indicator for latency performance within the cluster slice. The PIR measures the time interval between two successively received messages, and is used to indicate the delay value. Given that each cluster slice has a reserved duration of 1 ms and a period of 10 ms, the metric *(PIR - 10 ms)* can represent the average packet delay. The red dashed line signifies the delay bound mandated by URLLC requirements, which should not exceed 1 ms.
Our results show that, across different cluster topologies, the latency constraints can be comfortably met when the cluster size is fewer than 8 vehicles (including 1 receiver and 7 transmitters). However, when this number exceeds 8, a random resource allocation strategy is employed, thereby increasing the probability of collision and consequently degrading latency performance. Considering the PRR findings under same topology conditions, it can be concluded that with fewer than 8 vehicles in a single cluster, the communication among cluster members can reliably achieve a 99.99% success rate within the reserved 1 ms cluster slice period.
In conclusion, the proposed combined slice design can provide cluster vehicles with URLLC service, achieving high reliability and low-latency communication. However, sustaining this high quality of service necessitates strict admission controls, limiting cluster sizes to fewer than 8 vehicles.

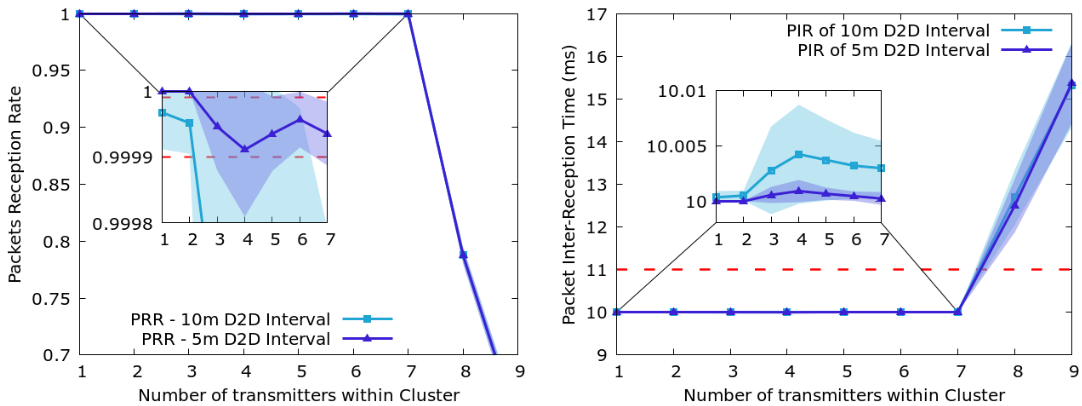

(a) PRR (b) PIR

Figure 4.12: 5G-NR Sidelink URLLC Slice Communication Performance

4.4 Conclusion

In this chapter, we introduced a URLLC Slicing service for dependable 5G-NR Sidelink communication. Extending the URLLC service from Chapter 3, this chapter provided a 5G-NR Sidelink Slicing parameter set, an architecture and a methodology to operate V2X and URLLC services in two dedicated 5G-NR Sidelink slices. Operating URLLC

in a dedicated Sidelink slice is necessary, first as it is not possible to change the default parameter set defined by ETSI ITS for the V2X service, and second to avoid V2X messages to interface with the URLLC messages. It is also important to be able to jointly operate URLLC and V2X services on the same spectrum.
This chapter therefore introduced a 5G-NR Sidelink URLLC slice orchestrator, which relies on the URLLC admission control mechanism defined in Chapter 3 to either accept or reject the presence of a UE on the URLLC slice. We then proposed to rely on the 3GPP Proximity Services (ProSe) specification to enable the first 5G-NR Sidelink URLLC Slicing service, where vehicles announce URLLC services, join a group and communicate on a protected slice operating on the PC5 interface without the involvement of a gNB.
URLLC sharing resources with V2X services, we dimensioned the URLLC Sidelink slice to have a minimal impact on the V2X service and demonstrated via simulation that URLLC communication may be supported on the dedicated URLLC slice with a minor impact on the performance of the V2X services. Defining the mandatory V2X services operating on a dynamically adjustable 5G-NR Sidelink C-ITS slice, this chapter therefore evaluated the first dual C-ITS & URLLC slice operation for 5G-NR Sidelink on the PC5 interface. It is a first step for the 5G-NR PC5 interface to operate similarly to the Uu interface and support the same 4 slices (URLLC, eMBB, mMTC and V2X), and will impact potential future development towards multi-vendor, multi-tenant, multi-service slicing operation on the 5G-NR PC5 interface.
In the next chapter, we evaluate the impact of the 5G-NR Sidelink URLLC slice for stable platoon operations, jointly operating a 5G-NR Sidelink C-ITS Slice supporting services, such as safety-critical perception and awareness messages.

Chapter 5
Dependable 5G NR Sidelink Communication for Vehicular Platoons

In the previous chapters, we showed that URLLC is possible for dependable V2X communication on 5G-NR Sidelink. In this chapter, we will show that URLLC is required for critical V2X use cases. Without loss of generalities, we opted for a Platooning scenario and will evaluate the benefit of a 5G-NR Sidelink URLLC slice on platoon stability.
We will first introduce the basics of vehicular platooning as well as the platoon management messages introduced by the European project ENSEMBLE [93]. We then propose an integrated URLLC Platoon management service by integrating the messages developed by ENSEMBLE to manage & control platoon dynamics with the ProSe messages handling the URLLC slice described in Chapter 4. We finally evaluate, first theoretically then via simulation, the impact of system-level V2X communication errors on platooning, then the benefit of relying on a URLLC slice supporting dependable platoon communication on 5G-NR Sidelink.

5.1 The Basic of Vehicular Platooning Mechanism

Vehicular platooning represents a significant technological advancement in intelligent transportation systems, as illustrated in Fig. 5.1. In this system, groups of vehicles travel closely together at highway speeds, meticulously controlling speed and acceleration in response to the surrounding platoon and infrastructure communications.
This practice leverages advanced vehicle sensing and communication technologies to enhance road capacity, mitigate traffic congestion, and boost fuel efficiency. Moreover, platooning improves safety by enabling vehicles within the platoon to share dynamic data about their speed, position, and other driving conditions. This shared information allows for nearly instantaneous adjustments to each vehicle's movements, significantly enhancing the overall safety and efficiency of road travel.
However, the proximity and speed of the vehicles in a platoon demand rapid response capabilities. Effective control theory is essential, requiring up-to-date information about the current platoon status to be relayed to control systems, thereby enabling the application of precise and timely control inputs.
To address these challenges, this section begins with an analysis of the control theories applied in this study, focusing on how they facilitate responsive and cohesive platoon

Figure 5.1: Vehicular Platooning on the Road [94]

dynamics. We then explore the vehicular communication messages required for efficient operation, detailing the types and purposes of messages that ensure continuous and reliable communication within the platoon. Finally, to uniformly assess platoon performance, we introduce a matrix based on several mobility factors. This matrix formalizes the analytical labels used to evaluate and compare different platooning scenarios, providing a structured approach to understanding the impacts and effectiveness of vehicular platooning.

5.1.1 Vehicular Platooning Control

In this study, our primary objective is to enhance the QoS within the framework of Connected and Automated Mobility (CCAM). As we dig deeper into V2X applications in Chapter 4, vehicular platooning has been selected as our focal use case. This choice is driven by the stringent and critical requirements of vehicular platooning, which exemplify the challenges and demands typical of CCAM applications.

To effectively maintain close distances among all platoon vehicles at high speeds and swiftly react to unexpected emergency scenarios, such as sudden braking or acceleration, the application of sophisticated control laws is a key element in the successful implementation of vehicular platooning. These control systems are crucial for ensuring the safety and efficiency of the platoon by dynamically adjusting each vehicle's speed and positioning in real time. The applied law governs the automated driving algorithms that dictate how each vehicle in the platoon responds to the dynamic driving environment. They are specifically designed to maintain a steady, optimal distance between vehicles, ensuring synchronized acceleration and braking. Control laws heavily depend on real-time data from V2V communications and accurate sensor information exchange to adjust vehicle behavior quickly and precisely.

To thoroughly analyze the performance of vehicular platooning, we begin by defining the notations used to describe the control algorithm, as detailed below:

$$X_{i,des} = x_{i-1} - L_i \tag{5.1}$$

$$\epsilon_i = x_i - x_{i-1} + L_i \tag{5.2}$$

$$a_i = \ddot{x}_i \text{ for } i = 1, ..., n \tag{5.3}$$

In Eq. 5.1, $X_{i,des}$ represents the desired position of the $(i-1)$-th vehicle within the platoon, factoring in the length of the vehicle L_i. Eq. 5.2 measures the spacing error of the i-th vehicle, highlighting discrepancies in the intended formation. Additionally, Eq. 5.3 denotes the acceleration, which is also equal to $\ddot{x}_i$ the second derivative of X_i with respect to time, required for the i-th vehicle in the platoon to maintain the desired spacing and speed.
Building on the established framework, we implement the control algorithm originally proposed by Rajesh Rajamani in Chapter 6 [95], a model that has become a standard in vehicular platooning scenarios. This algorithm calculates the desired acceleration of the i-th vehicle as $a_{i,des}$, as shown in below by using a combination of several dynamic inputs and predefined conditions. It provides a precise and robust mechanism for modulating each vehicle's speed to maintain optimal spacing and alignment within the platoon, thereby ensuring both safety and efficiency under various traffic conditions. This carefully designed function is critical for the coordinated operation of vehicles in a platoon, where precise movement control is essential.

$$\begin{aligned} a_{i,des} = \ddot{x_{i,des}} = (1 - C_1) \times a_{i-1} + C_1 \times a_0 \\ - (2\xi - C_1(\xi + \sqrt{\xi^2 - 1}))\omega_n(\nu_i - \nu_{i-1}) \\ - (\xi + \sqrt{\xi^2 - 1})\omega_n C_1(\nu_i - \nu_0) - \omega^2 \epsilon_i \end{aligned} \tag{5.4}$$

In this function, the control algorithm leverages three critical parameters to optimize platoon behavior and responsiveness. The gain C_1 modulates the influence of the lead vehicle's acceleration and velocity on following vehicles, enhancing the platoon's responsiveness or smoothness based on driving conditions and platoon configuration. The damping ratio ξ, set at 1 for critical damping, ensures stable and oscillation-free convergence to the desired state, preventing the "accordion" effect that could compromise efficiency and safety. Lastly, the control bandwidth ω_n dictates the system's response speed to positional and velocity changes, balancing quick reactions with the risk of sensitivity to noise, ensuring overall system stability. Together, these parameters are finely tuned to maintain a harmonious and safe platoon dynamic. The function also incorporates terms involving differences in velocity $\nu_i - \nu_{i-1}$ and the spacing error ϵ_i, which are vital for adjusting each vehicle's speed and position relative to others in the platoon. This ensures that each vehicle maintains an optimal distance that maximizes both safety and road efficiency.
From a general overview of the control function, the control algorithm for vehicular platooning showing its crucially relies on accurate and timely data concerning vehicle dynamics such as acceleration, velocity, and positional changes. This data forms the basis info of real-time calculations necessary for adjusting the acceleration of each vehicle within the platoon. To ensure precision, the information is sourced from two distinct but equally critical impact factors: the local sensing data collection and its communication data collection via communication access technologies, specifically over the 5G-NR Sidelink.
The cooperative combination of these data collection methods—local sensing and 5G-NR Sidelink communications—is illustrated in Figure 5.2, which details the roles and

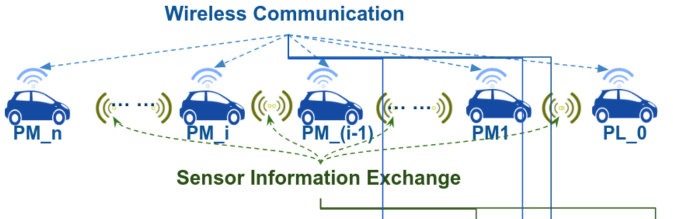

$$
\begin{aligned}
a_{i,des} = \ddot{x_{i,des}} = (1 - C_1) \times a_{i-1} + C_1 \times a_0 \\
- (2\xi - C_1(\xi + \sqrt{\xi^2 - 1}))\omega_n(\nu_i - \nu_{i-1}) \\
- (\xi + \sqrt{\xi^2 - 1})\omega_n C_1(\nu_i - \nu_0) - \omega^2 \epsilon_i
\end{aligned}
$$

Figure 5.2: Platoon Control Information Collection

contributions of each method. From a local sensing perspective, vehicles are equipped with advanced sensors that continuously gather data, but limited to its adjacent vehicles, on immediate mobility parameters and then derived into the spacing error ϵ_i value, this value is essential for maintaining safe distances between vehicles.

These sensors also measure the current local velocity v_i, providing real-time input that directly influences the vehicle's control responses. Such localized data collection is indispensable as it provides the foundational layer of raw, immediate environmental inputs necessary for the basic operational safety and responsiveness of the platoon.

On the communication front, the implementation of 5G-NR Sidelink communication profoundly enhances the dynamic interaction within the platoon. This communication technology is pivotal in synchronizing the behavior of vehicles throughout the entire platoon—from the lead to the tail—by disseminating critical operational parameters. These parameters include the lead vehicle's acceleration acceleration a_0 and velocity v_0, along with the acceleration a_{i-1} of the vehicle immediately ahead, ensuring cohesive movement across all units. These parameters are critical components of the control function, affecting how each vehicle individually adjusts its speed and spacing in response to changes observed in the leader and adjacent vehicles. The ability to share v_0, a_0 and a_{i-1} across the network ensures that all vehicles in the platoon have access to the same baseline data, crucial for maintaining uniformity in response to the lead vehicle's actions. This uniform data access helps in mitigating any lag in reaction times across the platoon, which is vital for the platoon's stability and safety. Meanwhile, the real-time transmission of ϵ_i helps each vehicle calibrate its position relative to others, ensuring that the platoon maintains optimal inter-vehicle spacing.

The update rate at which the calculated desired acceleration (as depicted in Fig. 5.3) is applied to each vehicle in the platoon needs to be defined carefully. It should be lower or equal to the rate at which sensor and communication information is updated. If the update rate of the desired acceleration is higher than that of the sensor/communication update rates, it may lead to redundant updates, resulting in inefficiencies. Based on empirical research, an update interval of 50 ms is commonly recommended [93]. This rate is considered optimal due to the limitations of the system's mechanics and the motor engine's response time, ensuring that the updates are timely enough to be effective yet not so frequent as to exceed the system's capability to respond.

The difference between the message update rate and the system control application rate

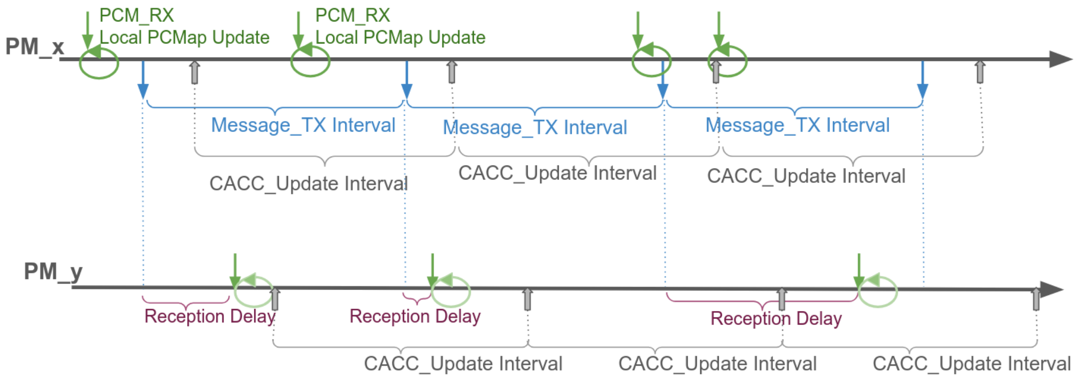

Figure 5.3: Platooning Control and Communication Rate Relationship

may influence performance; however, this aspect lies beyond the scope of the current study and is designated for future research. This investigation concentrates on scenarios where the message update rate equals to the system control application rate, as depicted in Fig. 5.3 . Consequently, the primary factor affecting control updates in this study is communication quality, which is the central focus of our analysis.

5.1.2 Vehicular Platooning Communication

This section investigates into the communication mechanisms employed for vehicular platooning, detailing the structure and function of related messages. The architecture proposed here is based on the prominent ENSEMBLE project, which sets a standard for collaborative vehicular operations.

Ensemble Platoon Project

The ENSEMBLE project [93] is advancing vehicular platooning by focusing on interoperability, safety, and practical application across diverse truck brands. It is the ambition of ENSEMBLE to realise pre-standards for interoperability between trucks, platoons and logistics solution providers, to speed up actual market pick-up of (sub)system development and implementation and to enable harmonization of legal frameworks in the member states. Collaboration with road authorities helps establish necessary regulatory frameworks, reflecting platoon impacts on roads and infrastructure. Real-world testing across national borders validates the efficacy and safety of multi-brand platooning. Additionally, ENSEMBLE integrates platooning with cloud-based logistics to improve operational efficiency. The project defines platooning as both a support function—enhancing safety and traffic fluency—and an autonomous function, optimizing fuel efficiency and logistics operations. Platooning utilizes a specific set of messages to facilitate vehicle coordination within a formation. Vehicles express their readiness to join a platoon through Cooperative Awareness Messages (CAMs), which include a new container featuring a flag called *isJoinable*. However, for real-world deployment, due to long-term backward compatibility issues, CAMs will be replaced by service announcement messages, though CAMs were initially selected by the ENSEMBLE project to simplify the system without adding unnecessary complexity. This substitution does not alter the underlying platooning logic or affect other protocol messages outlined in the current deliverable.

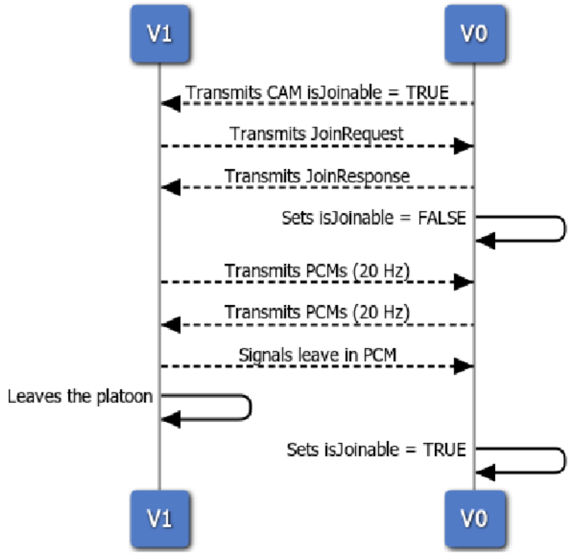

Figure 5.4: Ensemble Message Flow [93]

Platooning messages are categorized into two types: platooning management messages (PMMs) and platooning control messages (PCMs). PMMs are further divided into three subtypes: *JoinRequest*, *JoinResponse*, and *PlatoonUpdate* (previously known as KeyUpdate). A *JoinRequest* is initiated by a vehicle that identifies a potential platoon via CAMs indicating an *isJoinable* flag is set to true. The corresponding *JoinResponse* is a reply to this request, and *PlatoonUpdate* involves actions like regularly updating the encryption key for secure PCMs communication.
The Ensemble designed communication message exchange flow is illustrated in Figure. 5.4. PMM join requests and responds are piggybacked on CAM messages. Once accepted into the platoon, PCMs are broadcasted by all vehicles at a frequency of 20 Hz, aka every 50ms, and to simply the system no explicit acknowledgments are employed, instead all platoon members expecting a new PCM every 50 ms. When a platoon vehicle wants to leave, vehicles communicate their intent to exit the platoon through PCMs, ensuring ongoing information exchange throughout the separation process.

The Proposed Platooning Communication Architecture

Building on the ENSEMBLE Project's [93] design of PMM and PCM messages, which integrates a platooning protocol compatible with the existing ITS ecosystem for day-one applications, we further refine our proposed architecture to incorporate these message exchanges effectively.
We persist in utilizing the two primary platoon messages, the Platooning Management Message (PMM) and the Platooning Control Message (PCM), for essential platooning operations within our system. Unlike previous methods that piggybacked these messages on CAMs, our architecture assigns independent roles to each. Additionally, we aim to differentiate the QoS provided to each message type, reflecting their distinct roles and requirements. This differentiation ensures tailored handling of management and control functionalities, which we will explore in detail in the subsequent section.
The PMM message is essential for initiating platoon formation and dynamically managing

its composition. This message type ensures the platoon remains cohesive and can adapt to changes in its configuration or external conditions, functioning similarly to CAMs in terms of performance requirements. On the other hand, the PCM, issued by the platoon leader to all members, plays a pivotal role in centralized control. These messages communicate essential instructions related to velocity, acceleration, and precise positioning, crucial for the control mechanisms depicted in Figure. 5.2. Unlike PMM and CAM messages, PCM demands significantly higher reliability and lower latency to ensure effective execution of these directives, underscoring their critical nature in platooning operations.

Additionally, all vehicles must support general Cooperative-ITS (C-ITS) messages, such as Cooperative Awareness Messages (CAM), Decentralized Environmental Notification Messages (DENM), and Collective Perception Messages (CPM), as introduced in Section 2.3.3. These are crucial for establishing a foundational level of vehicular awareness and enhancing road safety. Typically transmitted at constant rates, these C-ITS messages require the allocation of specific resources to ensure continuous and reliable communication.

Combining the previous messages altogether, we can observe that vehicular platooning requires a 5G-NR Sidelink communication design that supports various message types with distinct requirements, as indicated in Figure. 5.5, even under heavy traffic conditions. The challenge lies in dynamically and efficiently allocating resources tailored to each service's needs within the constrained spectrum—typically 10 or 20 MHz allocated for V2X communication. Developing a method to manage these resources effectively is crucial to maintain reliable and efficient communication across diverse platooning scenarios.

Work by Giambene et al. [96] provides an analytical model to analyze the performance of direct V2V CAM messages over LTE-V technology, where resource allocation is managed through eNB assignment. This work analysed the performance of CAM communication within platoon under the same cell, it gave some deep analysis over different MCS value. To address these issues, Cao et al. [97] proposed an enhanced random resource selection from PL for platoon members and applied reinforcement learning-based semi-persistence for intra-platoon communication, significantly reducing external communication impact. Wang et al. [98] proposed combined predecessor-leader communication from PMs to PL, facilitating platoon formation and ensuring high QoS. However, details about manipulating unicast and groupcast communication modes were not provided.

Building on the findings from Chapter 4, which demonstrate an applicable structure of realizing direct network slicing on 5G-NR Sidelink, the novel designed system explores the dynamic allocation of resources tailored to specific slice requirements. This approach promises to effectively address the challenges identified, leveraging dynamic resource management to optimize network performance. The upcoming sections will inspect into the architectural design that implements this strategy to adapt to the vehicular platooning system.

Another key aspect we need to consider for vehicular platooning is an admission control mechanism. This concept is essential to effectively manage the platoon size, whereas the platoon leader can control the number of platoon members under a limit so as to support good QoS services among all vehicles within the limited resources. Platoon services, communicated through service announcements, must be broadcasted widely to reach as many ITS stations as possible, as pointed out by the ETSI standard [99]. By the meantime CAM messages are broadcast with the goal of maximizing coverage among ITS stations to ensure basic vehicular safety and therefore lead to Ensemble Project [93] to piggy-

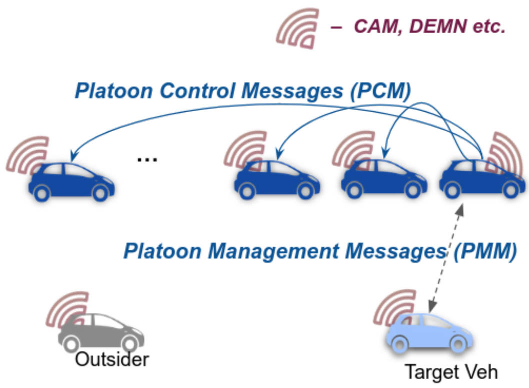

Figure 5.5: Platooning Communication Messages

back platoon service announcements on CAM. This approach guarantees that availability announcements are disseminated efficiently across CAM messages.
To achieve effective message communication among all platoon vehicles, it is essential to dynamically adapt the message structure and design a robust resource allocation mechanism. For C-ITS messages, which often involve heavy data transmitted at a fixed rate, sufficient resource allocation is crucial. PMM messages, on the other hand, can be formatted similarly to CAM, which have comparable requirements. However, the PCM messages are vital as they update control systems with the latest information on vehicle movements, significantly influencing platoon performance. These PCM messages must be precise and constrain to low latency to ensure that updates to control calculations are based on the most current data.
Michał et al.[100] analyzed platoon performance across varying communication quality levels using IEEE 802.11p technology. They employed the same CACC algorithm as we've shown in Section. 5.1.1. This work found that a 5% message loss can render vehicular platooning non-functional. Their research highlights that ideal communication conditions—where actuation lag, communication delay, and message rate are optimally managed—are crucial for maintaining platoon performance.
In order to tackle the high QoS requirements for platooning control messages which is curitially impacting CACC algorithm. These algorithms, as suggested by Lefeber et al. [101], are designed to automate acceleration and braking based on multi-vehicle communication, enhancing the platoon's ability to maintain uniform and safe distances between vehicles.
To dynamically assign resources for vehicular platooning, much of the current research has focused on assistance from gNB or higher core network levels. For instance, Gao et al.[102] introduced a dynamic spectrum sensing scheduling scheme with support from network clouds and roadside units (RSUs). The primary goal of this approach is to separate platoon control from data channels, enhancing the efficiency and reliability of communications within vehicular platoons. Similarly, Pengfei W. et al.[103] designed an algorithm that enables base stations to optimize power control and subchannel allocation for platoon vehicles. However, the question remains open on how to implement a pure Sidelink dynamic resource allocation that meets the stringent requirements of vehicular platooning.

5.1.3 Mobility Metrics for Analyzing Vehicular Platooning

To systematically evaluate the mobility performance of vehicular platooning, we propose a structured approach using four key elements. Each element represents a distinct aspect of platooning mobility, enabling the system to measure the actual performance of vehicular platooning. Additionally, we establish specific limits and thresholds for each parameter to provide a standardized framework for analysis:

Speed Overshoot (m/s)

Speed overshoot is representing the speed differences between the platoon leader and the last vehicle of the platoon, the definition of platoon is as follows:

$$\zeta_i(t) = v_{pl}(t) - v_{pm}(t) \tag{5.5}$$

where $\zeta_i(t)$ denotes the speed overshoot at time t,$v_{pl}(t)$ is the speed of the platoon leader, and $v_{pm}(t)$ is the speed of the following or monitored vehicle.
A positive value of $\zeta_i(t)$ indicates that the following vehicle is moving faster than the platoon leader at the specific time t. This condition is often observed when the following vehicle is attempting to reduce the distance between itself and the leader, possibly due to a previous increase in the gap or slow initial response. While this can be a normal occurrence in adjusting the spacing within the platoon, it also carries the potential risk of a collision if the speed differential is too great or if it is not adjusted back to a safer level promptly.
Conversely, a negative speed overshoot suggests that the following vehicle is traveling slower than the platoon leader at time t. This could be a result of the following vehicle intentionally slowing down, possibly in response to an anticipated deceleration by the leader or as a delayed reaction to previous changes in the leader's speed. A persistent negative speed overshoot could lead to an increased gap between vehicles, which might compromise the efficiency and safety benefits of platooning by reducing the aerodynamic and fuel advantages gained from closer spacing.
A zero speed overshoot implies that both the platoon leader and the following vehicle are moving at identical speeds at that moment. This is the ideal state in platoon dynamics, indicating a well-synchronized movement between the vehicles. Maintaining zero or minimal speed overshoot is crucial for ensuring the stability and safety of the platoon, as it prevents unnecessary oscillations and maintains consistent spacing across the platoon.
Effective control of the speed overshoot is crucial for platoon safety. As discussed before, a smaller overshoot ensures that following vehicles closely match the leader's speed, reducing collision risks, while a larger overshoot increases these risks, especially during sudden maneuvers by the leader. Our study investigates the impact of communication quality on speed overshoot, focusing on how delays and information loss can cause speed fluctuations and affect platoon stability. This analysis will help identify strategies to enhance communication reliability and improve safety in platooning dynamics.

String Stability (m^2/s)

String stability has been widely studied in vehicular platooning and can be applied to analyze the functionality of platoon mobility performance. Defined as σ, string stability is represented in terms of the variance of the acceleration difference between the following vehicle and the leader, normalized by the variance of the leader's acceleration:

$$\sigma_i(t) = |a_0(t) - a_i(t)| \tag{5.6}$$

Here, $a_0(t)$ represents the acceleration of the platoon leader at time t, and $a_i(t)$ denotes the acceleration of the following vehicle. String stability is particularly concerned with how well acceleration perturbations among platoon members are damped out as they propagate through the platoon.

A lower value of $\sigma_i(t)$ indicates that the accelerations of the following vehicles closely mirror that of the leader, suggesting a stable platoon where disturbances are quickly attenuated. Conversely, a higher σ value implies that disturbances are amplified as they propagate back through the platoon, potentially leading to unstable behavior and increased risk of oscillatory movements or collisions.

The question of what constitutes a reasonable limit for $\sigma_i(t)$ to ensure string stability is complex and can depend on several factors including the dynamic capabilities of the vehicles, the desired spacing between vehicles, and the specific operating conditions of the platoon. Typically, a $\sigma_i(t)$ value close to zero is ideal, indicating that following vehicles are perfectly mirroring the leader's acceleration without amplification of disturbances.

Understanding and controlling string stability is crucial for the safe operation of vehicular platoons, especially under varying traffic conditions and in environments that require rapid responsiveness to dynamic changes. This aspect of platoon dynamics underscores the importance of advanced control mechanisms and robust communication systems within the platoon to maintain cohesive and stable vehicle behavior.

Headway Time (s)

Time headway, denoted as $\gamma(t)$, is a vital metric for assessing both the safety and efficiency of a vehicular platoon. This measure quantifies the temporal distance between the leader and any following vehicle within the platoon, providing an indication of the time available for a following vehicle to respond to the maneuvers of the vehicle ahead. The mathematical definition of time headway is given by:

$$\gamma(t) = \frac{x_0(t) - x_i(t)}{v_{max}} \tag{5.7}$$

where $x_0(t)$ and $x_i(t)$ represent the positions of the platoon leader and the current following vehicle, respectively, and v_{max} denotes the maximum permissible speed for vehicles in the platoon.

Maintaining an appropriate time headway is crucial for ensuring that platoon vehicles have enough time to react to sudden changes in the leader's speed or direction, thereby preventing potential collisions and maintaining a smooth flow of traffic. A well-adjusted time headway balances safety and traffic efficiency: if the headway is too large, road space is underutilized, which can lead to decreased overall traffic throughput and may even impact the quality of wireless communications within the platoon due to increased distances between vehicles. Conversely, if the headway is too short, the risk of collisions increases, especially in emergency braking scenarios where the following vehicle may not have sufficient time to respond effectively.

The optimal time headway can vary based on numerous factors, including traffic conditions, speed, weather, and the technological capabilities of the vehicles (such as braking efficiency and communication latency). Advanced driver-assistance systems (ADAS) and autonomous driving technologies are often employed to dynamically adjust time headway based on real-time conditions, optimizing safety while maximizing road capacity and maintaining efficient platoon dynamics.
This in-depth understanding of time headway is essential for developing and implementing effective platooning strategies that enhance both the safety and efficiency of modern automated transportation systems.

Jerk (m^3/s)

Jerk, denoted as $J_i(t)$, is an important dynamic parameter in vehicular control, particularly in the context of automated driving and advanced driver-assistance systems. Defined mathematically as the rate of change of acceleration over time, jerk provides insight into the smoothness of a vehicle's motion. The formal continuous definition of jerk and its discrete-time approximation are given by:

$$J_i(t) = \frac{d}{dt} a_i(t) \tag{5.8}$$

$$J_i(t) \approx \frac{a_{i+1} - a_i}{t_{i+1} - t_i} \tag{5.9}$$

The concept of jerk is particularly relevant when evaluating the quality of the driving experience. High levels of jerk are typically undesirable as they relate directly to how passengers perceive the comfort and safety of their journey. Sudden changes in acceleration, which lead to high jerk values, can cause discomfort and even distress to passengers. This is due to the human body's sensitivity to unanticipated and rapid movements, which can be both startling and physically unpleasant.
In the realm of autonomous vehicle systems, managing jerk is crucial not only for passenger comfort but also for the overall stability and safety of vehicle operations. High jerk may not only reduce passenger comfort but can also place additional stress on the vehicle's mechanical components, potentially leading to quicker wear and tear or even failures in extreme cases.
Therefore, in designing and tuning the control algorithms for autonomous vehicles and driver-assistance systems, minimizing jerk is a key objective. This involves sophisticated control strategies that ensure acceleration and deceleration occur smoothly over time. Effective jerk management helps in achieving a balance between dynamic performance and ride quality, making the driving experience more enjoyable and safe for all occupants. Moreover, reducing jerk is essential for broader acceptance of autonomous technologies. User acceptance and satisfaction, pivotal factors for the commercial success of such technologies, are greatly enhanced when vehicles operate smoothly. Thus, minimizing jerk not only contributes to technical and operational efficiencies but also plays a significant role in the marketability and user adoption of autonomous vehicle systems.

5.2 5G-NR ProSe-based Vehicular Platooning Architecture

This section examines the comprehensive architecture designed for vehicular platooning, building on the concepts from Chapter 4. In the previous chapter, we introduced a ProSe-based 5G-NR Sidelink URLLC slice management architecture. In this section, we integrate the ENSEMBLE [93] platoon management architecture with the Chapter 4 architecture to propose a ProSe-based Platooning Service supporting dependable 5G-NR Sidelink communication. This approach considers varying QoS requirements associated with different V2X & platooning messages. The proposed dual-slice design is depicted on Fig. 5.6, where one URLLC slice is dedicated to the PCM to ensure dependable critical platoon control updates. The other C-ITS slice supports the PMM and meets other general communication requirements as per the ETSI C-ITS standards. This dual-slice approach effectively segregates and manages the distinct data flows essential for efficient platooning operations.

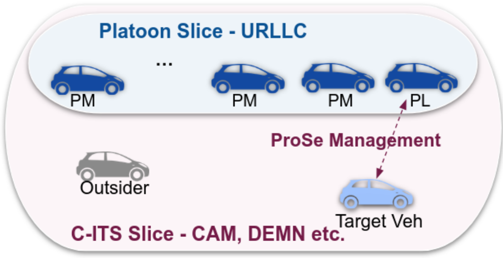

Figure 5.6: Vehicular Platooning Slicing Scheme

5.2.1 Platoon Configuration Procedure

The slicing design, as illustrated in Figure 5.6, introduces a novel framework specifically tailored for platooning communication. This framework segregates communication into separate slices: one dedicated to fundamental V2X communication and PMM message for vehicular management, and the other to PCM for collecting information to apply for platooning control mechanism. This separation minimizes interference and ensures that operations within each slice are independent. The V2X slice allocates the majority of resources to basic communication, while the platooning slice is specifically designed to support URLLC for critical intra-platoon messages.

Additionally, Proximity Services (ProSe) are utilized to manage platoon services, particularly facilitating the joining and leaving functions. Consequently, platoon configuration and management-related messages, known as PMMs, are encapsulated within ProSe-related messages. By leveraging direct ProSe-based service announcements, efficient configuration and management of vehicular platooning are achieved, as depicted in Figure. 5.7. Specific functions represented by PMMs for certain scenarios are directly translated into corresponding ProSe functionalities. Considering platooning as a service, ProSe can seamlessly transition from group management to platoon management, simplifying the linkage to physical layer resource allocation management. The *Ensemble* Project [93] notably pointed out the need of service announcement for platoon communication due to backward compatibility issues. 5G ProSe also provides enhanced safety and privacy for group management during the direct discovery procedure.

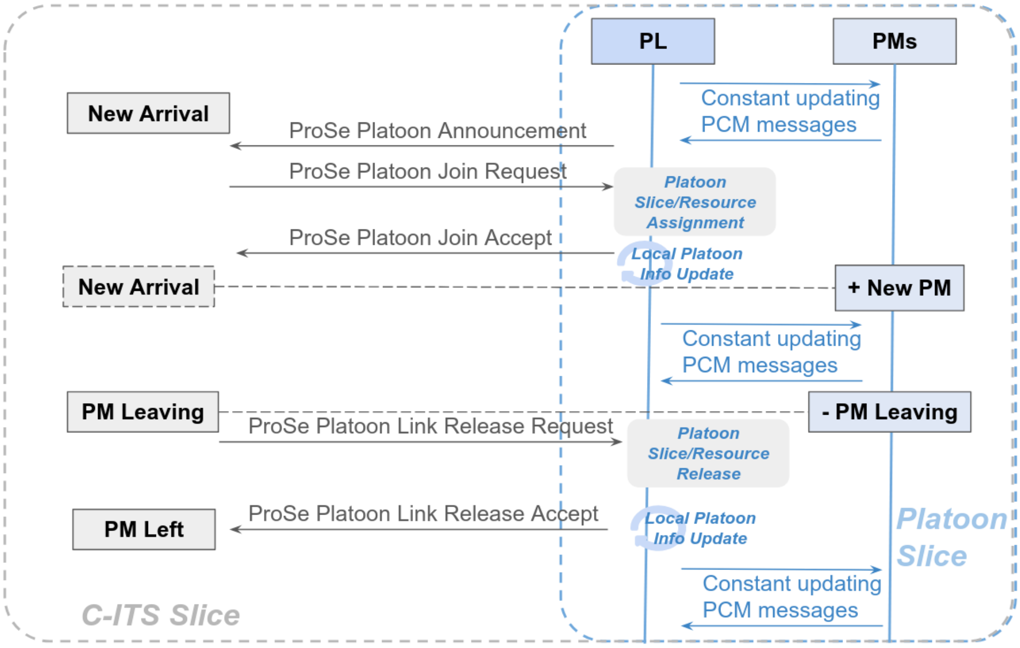

Figure 5.7: ProSe-based Platooning Frame Architecture

Meanwhile, PCM messages remain securely within their designated platoon slice, which aims to provide high reliability and low-latency communication. The detailed design of this slice mirrors what was introduced in Section. 4.3.3. To avoid repetition in this thesis, readers are encouraged to refer back to Chapter 4 for a comprehensive overview. Briefly, limited resources are allocated to the protected platoon slice—specifically, 1 ms over every 10 ms—to ensure the majority of resources are available to handle the more demanding basic safety communication needs from C-ITS. Within the URLLC slice, a higher numerology is employed to shorten the duration per slot in the time domain, thereby enhancing system capacity for short-term reservations and reducing communication delays. Additionally, a deterministic MAC layer scheduler is implemented, assigning fixed slots to each vehicle to ensure high reliability.

The actual message exchange procedure are illustrated in Figure. 5.7. Within the platoon slice, the platoon leader (PL) and platoon members (PMs) are in constant communication, updating PCM messages to apply the correct control methods. For platoon management scenarios, such as a new vehicle joining or a PM departing, ProSe is integral. When a vehicle wishes to join the platoon, ProSe join request and acceptance messages are exchanged between the vehicle and the PL, who then allocates the necessary resources within the platoon slice to ensure the new arrival meets the required communication quality standards. Similarly, when a PM wishes to depart, ProSe-related link release request and acceptance messages are exchanged to confirm the departure. Concurrently, the PL updates its local platoon information and releases the resources previously reserved for the departing member. For further details on the ProSe standard and its application in cluster management, please refer to Section 4.3.

5.2.2 Platoon Control Apply Procedure

Here we outline the algorithm. 2 for a control procedure for vehicular platooning, ensuring that multiple vehicles travel in a convoy while maintaining optimal distances and reacting to dynamic changes in speed. The control procedure is broken down into several phases: initialization, main simulation loop, and safety enforcement. Here's a detailed explanation:
Initialization: Several essential parameters are set here, number of the vehicles(N_{trucks}), total simulation time (T_{sim}), simulation time interval ($delta_t$), desired gap between vehicles ($g_{desired}$), maximum speed (v_{max}), minimum safe distance (d_{min}), and acceleration limits (a_{max}, a_{min}) Then an initial state is executed as for all platoon vehicles, to assign an initial values for speed (v), position (x), and acceleration (a).
Main simulation loop: The first step within the loop involves the platoon leader updating its speed at each time step based on a predefined speed function. Then the algorithm checks for updates based on predefined intervals (t_{update}) and processes them if received. Delays are calculated based on the distance to the leading vehicle, affecting the timing of updates. Next, for each Platoon Member (PM), the distance to the vehicle ahead is calculated. This distance is used to compute the desired acceleration (a_{des}) based on proportional (K_p) and derivative (K_d) gains aimed at maintaining the desired gap. Then, a kinematic update adjusts the desired acceleration, which must stay within the set maximum and minimum bounds, and is applied to update each vehicle's speed and position. This ensures that each vehicle adjusts its speed to maintain the correct formation dynamically.
Safety enforcement: A specific safety enforcement algorithm is activated in response to emergency scenarios. This is necessitated by the limitations of the analytical update time-step, which might lead to an emergency state within one time-step loop—where the current vehicle could exceed the maximum safety distance yet continue to accelerate. To address this, the algorithm continuously monitors the distance between each vehicle. If any vehicle comes too close to its predecessor, falling below the minimum safe distance (d_{min}), emergency braking is applied to quickly reduce speed and restore a safe following distance.
This procedure outlines a robust and dynamic algorithm for managing a platoon of vehicles within a controlled V2X environment, crucial for maintaining not only efficiency in transportation but also enhancing safety measures. By implementing a structured control sequence that adapts in real-time to the conditions of the road and the behavior of vehicles within the platoon, this algorithm effectively orchestrates synchronized vehicular movement. The inclusion of emergency protocols further ensures that the system can react swiftly to prevent accidents, thereby supporting the overarching goal of reducing road incidences and improving traffic flow.

5.3 Simulation and Result

5.3.1 Scenario Setup

In this study, we simulate a platoon of 6 vehicles, all moving at a constant speed from the beginning. At simulation time of 30 second, the platoon leader initiates a sinusoidal speed change to test the platoon's mobility performance. The details limitation and settings for the vehicle movements are listed in table. A.1.

Algorithm 2 Vehicular Platooning Control Procedure

Initialization:

Set parameters: $N_{\text{trucks}}, T_{\text{sim}}, \delta_t, g_{\text{desired}}, v_{\max}, d_{\min}, a_{\max}, a_{\min}$.

Initialize $time[0, T_{\text{sim}}]$ with interval δ_t, and platoon leader initial parameters: $v[1,0]$, $x[1,0]$, $a[1,0]$.

Initialize platoon member states $v[j,0], x[j,0], a[j,0]$ for $j = 2$ to N_{trucks}.

Main Simulation Loop:

for $t = 1$ to T_{sim} **do**

  Update leader's state using speed function:

  $v[1,t] = f_{\text{speed}}([t])$.

  $x[1,t] = x[1,t-1] + v[1,t] \cdot \delta_t$.

  $a[1,t] = (v[1,t] - v[1,t-1])/\delta_t$.

  Communication and Update Checks:

  Extract $delay(t)$ value based on current distance to the leading vehicle.

  if $time[t] \geq t_{\text{update}}$ and Message Received is "true" according to current PRR **then**

    Apply delay and update vehicles states accordingly.

    $v[j,t] = f_{\text{speed}}([t])$.

    $x[j,t] = x[j,t-1] + v[j,t] \cdot \delta_t$.

    $a[j,t] = (v[j,t] - v[j,t-1])/\delta_t$.

    $t_{\text{update}} = time[t] + \delta_t$.

  end if

  Vehicle Dynamics:

  for each following vehicle j from 2 to N_{trucks} **do**

    Calculate inter-vehicle distance: $d = |x[j-1,t-1] - x[j,t-1]| - g_{\text{desired}}$.

    Compute desired acceleration a_{des}:

$$a_{\text{des}} = K_p \cdot d + K_d \cdot (v[j-1,t-1] - v[j,t-1])$$

    Apply kinematic updates:

$$a[j,t] = \max(\min(a_{\text{des}}, a_{\max}), a_{\min})$$

$$v[j,t] = \max(\min(v[j,t-1] + a[j,t] \cdot \delta_t, v_{\max}), 0)$$

$$x[j,t] = x[j,t-1] + v[j,t] \cdot \delta_t$$

  end for

  Enforce Safety and Environmental Conditions:

  for each platoon member vehicle j from 2 to N_{trucks} **do**

    if $|x[j-1,t] - x[j,t]| < d_{\min}$ **then**

      Apply emergency braking: $a[j,t] = a_{\min}$.

    end if

  end for

end for

Table 5.1: Analytical Simulation Parameters Setting

Parameter	Value
Desired Inter-distance	5m
Maximum Speed	35 m/s
Constant Speed (0-30s)	20m/s
Sinusoidal Speed (30-100s)	$20 + 5\sin(0.2\pi(t-20))$ m/s
Communication Mode	Broadcast
Number of Platoon	6
Control Applied Rate	50ms

The control procedures are implemented across all vehicles according to the algorithm outlined in Algorithm 2 using MATLAB. The algorithm specifies that the current Packet Reception Ratio (PRR) and delay should be applied at each time step. However, the method for applying a realistic model that reflects the actual performance of inner platoon slice communications still needs to be determined.
Regarding the delay value, we implemented a distribution according to a correlated delay generation. This approach is based on the realistic scenario where the actual delay value at each time step should be correlated; therefore, we used an Auto-regression delay model (AR(1)). The definition is as follows:

$$X_t = \sum_{i=1}^{P} \Phi_i X_{t-i} + \epsilon_t \tag{5.10}$$

In the Eq. 5.10, X_t represents the delay at time t, P is the order of the auto-regressive model, Φ_i are the auto-regressive coefficients, and ϵ_t is the white noise error term, which accounts for random fluctuations in the delay. This AR(1) model captures the relationship between current and past delay values, effectively modeling the inherent correlation in delay patterns over time. This approach makes the system simulation more realistic by reflecting the tendency of delays to persist and fluctuate over time, rather than occurring independently.

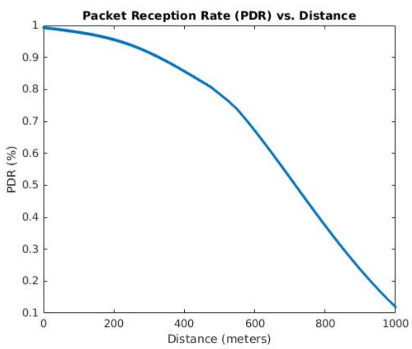

(a) PRR over distance

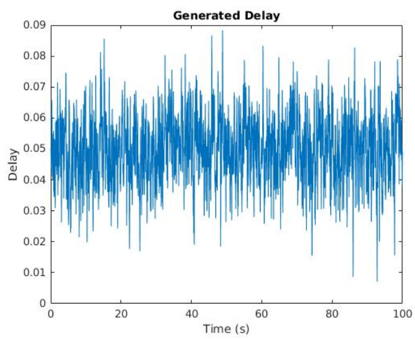

(b) Delay over time

Figure 5.8: Generated PRR and Delay over Time

To differentiate between two network slices—one for general C-ITS communication and the other specifically tailored for platooning control message exchanges—we have structured the slice settings based on parameters outlined in Table. 5.2. The numerology and MAC layer scheduler, derived from our findings in Chapters 3 and 4, ensure that the platoon slice delivers superior communication quality.

To assess the system's performance through simulation, we implemented an analytical model focusing on Packet Reception Rate (PRR) and delay metrics. The delay for each slice is modeled using the aforementioned auto-regression delay model, which provides correlated delay values over time. For the platoon slice, the average delay is set at 1 ms, reflecting the rapid reservation period specified by the resource allocation mechanism detailed in Chapter 4. In contrast, the delay for the C-ITS slice, based on realistic simulations conducted in NS3, averages around 50 ms, influenced by the physical and MAC layer settings specified.
The PRR for the C-ITS slice is based on studies by the UWICORE group [104], which explored the effects of 5G-NR V2X modulation on packet reception rates. Building on earlier work by Manuel et al. [105], which developed and validated analytical models of PRR for LTE-V Mode 4 performance based on transmitter-receiver distance, our study extends these findings to 5G-NR V2X. We implemented these updated results in our system representing the PRR impact by 5G-NR communication.
The PRR values, correlating to a packet size of 190 bytes and traffic density of 0.6 veh/m, were extracted from their findings. The relationship between PRR and transmission distance is illustrated in the referenced plot and included in our analysis as depicted in figure 5.8.
For the platoon slice, due to the adoption of mode 2(c) scheduler that allocates a fixed slot to each vehicle within the platoon, issues related to collisions are negligible. Additionally, packet loss from channel imperfections is considered minor and thus is not factored into the PRR for the platoon slice, ensuring an unimpeded communication flow within this critical application.

Slice Index	Numerology	Scheduler	Delay	PRR
Platoon Slice	2	mode 2(c)	$1ms\pm$	–
C-ITS Slice	0	mode 2(a)	$50ms\pm$	ref.to.graph

Table 5.2: Slices Design Details

5.3.2 Analytical Result Analysis

In this section, we compare results of the platoon slice design, in comparison of the C-ITS slice design. The main difference is the platoon slice is intended to support high reliability and low latency, however C-ITS slice is under 5G-NR mode 2 reliability, and generated correlated delay.
The result figures illustrated in Fig. 5.9 are plotted according to the mobility analysis matrix proposed in section 5.1.3. Direct plots are provided following the cumulative distribution function (CDF) of the values in a log-normal distribution. We extract only the steady-state simulation results, starting from a simulation time of 30 seconds, as it takes time for the platoon to reach a stable state.

Speed Overshoot Analysis

The speed overshoot results, depicted in Figure 5.9(a), highlight the growing disparity in speed between the following vehicles and the platoon leader, with a noticeable increase from the third follower onwards. This phenomenon, where speed overshoot values become

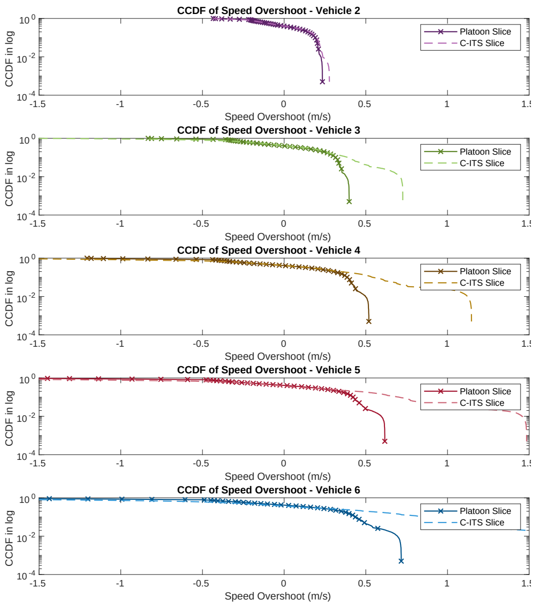

(a) Speed Overshoot in CCDF(log)

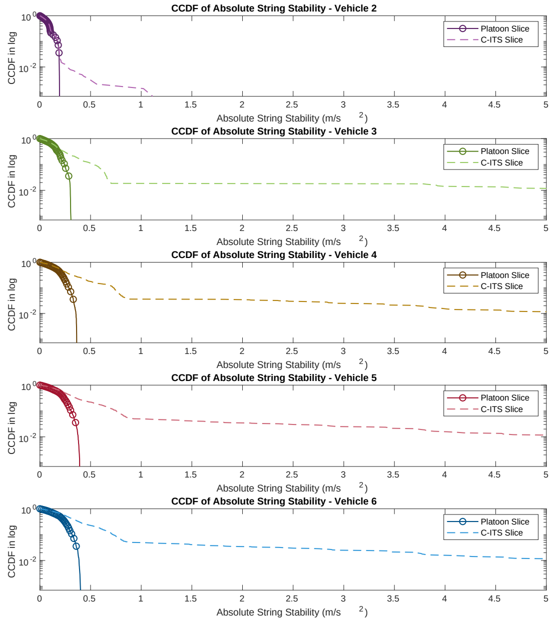

(b) String Stability in CCDF(log)

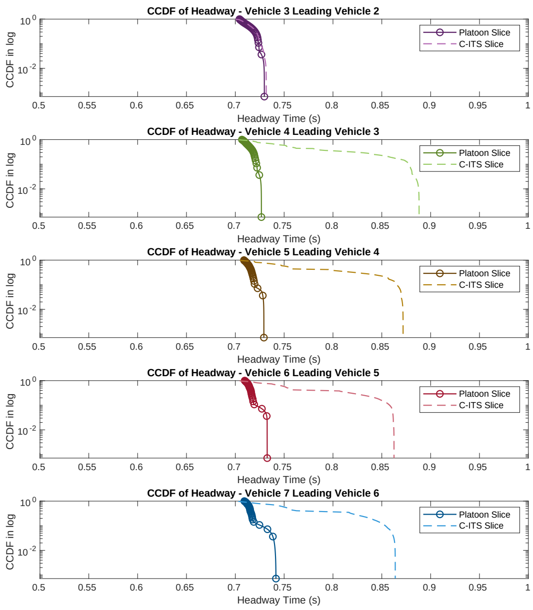

(c) Headway Time in CCDF(log)

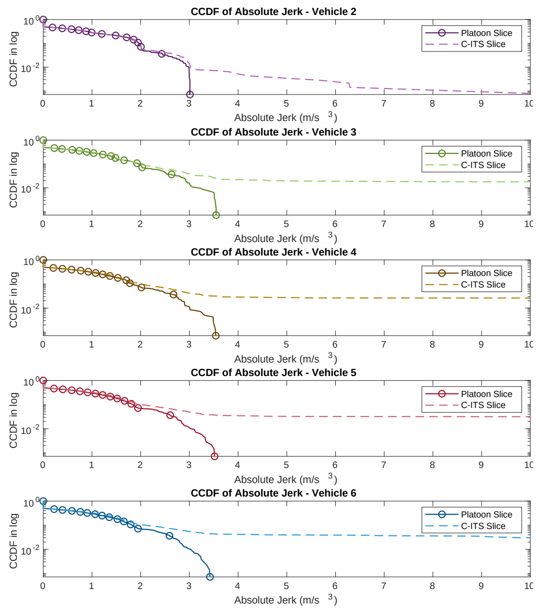

(d) Jerk in CCDF(log)

Figure 5.9: Mobility Matrix Result : Comparison between Different Slice Design

more pronounced in vehicles further back in the formation, is thoroughly examined in Table. 5.4. Here, we assess the overshoot values at the 0.9 and 0.8 probability levels, observing that the intervals between different slice designs not only widen but can escalate up to around 0.3m/s for subsequent vehicles in the platoon.
These increasing speed disparities pose significant risks as they may lead to higher chances of collision and overall platoon instability. Additionally, the variations in speed necessitate more frequent adjustments, which can elevate fuel consumption and, consequently, operational costs. Such inefficiencies undermine the primary objectives of vehicular platooning, which include enhancing road capacity and reducing environmental impact through more efficient driving practices.
However, the implementation of a specialized network slice design, termed the Platoon Slice, offers a promising solution. By providing a dedicated network resource tailored specifically for platooning applications, this design supports enhanced system responsiveness and enables more precise control over the vehicular speeds within the platoon. The Platoon Slice facilitates more synchronized and harmonious movements of all vehicles in the platoon, reducing the likelihood of speed overshoot and its associated risks. This targeted approach not only improves the safety and stability of the platoon but also optimizes fuel efficiency, aligning with the overarching goals of sustainable and safe intelligent transportation systems.

String Stability Analysis

The parameter of string stability is a critical measure used to assess the robustness of vehicular platooning systems against disturbances that can propagate through the platoon. This metric has been widely utilized to evaluate the stability of vehicle formations, ensuring that variations in acceleration do not escalate as they move from the lead vehicle to the following vehicles. In Figure. 5.9(b), the absolute string stability values between the current vehicle and the platoon leader are illustrated, showing how well disturbances are damped across the platoon.
For vehicles operating under the protected Platoon Slice, the string stability values consistently fall within a more desirable range of $(0, 0.5)m/s^2$. This indicates a higher level of damping of perturbations, suggesting a tighter and more cohesive platoon behavior. In contrast, vehicles managed within a normal C-ITS slice exhibit a wider variance in string stability, as summarized in Table. 5.3. Here, the probability of string stability values exceeding a certain threshold, specifically $0.5m/s^2$ and $2m/s^2$, is documented, highlighting a less controlled response to speed and acceleration changes.
Despite these differences in stability measures between the two slices, the overall integrity and string stability of the platoon are maintained. This effectiveness is reflected in the platoon's collective movement dynamics, where all vehicles adhere closely to the speed and acceleration patterns of the platoon leader, with minimal deviation. Such consistent behavior across the platoon minimizes the risk of collisions and enhances the overall flow of traffic, illustrating the critical role of string stability in maintaining safe and efficient vehicular operations. The Platoon Slice, in particular, offers significant advantages by ensuring that vehicles remain within a tighter control envelope, effectively minimizing the propagation of disturbances and maintaining a smoother and safer driving experience.

Headway Time Analysis

Headway time, the interval between vehicles, is a critical metric in traffic safety and efficiency. Under normal driving conditions, a standard recommended headway of approximately 2 seconds is advised to provide drivers ample time to react and brake safely. However, in the specialized environment of vehicular platooning, equipped with advanced synchronization and rapid response technologies, this headway can be significantly reduced.

In vehicular platooning scenarios, the integration of advanced communication systems allows vehicles to maintain much shorter headways safely. The data from Figure. 5.9(c) and Table. 5.4 demonstrate this capability effectively. Within the Platoon Slice, the headway times are consistently maintained below 0.75 seconds, illustrating the system's ability to optimize road space and enhance fuel efficiency by reducing the air drag at closer distances. In comparison, vehicles operating under the C-ITS slice show a slightly longer average headway time of approximately 0.87 seconds.

Although these variations are minor, the ability to safely reduce headway times below the standard 1 second highlights the technological advancements embedded within platooning systems. This reduction not only optimizes road usage by allowing more vehicles to travel closely and safely but also contributes to improved fuel efficiency due to reduced aerodynamic drag. The slight deviations from the 1-second standard are typically influenced by the initial settings for vehicle inter-distance, which are configurable based on specific traffic conditions and safety requirements. Adjustments to these settings can further refine the balance between safety and efficiency, tailoring the platoon dynamics to more realistic driving scenarios. This adaptability underscores the advanced capabilities of platooning technology in enhancing vehicular operations beyond traditional driving norms.

Jerk Analysis

The absolute jerk value, measuring the rate of change of acceleration, is a critical metric for assessing driving comfort. To ensure a smooth and comfortable ride, it is generally accepted that jerk values should remain below $10m/s^3$, as exceeding this threshold can cause discomfort or even motion sickness among drivers and passengers.

Our analysis of the data in Table. 5.3 focused on determining the probability of jerk values surpassing this comfort threshold. The findings reveal that under the protected Platoon Slice design, jerk values are consistently kept low, demonstrating the system's effectiveness in ensuring a smooth driving experience. This design's superior control mechanisms effectively minimize sudden changes in acceleration, thus maintaining jerk within comfortable limits.

In the C-ITS slice, the probability of exceeding the comfort jerk limit of $10m/s^3$ is low at about 0.05, but even this small rate is noteworthy as infrequent high jerk values can cause driver discomfort, potentially leading to delayed reactions or increased stress, which could compromise platoon safety. Addressing these high jerk occurrences in C-ITS slices is essential. Comparing with Platoon slice we can see that by refining communication protocols, we can minimize such issues, enhancing the safety, comfort, and overall efficiency of vehicular platoons.

In summary, while the overall mobility-related parameters in vehicular platooning show only slight improvements with the protected slice design, the key enhancements are par-

Table 5.3: Results - Probability of Reaching Specified Parameter Thresholds

Parameter	Slice Index	Vehicle 2	Vehicle 3	Vehicle 4	Vehicle 5	Vehicle 6
StringStability $\geq$ 0.5	Platoon Slice	0	0	0	0	0
	C-ITS Slice	0.003	0.113	0.178	0.219	0.22
StringStability $\geq$ 2	Platoon Slice	0	0	0	0	0
	C-ITS Slice	0	0.0182	0.03459	0.03458	0.03458
Jerk $\geq$ 2	Platoon Slice	0.08	0.0889	0.0831	0.0795	0.077
	C-ITS Slice	0.083	0.1126	0.116	0.118	0.1268
Jerk $\geq$ 8	Platoon Slice	0	0	0	0	0
	C-ITS Slice	0.0012	0.0227	0.0332	0.0403	0.0437
Jerk $\geq$ 12	Platoon Slice	0	0	0	0	0
	C-ITS Slice	0.0051	0.0222	0.0328	0.0343	0.0316

Table 5.4: Results - Parameter Values at Specific Probabilities

Parameter	Slice Index	Vehicle 2	Vehicle 3	Vehicle 4	Vehicle 5	Vehicle 6
$\mathbf{Prob_{Overshoot}} \geq \mathbf{0.9}$	Platoon Slice	0.04	0.06	0.07	0.0874	0.0873
	C-ITS Slice	0.039	0.057	0.088	0.2	0.3
$\mathbf{Prob_{Overshoot}} \geq \mathbf{0.8}$	Platoon Slice	0.07	0.124	0.158	0.169	0.173
	C-ITS Slice	0.072	0.121	0.2	0.345	0.499
$\mathbf{Prob_{Headway}} \geq \mathbf{0.9}$	Platoon Slice	0.704	0.707	0.709	0.71	0.71
	C-ITS Slice	0.703	0.73	0.731	0.7309	0.7308
$\mathbf{Prob_{Headway}} \geq \mathbf{0.8}$	Platoon Slice	0.706	0.708	0.71	0.7116	0.7118
	C-ITS Slice	0.7066	0.745	0.7467	0.7438	0.7413

ticularly notable in jerk reduction, which significantly increases passenger comfort under the Platoon Slice design. Although the string stability and consistency in vehicular following are largely maintained across both the Platoon and C-ITS slices, indicating that the C-ITS slice does not compromise the coherence of the platoon, the main differentiate lies in the system's response to dynamics. Speed overshoot and headway time analyses reveal that the Platoon Slice ensures tighter control over vehicular speeds and maintains shorter headways, suggesting a quicker and safer response in sudden emergency scenarios. These differences, albeit minor, highlight the importance of the protected slice in enhancing the overall safety and operational efficiency of vehicular platooning systems.

5.3.3 Simulation Result Analysis

Simulation Scenarios

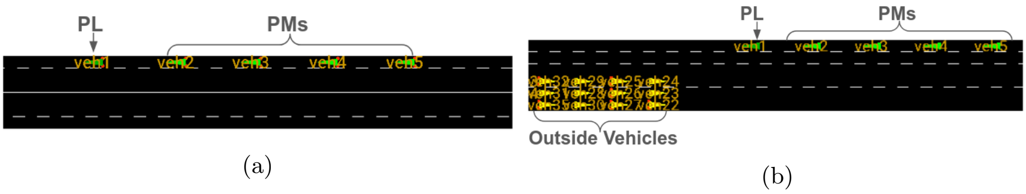

Figure 5.10: Scenario Setting Performance on SUMO platform

Based on the analytical mechanism, we built the similar architecture on NS3 simulator to execute a simulation results. We implemented our designed system on the MS-VANET model using NS3 [70], as detailed in Chapter 2. this simulator extends the analytical model to incorporate realistic platooning parameters. MS-VANET facilitates the integration of the NS3 simulator with the SUMO platform, enabling realistic mobility simulations tailored to platooning scenarios. As further explained in Chapter 2, MS-VANET enhances NS-3 capabilities by incorporating 3GPP Release 16 5G-NR-V2X and the ETSI C-ITS stack, crucial for building authentic platoon-based communication scenarios. Additionally, the NS3 simulator integrates the 3GPP Channel Model[92], which takes into account both fading and shadowing, producing a realistic physical channel environment for our simulations.

Table 5.5: NS3 Simulation Parameters Setting

Parameter	Value
Platoon Inter-distance	5m
Platoon Average Speed	35 m/s
Constant Speed (0-30s)	20m/s
Sinusoidal Speed (30-100s)	$20 + 5\sin(0.2\pi(t-20))$ m/s
Communication Mode	Broadcast
Number of Platoon	6
Outside Vehicles	20
Control Applied Rate	50ms
Channel Model	3GPP Channel Model [92]

In this section, on top of examining the impact of realistic channel degradation on platoon communication performance, we also investigate into analyzing platoon mobility under conditions of heavy traffic. The scenario parameters are detailed in Table.A.1. Initially, the platoon leader moves applying a sinusoidal speed pattern, as depicted in the left figure of Fig.5.10. Around 55 seconds into the simulation, the platoon encounters a cluster of external vehicles traveling on an adjacent road. These vehicles intensify the channel load by transmitting a higher rate of CAMs, set manually to fix the transmission frequency up to 10ms(100Hz). This scenario design helps to assess the robustness of platoon communications and mobility in response to increased external communication traffic and its associated channel load.

Simulation Result Analysis

Similar to the analytical simulation results, we analyze the outcomes across four primary mobility aspects: string stability, overshoot, headway time and jerk values.

The results, presented in Figure. 5.11, compare the traditional single slice design against our proposed double slice network slicing architecture. For clarity, averages are computed and displayed every 1000 ms, spanning multiple control updates, and the coherent standard deviation value is calculated within each time bin, this helps to better assess the impact of our slicing strategy on vehicular mobility performance.

The background color changed from blue to grey illustrates the progression of the platoon vehicles as they navigate through a heavy traffic scenario. Beginning at 55 seconds, the platoon approaches an area with dense external traffic, marking the onset of communication interference from nearby vehicles. This interaction continues until approximately 80 seconds, when the platoon moves beyond the influence of the external traffic, returning to a state unaffected by outside disturbances.

In typical traffic conditions (indicated by the blue zone in the graph), the single slice design which adheres to standard communication settings, in compared with the double slice design where one slice specifically supports URLLC services, the standard single slice setup exhibits higher deviations in string stability and jerk values. These changes are indicative of abrupt accelerations and deceleration within the platoon, potentially leading to discomfort for passengers and reduced adaptability in emergency situations.

Concerning the other two mobility metrics—headway time and speed overshoot—the average values fluctuate more under the single slice design compared to the URLLC-supported double slice design. This observation underscores the challenges faced by the system when navigating through densely traffic areas without the benefits of network slicing. By contrast, the double slice design consistently demonstrates stable performance, even amidst heavy external traffic. This stability is attributed to the enhanced protection offered by the network slicing architecture, ensuring reliable and timely communication within the platoon continuously. Such a setup not only mitigates the adverse effects of dense traffic but also enhances overall vehicular coordination and safety.

In summary, the simulation results corroborate the observations from the previous analytical simulations, demonstrating enhanced vehicular platooning performance. Specifically, the URLLC services contribute to improvements in string stability among other mobility metrics. In particular, the jerk metric shows significant enhancements, with a reduction in high jerk values, indicating smoother and more stable vehicular movements. Furthermore, the simulations under heavy traffic conditions—representing extreme scenarios—highlight the robustness of the protected slice. This slice exhibits superior resilience in emergency situations, affirming the necessity of implementing network slicing directly over the 5G-NR Sidelink for V2X communications. This is especially crucial for use cases with stringent requirements, where maintaining high reliability and responsiveness is paramount. These findings underscore the value of tailored network architectures like the multiple slice design in supporting advanced vehicular operations, ensuring that V2X communications are both reliable and efficient under diverse traffic conditions.

5.4 Conclusion

In this chapter, we evaluated the benefits of the URLLC slicing service described in Chapter 4 for a challenging Cooperative Connected Automated Mobility (CCAM) use case, namely vehicular platooning. Operating a safe and comfortable platoon require strict delay bounds in control messages exchanged between vehicles in the platoon, even under other interfering V2X communications.

The methodology was segmented into two parts. The first part proposed a platooning service operating on a 5G-NR Sidelink URLLC slice. We introduced a novel ProSe-based architecture integrating the messages defining the dependable slicing service described in Chapter 4 with platoon management messages described by the ENSEMBLE [93] project. From a broad perspective on what vehicles need to support for V2X communication—including general C-ITS V2X messages and exclusive platooning-related communication—we designed a dual-slice architecture. This consists of one general slice to support overall V2X communication and an exclusive, protected slice reserved solely for platoon control-related communication. Within these slices, different QoS levels were allocated, adhering to the structure recommended in Chapter 4.

The second part investigated the impact of vehicular communication on the complex vehicular platooning control methods. By leveraging 5G-NR Sidelink communication performance with realistic PRR and delay values, we integrated these factors into our vehicular platooning control procedure, providing a novel explanation of how to translate delay and the reliability of URLLC quality into actual performance.

The simulation results, analyzed through four mobility metrics, revealed specific advantages that a 5G-NR Sidelink URLLC services offer to vehicular platooning. Notably, there is a marked improvement in driving stability by effectively managing jerk values, contributing to a smoother driving experience. However, traditional metrics such as string stability also exhibit enhancements with the implementation of URLLC services.

Building on the theoretical framework, the system was further evaluated via simulation, incorporating realistic channel and mobility models tailored for platooning. The simulation corroborated the analytical findings, demonstrating significant mobility dynamics improvements in vehicular platooning. Additionally, the results highlighted the efficiency of the double slice design in managing stringent application requirements under heavy traffic conditions. This dual slice setup is crucial in safeguarding resources for high QoS demand applications within V2X communications.

In conclusion, this chapter demonstrated the need for dependable communication for future platooning services based on 5G-NR Sidelink communication. With the previous chapters demonstrating the feasibility of dependable communication on 5G-NR Sidelink, we closed the loop of our study investigating mechanisms at 5G RAN, 3GPP service and finally CCAM application layers towards dependable 5G-NR Sidelink communication.

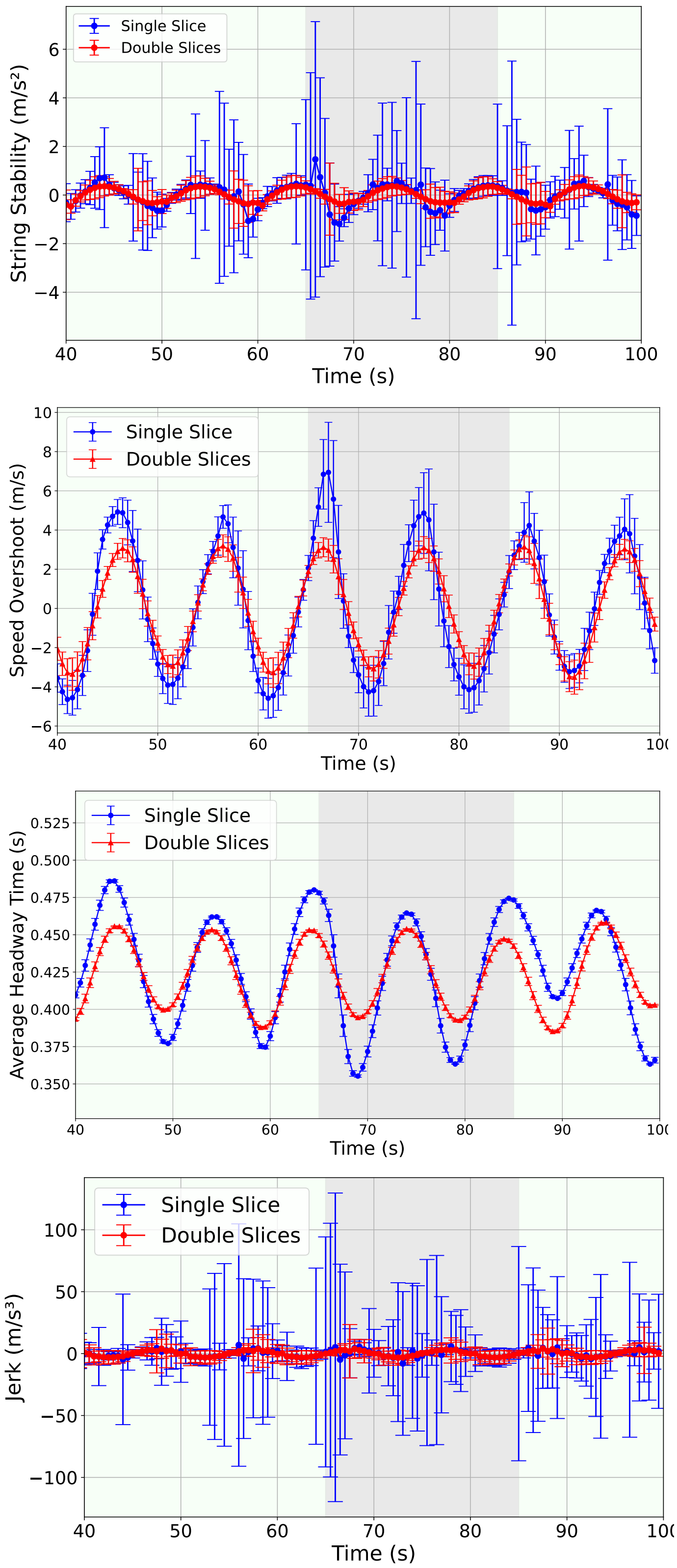

Figure 5.11: Simulation Results on Platooning Communication Conditions

Chapter 6
Conclusion & Perspectives

6.1 Conclusion

We are currently experiencing an era marked by extraordinary technological and scientific progress, characterized by widespread automation and the ubiquity of intelligent devices. In this swiftly changing environment, it is crucial to ensure robust and high-quality connectivity to support contemporary paradigms. As devices increasingly interconnect and integrate even with AI functionalities, the necessity for continuous dependable wireless connectivity becomes more noticeable. Managing the complex dynamics of shared data—which varies significantly in rate and size and demands reliable connections—poses a considerable challenge, far surpassing the demands of previous technological generations. A direct D2D communication framework can facilitate swift and efficient local information sharing, simplifying the network's architecture by reducing the complexity and delays comparing with vertical communications. Developing effective direct D2D communication methods is crucial for enhancing the efficiency of current and future connected and/or automated vehicles as well as next generation IoT ecosystems.

5G-NR communication is designed to offer high capability and dynamic adaptability to suit the evolving needs of the connected world. However, there has been limited research and development specifically targeting direct dependable D2D communication. This oversight is particularly critical given two key aspects that are currently unaddressed but essential for the realistic application of 5G technologies:

Firstly, while high-quality service provision cataloged as URLLC service, is actively being developed for 5G-NR communications, its application to 5G-NR D2D Sidelink communication remains largely unexplored. This gap highlights a crucial area where 5G-NR must evolve to support the stringent latency and reliability requirements expected in direct device interactions within modern IoT and industrial applications.

Secondly, providing a diverse QoS aiming to support different services, including the standard and URLLC requirements over Sidelink communication has yet not been adequately addressed. One key element on 5G-NR in regards of managing bandwidth and customizing to multiple services is network slicing, this strategy has seen extensive research within RAN and core network architectures. However, the extension of this concept to 5G-NR Sidelink communication has not been adequately addressed. This absence represents a significant shortfall, as network slicing could greatly enhance the efficiency and specificity of services provided directly between devices, a necessity for the future landscape of autonomous systems and smart city infrastructures.

To address these shortcomings in 5G-NR's approach to D2D Sidelink communication, initially, our study analyzed the feasibility of implementing URLLC services via 5G-NR Sidelink communication. We proposed a new architecture that reconfigures the 5G-NR parameters—MCS, numerology, and MAC layer scheduling. This configuration enhances reliability and reduces latency, enabling the system to meet the stringent requirements of URLLC services.
To evaluate the performance of this structure, we tested the system within a cluster-based V2X communication framework. The results demonstrated that by limiting the number of access points within the cluster, the communication within the cluster can effectively meet URLLC standards, achieving latency of lower than 1 ms and reliability of 99.99%. This pioneering step in the development of URLLC services over 5G-NR Sidelink communication opens up great potential for D2D communication with 5G-NR across various applications. Quality-critical use cases, such as autonomous driving and real-time remote control systems, stand to benefit significantly from these advancements. This system could also be instrumental in sectors like emergency response where rapid, reliable communication is crucial, and smart city infrastructure, which relies on seamless and efficient device interaction.

Under this innovative URLLC-supportive architecture, our proposed system encountered a challenge: its parameters diverge from the standardized settings recommended by ETSI [84] for V2X applications. Addressing this requires a system that can support multiple QoS levels through different resource groups for various services. Each group must allow dynamic parameter assignment and prevent interference between resource blocks, while remaining compatible with existing ITS stack standards.
To address this, we leveraged the ProSe standard (rel.17) to benefit from its robust service announcement and group management protocols to orchestrate a URLLC slicing service on 5G-NR Sidelink. This enabled the creation and management of RAN based slices on the PC5 interface using ProSe standard message exchanges and URLLC admission control mechanisms. A detailed evaluation of this innovative double URLLC/V2X slice configuration shows that the URLLC slice achieves high reliability and low latency for grouped UEs. Additionally, we assess the impact of this new URLLC slice on the C-ITS slice, demonstrating minimal disruption to V2X resources and ETSI ITS services. This indicated that the system can still support essential safety-related V2X communications, underlining the effectiveness of our approach in enhancing network flexibility and performance.
To carefully evaluate our proposed ProSe-based 5G-NR Sidelink network slicing and URLLC services, we focus on a critical V2X use-case: vehicular platooning. This analysis investigated the general mechanisms for vehicular platooning and assessed the impact of wireless communication factors (delay and reliability) on the platoon effective management (e.g. string stability, jerk,..). We conducted this study analytically first, then introduced the impact of mobility and wireless channel via simulation.
We demonstrated that a 5G-NR URLLC slice benefits key mobility factors such as string stability, while significantly improving jerk performance. This translates into increased passenger comfort in real-world scenarios. This study demonstrated that our proposed 5G-NR URLLC slicing architecture consistently safeguards QoS, maintaining high perfor-

mance and stability even in extreme traffic scenarios, thereby demonstrating the potential of dependable 5G-NR Sidelink communication for vehicular platooning.

6.2 Future Perspectives

Through this work, we identified challenging gaps required for future CCAM scenarios, and filled these gap by demonstrating the feasibility of dependable 5G-NR Sidelink communication. Each of these gaps are yet expected to bear a wider impact beyond this work, as URLCC or 5G Slicing on the PC5 interface are a required extension to complete the promises of 5G technology, and 5G-NR Sidelink should support the same functions as 5G-NR (via gNB).

PC5 Slicing: Our research has been based on a dual-slice design specifically tailored for 5G-NR Sidelink communication. The dual-slice (URLLC/C-ITS) has been protectively designed, but could be dynamically adjusted and enhanced with additional eMBB or mMTC slices dynamically orchestrated similarly to 5G-NR. Additional PC5 slicing features such as life-cycle management, real-time resource balancing between multiple slices are therefore promising aspects beyond this work. Moreover, enabling slicing on the PC5 interface opens the door to PC5 RAN intelligent controllers (RICs), which in turn enables robust xApp for 5G-NR Sidelink.

Advanced Platooning Management: Our initial simulations of vehicular platooning were conducted under the assumption that the platoon configurations were already established. However, real-world scenarios often present additional challenges that could significantly impact the coherence and performance of platoon systems. These scenarios include events such as platoon members departing, new vehicles joining, or external vehicles intersecting the platoon movement. To gain a deeper understanding of how such events affect platooning dynamics, it is essential to formalize and analyze these situations using realistic simulation models. By examining the effects of these complex interactions, we can better evaluate and enhance the mobility performance and stability of vehicular platoons.

Appendix A
Decentralized 5G-NR Sidelink URLLC Services

In the main body of this thesis, we have explored the implementation of network slicing over direct Sidelink communication for 5G-NR, specifically focusing on mechanisms for delivering Ultra-Reliable Low-Latency Communications (URLLC) services within designated slices. In this supplementary chapter, our primary goal is to expand from a dual-slice to a multi-slice architecture, while also examining the 5G-NR's capacity to provide URLLC services within each slice under a UE-only, decentralized Sidelink communication setup. This extension of our study enhances the architecture to include distributed group/cluster formation mechanisms. This supports a system where, under a purely Sidelink-driven approach, we optimize the delivery of maximum URLLC services per cluster with minimal interference among users. This exploration not only broadens the application scope of our initial findings but also leverages 5G-NR's capabilities to enhance the robustness and efficiency of vehicular and mobile communications in densely populated network environments.

A.1 Introduction

Ultra-reliable and Low Latency Communication (URLLC) is one of the paramount asset of the 5G New Radio (NR) [1] technologies. Various studies [106, 1] investigated URLLC for infrastructure-based 5G-NR (i.e. operated by one gNB or a Central Unit (CU)). 5G-NR Sidelink (SL) is a functionality of 5G-NR enabling direct communication between User Equipments (UEs) (i.e. devices). SL has been already introduced by 3GPP for the 4G technology in rel.12 and received more attentions from the automotive stakeholders for Vehicular-to-Everything (V2X) communications in rel.14. However the 4G SL limited performance, use cases and chipset availability did not manage to generate enough attractions from industrial stakeholders interested in cellular Device-to-Device (D2D) communications, which preferred to wait for 5G. 5G-NR SL URLLC is defined by 3GPP rel.17 as providing a 10^{-5} reliability within $1ms$ for 300 bytes, resp. 20 bytes packets for V2X or regular industrial wireless scenarios. It has been studied for 5G-NR V2X for the uplink/downlink (Uu) interface by [107]. Based on our previous work focus on 5G-NR

[1] The ITU defines URLLC as part of 5G technology. However, current commercial 5G technologies are not capable of URLLC.

URLLC on the SL interface, it showed that the tight URLLC requirements could be met only under strict admission control (limiting the number of devices involved in URLLC). 5G-NR SL URLLC considering a fully ad-hoc decentralized topology has to the best of the authors knowledge not been studied yet.
Decentralized 5G-NR SL URLLC is a critical feature for various use cases, such as *decentralized* platooning (a.k.a. Cooperative Adaptive Cruise Control-CACC) or cooperative robotics/cobots [108], where one static or moving stable coordinator is not available. Yet, decentralized 5G-NR SL URLLC is extremely challenging. For instance, the default 5G-NR SL mode 2(a) (ad-hoc) scheduler cannot meet URLLC requirements, and deterministic schedulers as mode 2(c) or 2(d) implicitly require coordinators. URLLC admission control and 5G SL slice management need to have a common orchestrator. Decentralized SL topologies require 5G-NR UEs to get time synchronized to be able communicate, thus requiring a synchronization entity (3GPP calls it a SyncRef UE). Finally, potential multi-hop relays defined in the 3GPP TR 22.866 rel.17 specification require the creation of optimal leaders in the form of a connected dominating (multi-hop) set (MCDS). As of 3GPP rel.19, it is not clear if these various entities would even coincide in a same node (syncRF UE, orchestrator, scheduler, relay, etc.). One key challenge is therefore to define an ad-hoc cellular topology considering these various entities.
In this work, we focus on a first step towards decentralized 5G-NR URLLC by providing a clustering algorithm capable of providing decentralized URLLC admission control. The contributions of this paper are threefolds: (i) a cluster formation algorithm, which weight function limits the size of the cluster to the URLLC maximum admissible UEs; (ii) a graph coloring algorithm to define orthogonal URLLC resources between clusters; (iii) an URLLC slice resource allocation on 5G-NR V2X SL resource pools. The cluster formation as well as the coloring algorithms have linear complexity and can be operated individually by each node (i.e. UE). Nodes within each cluster are capable of intra-cluster URLLC, we leave the inter-cluster URLLC to future work.

A.2 Methodology

All 5G-NR equipped devices must first be synced with their local leaders before enabling group-based URLL Sidelink communication. Under this assumption, we propose to create synchronized clusters in a distributed manner, along with assignments of local cluster heads; meanwhile, we employ admission control to control the size of cluster, allowing the system to support URLLC communication within the cluster.
As this is the first study of cluster-based 5G Sidelink URLL communication, to simplify the global perception, all nodes are assumed to move at a relative constant speed, i.e., no mobility needs to be taken into account. Instead, we regenerate node topology under a centred entity, and during each run, a new set of random nodes is generated under the Poisson Point Process (PPP), therefore dynamic adaptation under different topology is investigated. Detailed nodes generation settings are listed in Table A.1.

A.2.1 Cluster Formulation

Cluster formation is the foundation of establishing synchronized cluster groups and has a significant impact on realising 5G-NR Sidelink URLL communication. The cluster forma-

Table A.1: Simulation Parameters Setting

Parameter	Value
Independent Runs	30
Simulation Range	1km $\times$ 1km
Nodes Density	0.2 per $meter^2$
Transmission Range	120m

tion process is fully decentralized. As direct D2D Sidelink communication is the targeted communication technology, the formation of clusters also needs to be decentralised. Additionally, as cluster size need to be controlled, an admission control methodology is applied in respect of URLL communication. Finally, the complexity of the algorithm needs to be calculated.

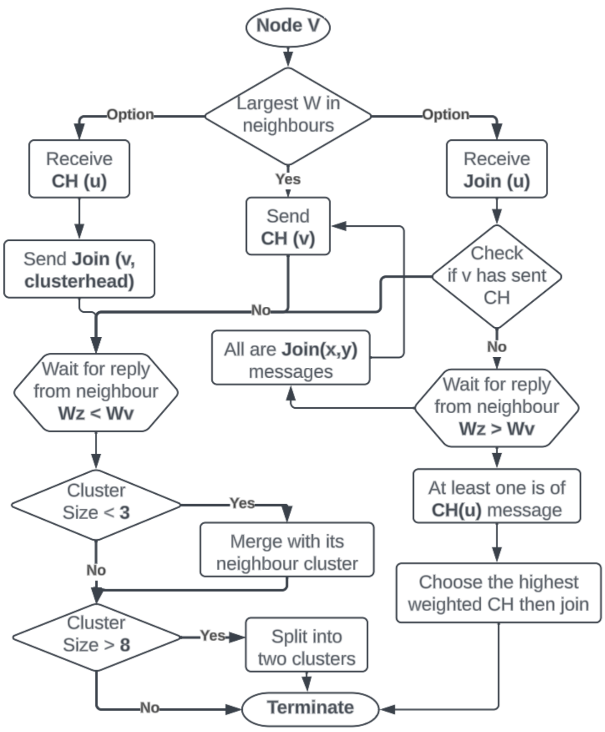

Figure A.1: Cluster Formation Procedure

Cluster Formulation Procedure

We design a clustering algorithm based on the distributed clustering algorithm (DCA) proposed by S. Basagni et al.[109]. Detailed procedure of this algorithm is illustrated in the flow chart Figure. A.1. Our proposed distributed clustering procedure limits the topology knowledge to a localised environment understanding, i.e., only one-hop neighbouring info was required.

Neighbour degrees are applied for weighing different nodes during cluster head election. We make an operational assumption that all the nodes weights are known. Message communication, especially within the communication range, is considered all to be successfully received.[2]

Admission control in cluster formation

Despite the algorithm's simplicity, it has the potential to produce clusters with either too few or too many members. Since the size of the cluster has a significant impact on the URLLC services that follow, we further apply an admission control regarding to URLLC criteria.
In order to guarantee a overall systematic efficiency, we set the lower bound of cluster size of 3; for maximum boundary, as explain in chapter 3, under numerology-3, every 1 ms there are 8 mini-slots available. Since we intended to reduce the latency meanwhile maintaining the reliability, for each cluster, we assign a limited 1 ms, resulting in a correlated upper bound cluster size of 8. Further resource allocation details will be explained in the following section A.2.2.

Algorithm Time Complexity

As this algorithm is a modified version of Domestic Clustering Algorithm, the complexity of message is calculated by work from Basagni et al. [109], in which Corollary-2 pointed out that the message complexity of the DCA is n.
From the distributed clustering algorithm, each message is processed by a fixed number of computation steps. From Theorem 2, there are only messages in the system. Thus, the time complexity is $\mathcal{O}(n)$ [110]. In our algorithm, on top of DCA, we added two rounds of communication, for either merging or splitting, each node sends one more message, which is equivalent to the complexity of DCA, therefore, the overall algorithm complexity is $\mathcal{O}(3n) \rightarrow \mathcal{O}(n)$.

A.2.2 Cluster Resource Sharing Strategy

Once the clusters are formed, adjacent clusters must be granted separate resources from their neighbouring clusters in order to provide group communication without interference. In a cellular network, this isolation can be achieved either on frequency- or time-domain division. In this study, we approach the segmentation among different clusters through time-domain division. As depicted in Fig. A.2, different colours represent the various clusters' allocated resources.

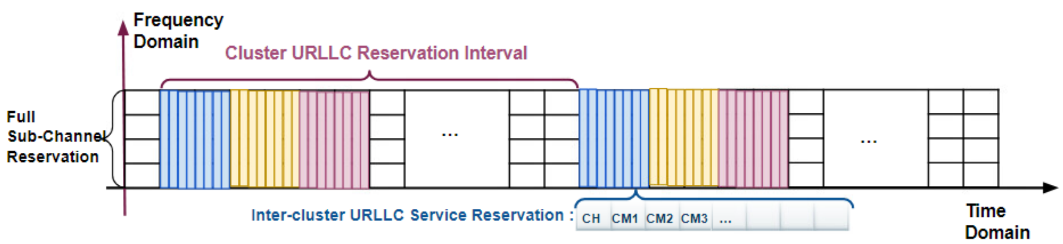

Figure A.2: Resource Allocation on Cluster-based Slices

[2]Although this is not feasible in practical wireless communication, reliability within short range can be guaranteed and improved by multiple retransmission.

We formulate the problem of resource assignments for different clusters into a graph colouring problem. As the first study to address this issue, we approach the problem using a greedy colouring algorithm. Although greedy colouring might end up in utilising more colours than optimal, its simplicity can help to reduce system complexity. Detailed design of the graph colouring algorithm is explained in Algorithm 3.
In addition, the complexity of greedy colouring can be assumed as $\mathcal{O}(V+E)$, in which V is the vertical(nodes) number, E is the total edge(connected links) number. Both V and E are linearly proportional to total number of nodes N, therefore combining the analysis in Section A.2.1, the overall system algorithm complexity stays $\mathcal{O}(n)$.
To meet the strict demands for URLL communication among cluster members. On the physical layer, firstly a higher numerology-3 is applied, thus the slot time is reduced to 0.125 ms, as demonstrated in chapter 4. This can help the system to achieve lower latency. Secondly, in order to avoid half-duplex problem, a pure time-domain multiplexing is applied, all full available physical resource blocks are uniformly assigned to one user. Under this setting, each transmission slot can support up to 300 bytes, however for smaller controlled based packets for Sidelink, the system can support larger cluster formation combining the admission control algorithm explained in Section A.2.1. Under this configuration, each transmission slot can accommodate up to 300 bytes. Furthermore, controlled-based 5G-NR Sidelink packets are generally small, allowing admission control to construct larger clusters. This suggests the system has greater capacity potential.
Thirdly, as mentioned in previous section, certain scheduler modes in 5G-NR Sidelink have the potential to support URLLC. We hereby apply a deterministic Time-Division Multiple Access (TDMA) scheduler mode 2(c) to meet the URLLC delay requirements. A pre-allocated pattern is created by the cluster leader and disseminated to its members, as indicated in Fig. A.2, within each cluster resource, eight different time-slots are available for its members communication. When the size of cluster is lower than eight, a fixed transmission pattern is allocated to members; if the size exceeds, random selection is generated.
The URLLC communication reserve period T_{int} is set to 10 ms from a global view. Since each millisecond is reserved for a specific cluster, the system is capable of providing a overall coherent URLLC communication by supporting 10 separate cluster-based resource assignments.

Algorithm 3 Greedy Colouring Algorithm

Require: Array $Colour$ summarises colour list that is being used for colouring.
d= number of neighbours of current nodes v.
Array $UsedC$ summarises list of already applied colour in Boolean label.

```
for w = 1 : 1 : d do                          ▷ loop over all neighbours applied colours
    UsedC[colour[w]] = true;
end for
return smallest c such that
    UsedC[c] = false;                         ▷ Get the smallest unused colour to apply
```

A.3 System Performance Analysis

We implement the aforementioned methodology on Matlab. This section is to analyse the system performance. In order to acquire a statistical performance results, we simulate 30 independent runs, during each run, a new set of nodes are regenerated and topology are reallocated according to Poisson Point Process (PPP), this process helps the system to generate points scattered homogeneously in a random manner.

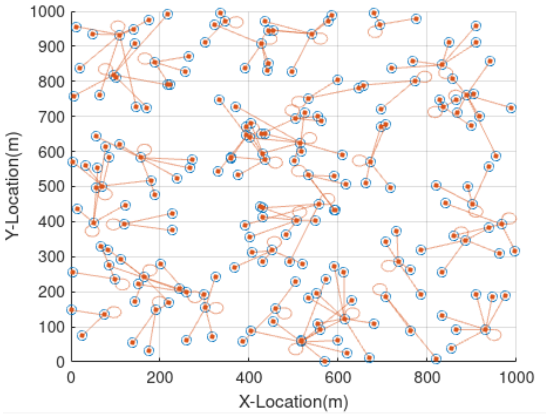

(a) Clustered Nodes

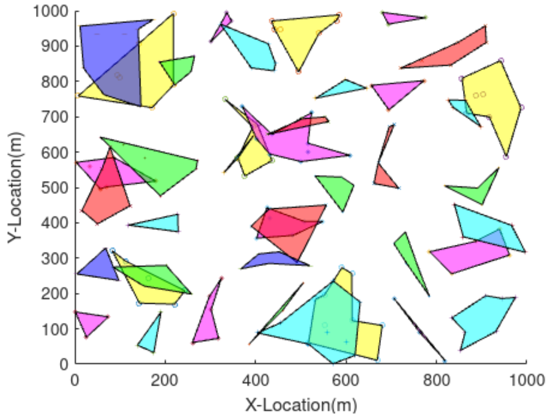

(b) Coloured Clusters

Cluster Forming and Resource Allocation Result

The cluster formation is realised by the procedure shown in Fig. A.1. One simulation result is depicted in Fig. A.3(a), nodes with self-loop representing the selected cluster heads. Moreover, a corresponding colouring result based on the graph colouring methodology is shown in Fig. A.3(b). This clustering topology requires 7 different colours in total. Combining the both, we get a broad impression that nodes are clustered in a scattered way and under a controlled cluster size.

Furthermore we obtain the statistical results for the required colour number over 30 separate runs. As illustrated in bar Fig. A.4, for cluster-based URLLC communication, the system typically requires 7 separate resource blocks as the majority of simulations require up to 7 colors. As a result, this system can assign various resources to independent cluster communication without interference, using the suggested 10 ms reservation period.

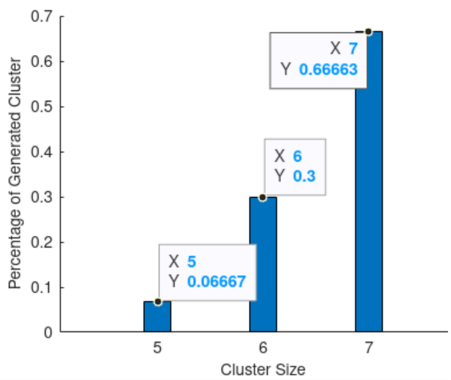

Figure A.4: Number of Needed Colour for Resource Allocation

URLLC-related Reliability Result

The reliability of URLL communication mostly depends on the size of formed clusters, due to the fact that the deterministic scheduler is applied according to Section A.2.2. Within the reserved 1ms per cluster, 8 slots are available, therefore a certain 100% reception rate[3] can be guaranteed when the cluster size is lower than 8. However if the size is larger than this limit, a random selection need to be generated, therefore a lower packet reception rate can be guaranteed.

We firstly illustrate the distribution of generated cluster size over 30 runs in Table A.2, it is evident that the majority of the formed clusters meet under the size restriction. However, because we only perform the segmentation once throughout the cluster generation, some large clusters can still be produced. We reserved to perform this segmentation once due to the trade-off between system complexity and cluster size reduction.

To further analyse the system packet reception rate (PRR) performance, given the generated N number of clusters under size of $S_1, S_2, ..., S_N$, the packet reception rate (PRR) calculation can be formulated as :

$$rho(i) = \begin{cases} 1 & \text{if } S_i \leq 8 \\ 8/S_i & \text{if } S_i > 8. \end{cases} \tag{A.1}$$

$$PRR = \frac{\sum_{i=1}^{N} \rho(i)}{N} \tag{A.2}$$

In which, ρ representing the PRR over different cluster size. When the cluster size is under the controlled restriction, 100% of PRR is achieved under perfect channel condition, for larger cluster size, random resource slot selection is generated, correspondingly a lower PRR is acquired. PRR representing the average packet reception rate over all cluster members.

We hereby plot the analytical PRR distribution in Fig. A.5(a), represented in blue line. The x-axis of connected nodes is equivalent to the cluster size. One can observe a gradual degradation of reliability once the cluster size is exceeded 8. The aforementioned function is assuming all nodes are occupied throughout the simulation, which is not the case in reality. We therefore further analyse the actual availability for each node within the URLL transmission pool. Under assumption of events occurrences are according to Poisson distribution, the theoretical calculation is plotted in red line in the same figure.

We can observe a higher probability for transmission availability than packet reception rate, as a probability is introduced for transmission availability, not all collisions happen in full certainty. However, once the number of connected nodes exceeds around 20, the degradation of transmission availability worsens faster than the packet reception rate. This is due to an increased number of nodes generates a higher possibility of events, which dominates the deterioration.

We can conclude that controlling the size of clusters through admission control is critical in achieving high reliability performance for URLL communication system.

Further simulation results are obtained through 30 independent runs, listed in table A.2. For size of smaller than 8, 100% packet reception rate is achieved, and the results show that on average under a confidential interval of 0.95, 0.9923 ± 0.00504 chance the system is able to support full successful communication. As conclusion, for packet reception rate

[3] Under perfect channel conditions.

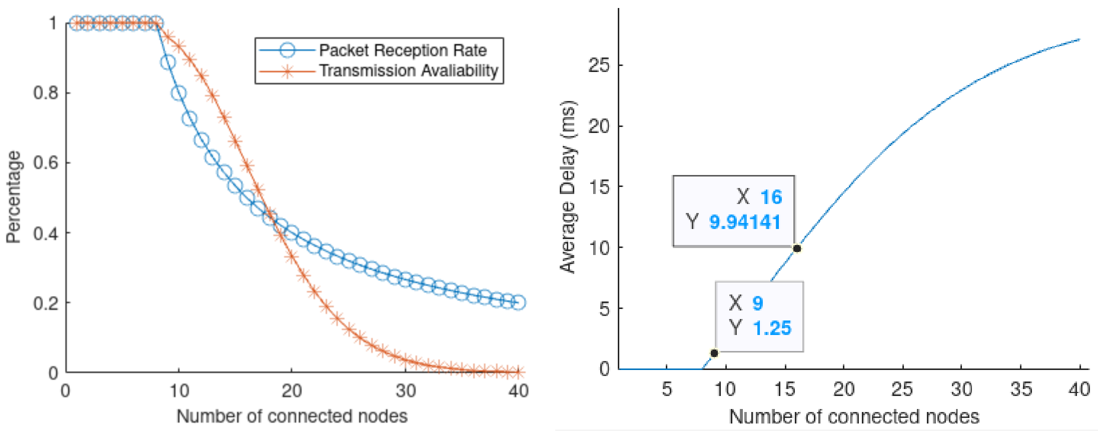

(a) PRR and Transmission Availability Analysis

(b) Average Delay Result in ms

this system is able to support up to 99% chance of a full 100% PRR, which is corresponding to URLL communication.

Index	Size <= 8	Size > 8
Average	0.9636	0.0364
Confident Interval of 0.95	0.01830	0.01830

Table A.2: Cluster Size Distribution over Simulation Result

URLLC-related Latency Result

According to Section A.2.2, the reservation periodic for the URLLC communication pool is defined as T_{int} of 10 ms. URLLC latency is mainly caused by the failure of transmission on the current reservation period, of which case, nodes will have to wait for the next period reservation. This average delay can be calculated in the following function :

$$Delay_m = T_{int} * P_m \sum_{i=1}^{M} i * (1 - P_m)^i \quad \text{(A.3)}$$

In which, P_m representing the average packet reception rate result from Section. A.3, under the connected number of nodes size of m. A corresponding analytical result is plotted in Figure. A.5(b), it can be seen that only when the connected nodes number are lower than 8, this system can meet the delay bound of 1 ms. Combining the previous section, we can conclude that this methodology can satisfy the URLLC latency criterion because the majority of cluster sizes generated in our system are significantly less than 8.
Furthermore, 10 ms is also considered as a typical inter-packet gap for most use cases in robotics and Cooperative, Connected and Automated Mobility (CCAM), under a deterministic scheduler, a delay of 10 can therefore also be acceptable. In this case, this system can support up to 16 nodes, doubled the capability under an acceptable delay tolerant.

A.4 Conclusion

This study proposes a fully distributed cluster formation methodology, which restricts the cluster's size to the URLLC's maximum allowable UEs and creates synchronized cluster entities. Additionally, we suggest modifications to the 5G-NR Sidelink physical layer and apply a different resource scheduling mode. We analyse the performance of the system based on an analytical configuration; in the future we intend to analyse the precise node mobility based on use-case oriented applications, and examine system performance with more realistic channel models.

We demonstrate that this methodology can support inner-cluster communication with high reliability and low latency, meeting the URLL communication requirements with high probability. The further inter-cluster communication will be addressed in a following study.

Bibliography

[1] Rashid Ali et al. URLLC for 5G and Beyond: Requirements, Enabling Incumbent Technologies and Network Intelligence. In: *IEEE Access* 9 (2021), pp. 67064–67095. 10.1109/ACCESS.2021.3073806.

[2] Petar Popovski et al. Wireless Access in Ultra-Reliable Low-Latency Communication (URLLC). In: *IEEE Transactions on Communications* 67.8 (2019), pp. 5783–5801. 10.1109/TCOMM.2019.2914652.

[3] 5G Americas. New Services and Applications with 5G Ultra-Reliable Low Latency Communications. In: *5G Americas White Paper* (2018).

[4] Gabriel Brown. Ultra-Reliable Low-Latency 5G for Industrial Automation. In: *A Heavy Reading white paper produced for Qualcomm Inc.* ().

[5] John B Kenney. Dedicated short-range communications (DSRC) standards in the United States. In: *Proceedings of the IEEE* 99.7 (2011), pp. 1162–1182.

[6] ETSI. In: *ETSI TR 101 607 (v1.1.1), Intelligent transport systems (ITS); Cooperative ITS (C-ITS); Release 1* (2013).

[7] ETSI. In: *3GPP TS 36.300: "Evolved universal terrestrial radio access (E-UTRA) and evolved universal terrestrial radio access network (E-UTRAN); overall description; stage 2"* (2016).

[8] Dan Wang and Tao Sun. Leveraging 5G TSN in V2X Communication for Cloud Vehicle. In: *2020 IEEE International Conference on Edge Computing (EDGE)*. 2020, pp. 106–110. 10.1109/EDGE50951.2020.00023.

[9] ETSI. In: *ETSI EN 302 663 V1.3.0: Intelligent Transport Systems (ITS);ITS-G5 Access layer specification for Intelligent Transport Systems operating in the 5 GHz frequency band* (2019).

[10] ETSI TR 137 985 V16.2.0. In: *LTE; 5G; Overall description of Radio Access Network (RAN) aspects for Vehicle-to-everything (V2X) based on LTE and NR* (2024-01).

[11] Qualcomm. How will sidelink bring a new level of 5G versatility? In: *www.qualcomm.com/news/ onq/ 2022/09/how-will-sidelink-bring-a-new-level-of-5g-versatility* (2022-09).

[12] Ahmad Alalewi, Iyad Dayoub, and Soumaya Cherkaoui. On 5G-V2X Use Cases and Enabling Technologies: A Comprehensive Survey. In: *IEEE Access* 9 (2021), pp. 107710–107737. 10.1109/ACCESS.2021.3100472.

[13] TR 21.918 V1.1.0. In: *Technical Report 3rd Generation Partnership Project;Technical Specification Group Services and System Aspects; Release 18 Description;Summary of Rel-18 Work Items* (2024-09).

[14] ETSI. Part 2: Specification of Cooperative Awareness Basic Service. In: *ETSI EN 302 637-2 V1.4.1: Intelligent Transport Systems (ITS); Vehicular Communications; Basic Set of Applications;* (2019).

[15] ETSI. Part 3: Specifications of Decentralized Environmental Notification Basic Service. In: *ETSI EN 302 637-3 V1.3.1: Intelligent Transport Systems (ITS); Vehicular Communications; Basic Set of Applications;* (2019).

[16] Sudeep Hegde et al. Sidelink Group Resource Scheduling for Platoons in Cellular Vehicle-to-Vehicle Communications. In: *2021 IEEE 93rd Vehicular Technology Conference (VTC 2021 - Spring)*. 2021, pp. 1–5. 10.1109/ VTC2021 - Spring 51267.2021.9449009.

[17] Luca Barbieri et al. Decentralized federated learning for extended sensing in 6G connected vehicles. In: *Vehicular Communications* 33 (2022), p. 100396. 2214-2096. https://doi.org/10.1016/j.vehcom.2021.100396. https://www.sciencedirect.com/science/article/pii/S2214209621000656.

[18] ETSI. System Reference document (SRdoc); Road ITS equipment operating in the 5,9 GHz band with channel bandwidths larger than 10 MHz. In: *ETSI TR 103 853 V1.1.1 (2023-01)* (2023).

[19] M. Carmen Lucas-Estañ and J. Gozalvez. Sensing-Based Grant-Free Scheduling for Ultra Reliable Low Latency and Deterministic Beyond 5G Networks. In: *IEEE Transactions on Vehicular Technology* 71.4 (2022), pp. 4171–4183. 10.1109/TVT.2021.3136725.

[20] Lei Feng et al. Joint Computation Offloading and URLLC Resource Allocation for Collaborative MEC Assisted Cellular-V2X Networks. In: *IEEE Access* 8 (2020), pp. 24914–24926. 10.1109/ACCESS.2020.2970750.

[21] Xiaohu Ge. Ultra-Reliable Low-Latency Communications in Autonomous Vehicular Networks. In: *IEEE Transactions on Vehicular Technology* 68.5 (2019), pp. 5005–5016. 10.1109/TVT.2019.2903793.

[22] ETSI. Intelligent Transport Systems (ITS); Access layer part; Congestion Control for the Cellular: V2X PC5 interface. In: *ETSI TS 103 574 V0.3.1* (2018).

[23] Claudia Campolo et al. 5G Network Slicing for Vehicle-to-Everything Services. In: *IEEE Wireless Communications* 24.6 (2017), pp. 38–45. 10.1109/MWC.2017.1600408.

[24] Hamza Khan et al. On the Application of Network Slicing for 5G-V2X. In: *European Wireless 2018; 24th European Wireless Conference*. 2018.

[25] Alexios Lekidis and Faouzi Bouali. C-V2X network slicing framework for 5G-enabled vehicle platooning applications. In: *2021 IEEE 93rd Vehicular Technology Conference (VTC2021-Spring)*. 2021, pp. 1–7. 10.1109/VTC2021-Spring51267.2021.9448769.

[26] Ruyan Wang, Jiaxing Wu, and Junjie Yan. WO2019221826A1: Resource slicing on a sidelink interface. In: *World Intellectual Property Organization(PATENT)* (2019).

[27] Ciprian Zamfirescu et al. Network slice allocation for 5G V2X networks: A case study from framework to implementation and performance assessment. In: *Vehicular Communications* 45 (2024), p. 100691. 2214-2096. https://doi.org/10.1016/j.vehcom.2023.100691. https://www.sciencedirect.com/science/article/pii/S2214209623001213.

[28] Hiroki Baba et al. End-to-end 5G network slice resource management and orchestration architecture. In: *2022 IEEE 8th International Conference on Network Softwarization (NetSoft)*. 2022, pp. 269–271. 10.1109/NetSoft54395.2022.9844088.

[29] Jin Yan and Jérôme Härri. MCS Analysis for 5G-NR V2X Sidelink Broadcast Communication. In: *2022 IEEE Intelligent Vehicles Symposium (IV)*. 2022, pp. 1347–1352. 10.1109/IV51971.2022.9827311.

[30] Jin Yan and Jérôme Härri. On the Feasibility of URLLC for 5G-NR V2X Sidelink Communication at 5.9 GHz. In: *GLOBECOM 2022 - 2022 IEEE Global Communications Conference*. 2022, pp. 3599–3604. 10.1109/GLOBECOM48099.2022.10000606.

[31] Jin Yan and Jérôme Härri. Towards 5G NR ProSe-Based Platoon Services Supporting URLL Vehicular Communication. In: *ICC 2024 - IEEE International Conference on Communications*. 2024, pp. 1017–1022. 10.1109/ICC51166.2024.10622239.

[32] 3GPP TR 21.915 V15.0.0. In: *Technical Report 3rd Generation Partnership Project;Technical Specification Group Services and System Aspects; Release 15 Description;Summary of Rel-15 Work Items* (2019-09).

[33] ETSI. In: *ETSI TS 123 287 V16.4.0 : "Architecture enhancements for 5G System (5GS) to support Vehicle-to-Everything (V2X) services(3GPP TS 23.287 version 16.4.0 Release 16)"* (2020).

[34] ETSI TS 138 300 V16.2.0. In: *5G;NR;NR and NG-RAN Overall description;Stage-2* (2020-07).

[35] 3GPP TR 22.804. In: *Study on Communication for Automation in Vertical Domains (Release 16)* (2021-06).

[36] 3GPP TR 21.917 V19.0.0. In: *Technical Report 3rd Generation Partnership Project;Technical Specification Group Services and System Aspects; Release 17 Description;Summary of Rel-17 Work Items* (2022-12).

[37] 3GPP 21.916 V16.0.0. In: *Technical Report 3rd Generation Partnership Project;Technical Specification Group Services and System Aspects; Release 16 Description;Summary of Rel-16 Work Items* (2021-06).

[38] RP-201385. In: *WID revision: NR sidelink enhancement, 3GPP* (2020).

[39] Muhammad Waqas et al. A Comprehensive Survey on Mobility-Aware D2D Communications: Principles, Practice and Challenges. In: *IEEE Communications Surveys Tutorials* 22.3 (2020), pp. 1863–1886. 10.1109/COMST.2019.2923708.

[40] ETSI. In: *ETSI TS 133 533 V18.2.0 : "Security aspects of ranging based services and sidelink positioning"* (2024).

[41] Mario H. Castañeda Garcia et al. A Tutorial on 5G NR V2X Communications. In: *IEEE Communications Surveys Tutorials* 23.3 (2021), pp. 1972–2026. 10.1109/COMST.2021.3057017.

[42] Chia-Hao Yu et al. Resource Sharing Optimization for Device-to-Device Communication Underlaying Cellular Networks. In: *IEEE Transactions on Wireless Communications* 10.8 (2011), pp. 2752–2763. 10.1109/TWC.2011.060811.102120.

[43] Zoraze Ali, Sandra Lagén, and Lorenza Giupponi. On the impact of numerology in NR V2X Mode 2 with sensing and no-sensing resource selection. 2021. arXiv: `2106.15303 [eess.SP]`. https://arxiv.org/abs/2106.15303.

[44] Claudia Campolo et al. Improving Resource Allocation for beyond 5G V2X Sidelink Connectivity. In: *2021 55th Asilomar Conference on Signals, Systems, and Computers*. 2021, pp. 55–60. 10.1109/IEEECONF53345.2021.9723155.

[45] Rafael Molina-Masegosa, Javier Gozalvez, and Miguel Sepulcre. Configuration of the C-V2X Mode 4 Sidelink PC5 Interface for Vehicular Communication. In: *2018 14th International Conference on Mobile Ad-Hoc and Sensor Networks (MSN)*. 2018, pp. 43–48. 10.1109/MSN.2018.00014.

[46] Claudia Campolo et al. 5G NR V2X: On the Impact of a Flexible Numerology on the Autonomous Sidelink Mode. In: *2019 IEEE 2nd 5G World Forum (5GWF)*. 2019, pp. 102–107. 10.1109/5GWF.2019.8911694.

[47] Hamidreza Bagheri et al. 5G NR-V2X: Toward Connected and Cooperative Autonomous Driving. In: *IEEE Communications Standards Magazine* 5.1 (2021), pp. 48–54. 10.1109/MCOMSTD.001.2000069.

[48] Mujahid Muhammad and Ghazanfar Ali Safdar. 5G-based V2V broadcast communications: A security perspective. In: *Array* 11 (2021), p. 100084. 2590-0056. https://doi.org/10.1016/j.array.2021.100084. https://www.sciencedirect.com/science/article/pii/S2590005621000321.

[49] K. B. Shashika Manosha et al. Admission Control Algorithms for QoS-Constrained Multicell MISO Downlink Systems. In: *IEEE Transactions on Wireless Communications* 17.3 (2018), pp. 1982–1999. 10.1109/TWC.2017.2787641.

[50] Nipuni Uthpala Ginige et al. Admission Control in 5G Networks for the Coexistence of eMBB-URLLC Users. In: *2020 IEEE 91st Vehicular Technology Conference (VTC2020-Spring)*. 2020, pp. 1–6. 10.1109/VTC2020-Spring48590.2020.9129141.

[51] 3GPP Technologies Report. 5G Network slice management. In: *www.3gpp.org/ technologies/ slice-management* (2023-07).

[52] Nokia. Network slicing Enabling business-intent driven networking. In: *www.nokia.com/ networks/ network-slicing/* (2024).

[53] O-RAN. O-RAN Work Group 1 (Use Cases and Overall Architecture) Use Cases Analysis Report. In: *WG1.Use-Cases-Analysis-Report-R003-v14.00* (2024).

[54] ETSI. 5G; Management and orchestration; Architecture framework. In: *ETSI TS 128 533 V15.0.0* (2018-10).

[55] Li Da Xu, Wu He, and Shancang Li. Internet of Things in Industries: A Survey. In: *IEEE Transactions on Industrial Informatics* 10.4 (2014), pp. 2233–2243. 10.1109/TII.2014.2300753.

[56] Ben-Jye Chang et al. Dynamic Keeping Reserved Resource Probability with Slicing Flow Steering in 5G Sidelink SPS for Platooning ADAS and Autonomous Self Driving. In: *2020 International Automatic Control Conference (CACS)*. 2020, pp. 1–6. 10.1109/CACS50047.2020.9289794.

[57] Official Journal of the European Union. In: *Commission Implementing Decision (EU) 2020 /1426 of 7 October 2020 on the harmonised use of radio spectrum in the 5 875-5 935 MHz frequency band for safety-related applications of intelligent transport systems (ITS) and repealing Decision 2008/671/EC* (2020).

[58] Mario H. Castañeda Garcia et al. A Tutorial on 5G NR V2X Communications. In: *IEEE Communications Surveys Tutorials* 23.3 (2021), pp. 1972–2026. 10.1109/COMST.2021.3057017.

[59] ETSI. Analysis of the Collective Perception Service (CPS); Release 2. Tech. In: *ETSI TR 103 562 V2.1.1: Intelligent Transport Systems (ITS); Vehicular Communications; Basic Set of Applications;* (2019).

[60] ETSI. Intelligent Transport Systems (ITS); Vehicular Communications; Manoeuvre Coordination Service (MCS); Pre-standardization study; Release 2. In: *ETSI TR 103 578 V2.1.1* (2024).

[61] TransAID. TransAID: D5.1 Definition of V2X message sets; Definition of V2X message sets Project Acronym TransAID;Transition Areas for Infrastructure-Assisted Driving;Work Package WP5 Connectivity and Signalling. In: *Horizon 2020 ART-05-2016 – GA Nr 723390* (2016).

[62] ETSI. In: *ETSI TS 122 186 V17.0.0: 5G; Service requirements for enhanced V2X scenarios (3GPP TS 22.186 version 17.0.0 Release 17)* (2022).

[63] ETSI GR MEC 024 V2.1.1. In: *Multi-access Edge Computing (MEC); Support for network slicing* (2019-11).

[64] Giampaolo Cuozzo et al. Enabling URLLC in 5G NR IIoT Networks: A Full-Stack End-to-End Analysis. In: *2022 Joint European Conference on Networks and Communications 6G Summit (EuCNC/6G Summit)*. 2022, pp. 333–338. 10.1109/EuCNC/6GSummit54941.2022.9815750.

[65] Natale Patriciello et al. An E2E simulator for 5G NR networks. In: *Simulation Modelling Practice and Theory* 96 (2019), p. 101933.

[66] Zoraze Ali et al. 3GPP NR V2X Mode 2: Overview, Models and System-level Evaluation. In: *IEEE Access* PP (June 2021), pp. 1–1. 10.1109/ACCESS.2021.3090855.

[67] András VargaAndrás Varga. The OMNET++ discrete event simulation system. In: *Computer Science, Engineering* (2000).

[68] Florian Kaltenberger et al. OpenAirInterface: Democratizing innovation in the 5G Era. In: *Computer Networks* 176 (2020), p. 107284. 1389-1286. https://doi.org/10.1016/j.comnet.2020.107284. https://www.sciencedirect.com/science/article/pii/S1389128619314410.

[69] Pablo Alvarez Lopez et al. Microscopic Traffic Simulation using SUMO. In: *2018 21st International Conference on Intelligent Transportation Systems (ITSC)*. 2018, pp. 2575–2582. 10.1109/ITSC.2018.8569938.

[70] F. Raviglione et al. ms-van3t: An integrated multi-stack framework for virtual validation of V2X communication and services. In: *Computer Communications* 217 (2024), pp. 70–86. 0140-3664. https://doi.org/10.1016/j.comcom.2024.01.022. https://www.sciencedirect.com/science/article/pii/S0140366424000227.

[71] Karl Schrab et al. Modeling an ITS Management Solution for Mixed Highway Traffic With Eclipse MOSAIC. In: *IEEE Transactions on Intelligent Transportation Systems* 24.6 (2023). 10.1109/TITS.2022.3204174.

[72] Christoph Sommer, Reinhard German, and Falko Dressler. Bidirectionally Coupled Network and Road Traffic Simulation for Improved IVC Analysis. In: *IEEE Transactions on Mobile Computing* 10.1 (2011), pp. 3–15. 10.1109/TMC.2010.133.

[73] ETSI. 5G;NR;Study on Scenarios and Requirements for Next Generation Access Technologies. In: *3GPP TR 38.913 version 17.0.0 Release 17* (2022-03).

[74] ETSI. In: *3GPP TS 38.214 V17.1.0: 5G; NR;Physical layer procedures for data* (2022).

[75] Daniel Jiang, Qi Chen, and Luca Delgrossi. Communication Density: A Channel Load Metric for Vehicular Communications Research. In: *2007 IEEE International Conference on Mobile Adhoc and Sensor Systems*. 2007, pp. 1–8. 10.1109/MOBHOC.2007.4428734.

[76] Miguel Sepulcre, Javier Gozalvez, and Baldomero Coll-Perales. Why 6 Mbps is Not (Always) the Optimum Data Rate for Beaconing in Vehicular Networks. In: *IEEE Transactions on Mobile Computing* 16.12 (2017), pp. 3568–3579.

[77] J. Gozalvez R. Molina-Masegosa and M. Sepulcre. Comparison of IEEE 802.11p and LTE-V2X: An Evaluation With Periodic and Aperiodic Messages of Constant and Variable Size. In: *IEEE Transactions on Mobile Computing* 8 (2020), pp. 121526–121548.

[78] Andres Burbano-Abril et al. MCS Adaptation within the Cellular V2X Sidelink. In: *ArXiv* abs/2109.15143 (2021).

[79] Natale Patriciello et al. An E2E simulator for 5G NR networks. In: *Simulation Modelling Practice and Theory* 96 (May 2019), p. 101933. 10.1016/j.simpat.2019.101933.

[80] Tommaso Zugno et al. Implementation of A Spatial Channel Model for ns-3. In: *arxiv* (Feb. 2020).

[81] ETSI. In: *ETSI TR 103 300-1 V2.1.1, "Intelligent Transport Systems (ITS) Vehicular Communications; Vulnerable Road Users (VRU) awareness; Part 1: Use Cases definition"* (2018).

[82] Laurent Gallo and Jérôme Härri. Short paper: A LTE-direct Broadcast Mechanism for Periodic Vehicular Safety Communications. In: *2013 IEEE Vehicular Networking Conference*. 2013, pp. 166–169. 10.1109/VNC.2013.6737604.

[83] ETSI. 5G NR; Physical layer procedures for data. In: *3GPP TS 38.214 version 16.2.0 Release 16* (2020-07).

[84] ETSI. Intelligent Transport Systems (ITS);LTE-V2X and NR-V2X Access layer specification for Intelligent Transport Systems operating in the 5 GHz frequency band; Release 2. In: *ETSI EN 303 798 V2.0.1* (2023).

[85] IEEE Standard for Wireless Access in Vehicular Environments (WAVE)–Multi-channel Operation. In: *IEEE Std 1609.4-2010 (Revision of IEEE Std 1609.4-2006)* (2011), pp. 1–89.

[86] ETSI. 5G ; Proximity-services (ProSe) in 5G System (5GS) protocol aspects; Stage 3. In: *ETSI TS 124 554 V17.1.0* (2022).

[87] Shangwei Zhang et al. Envisioning Device-to-Device Communications in 6G. In: *IEEE Network* 34.3 (2020), pp. 86–91. 10.1109/MNET.001.1900652.

[88] 3GPP TS 28.530 V1.0.0. In: *3rd Generation Partnership Project;Technical Specification Group Services and System Aspects;Telecommunication management; Management of 5G networks and network slicing;Concepts, use cases and requirements* (2018).

[89] NGMN Alliance. Version 1.0. In: *NGMN 5G P1; Requirements Architecture;Work Stream End-to-End Architecture; Description of Network Slicing Concept* (2016).

[90] 3GPP. 3rd Generation Partnership Project; Technical Specification Group Services and System Aspects; Proximity-based Services (ProSe); Security aspects(Release 12). In: *3GPP TS 33.303 V12.0.0* (2014).

[91] 5GAA. V2X Functional and Performance Test Report; Test Procedures and Results. In: *5GAA P-190033* (2018).

[92] Tommaso Zugno et al. Extending the ns-3 spatial channel model for vehicular scenarios. In: *Proceedings of the 2021 Workshop on ns-3* (2021).

[93] ENSEMBLE. D2.8 Platooning protocol definition and communication strategy. In: *HORIZON 2020 H2020-ART-2016-2017/H2020-ART-2017-Two-Stages GA No. 769115* (2022).

[94] Sébastien Sabiron Christine Siméone. Le platooning, quand les camions circulent en peloton reliés par le wi-fi. In: *Radio France - Volvo* (2019). https://www.radiofrance.fr/franceinter/le-platooning-quand-les-camions-circulent-en-peloton-relies-par-le-wi-fi-1582167.

[95] Rajesh Rajamani. Vehicle Dynamics and Control. Springer, 2006. ISBN: 1461414326.

[96] Giovanni Giambene, MD Saifur Rahman, and Alexey Vinel. Analysis of V2V Sidelink Communications for Platoon Applications. In: *ICC 2020 - 2020 IEEE International Conference on Communications (ICC)*. 2020, pp. 1–6. 10.1109/ICC40277.2020.9148968.

[97] Liu Cao and Hao Yin. Resource Allocation for Vehicle Platooning in 5G NR-V2X via Deep Reinforcement Learning. In: *2021 IEEE International Black Sea Conference on Communications and Networking (BlackSeaCom)*. 2021, pp. 1–7. 10.1109/BlackSeaCom52164.2021.9527765.

[98] Ruyan Wang, Jiaxing Wu, and Junjie Yan. Resource Allocation for D2D-Enabled Communications in Vehicle Platooning. In: *IEEE Access* 6 (2018), pp. 50526–50537. 10.1109/ACCESS.2018.2868839.

[99] ETSI. Intelligent Transport Systems (ITS);Facilities layer function;Part 1: Services Announcement (SA) specification. In: *ETSI EN 302 890-1 V1.2.0* (2018-04).

[100] Michał Sybis et al. Communication Aspects of a Modified Cooperative Adaptive Cruise Control Algorithm. In: *IEEE Transactions on Intelligent Transportation Systems* 20.12 (2019), pp. 4513–4523. 10.1109/TITS.2018.2886883.

[101] Erjen Lefeber, Jeroen Ploeg, and Henk Nijmeijer. Cooperative Adaptive Cruise Control of Heterogeneous Vehicle Platoons. In: *IFAC-PapersOnLine* 53.2 (2020). 21st IFAC World Congress, pp. 15217–15222. 2405-8963. https://doi.org/10.1016/j.ifacol.2020.12.2304.

[102] Wei Gao et al. Communication Resources Management Based on Spectrum Sensing for Vehicle Platooning. In: *IEEE Transactions on Intelligent Transportation Systems* 24.2 (2023), pp. 2251–2264. 10.1109/TITS.2022.3148230.

[103] Pengfei Wang et al. Platoon Cooperation in Cellular V2X Networks for 5G and Beyond. In: *IEEE Transactions on Wireless Communications* 18.8 (2019), pp. 3919–3932. 10.1109/TWC.2019.2919602.

[104] Luca Lusvarghi et al. A comparative analysis of the semi-persistent and dynamic scheduling schemes in NR-V2X mode 2. In: *Vehicular Communications* 42 (2023), p. 100628. 2214-2096. https://doi.org/10.1016/j.vehcom.2023.100628. https://www.sciencedirect.com/science/article/pii/S221420962300058X.

[105] Manuel Gonzalez-Martín et al. Analytical Models of the Performance of C-V2X Mode 4 Vehicular Communications. In: *IEEE Transactions on Vehicular Technology* 68.2 (2019), pp. 1155–1166. 10.1109/TVT.2018.2888704.

[106] Gordon J. Sutton et al. Enabling Technologies for Ultra-Reliable and Low Latency Communications: From PHY and MAC Layer Perspectives. In: *IEEE Communications Surveys Tutorials* 21.3 (2019), pp. 2488–2524. 10.1109/COMST.2019.2897800.

[107] Ana Larrañaga et al. 5G Configured Grant Scheduling for 5G-TSN Integration for the Support of Industry 4.0. In: *2023 18th Wireless On-Demand Network Systems and Services Conference (WONS)*. 2023, pp. 72–79. 10.23919/WONS57325.2023.10062219.

[108] Yuanwei Liu et al. Robotic Communications for 5G and Beyond: Challenges and Research Opportunities. In: *IEEE Communications Magazine* 59.10 (2021), pp. 92–98. 10.1109/MCOM.111.2001118.

[109] S. Basagni. Distributed clustering for ad hoc networks. In: *Proceedings Fourth International Symposium on Parallel Architectures, Algorithms, and Networks (I-SPAN'99)*. 1999, pp. 310–315. 10.1109/ISPAN.1999.778957.

[110] C.R. Lin and M. Gerla. Adaptive clustering for mobile wireless networks. In: *IEEE Journal on Selected Areas in Communications* 15.7 (1997), pp. 1265–1275. 10.1109/49.622910.